63-1-5

290 286

NOX

HUGHES TOOL COMPANY · AIRCRAFT DIVISION
Culver City, California

Report 285-17 (62-17)

CONTRACT AF 33(600)-30271

HOT CYCLE DESIGN & DEVELOPMENT PROGRAM

TECHNICAL SUMMARY REPORT

March 1962
Revised June 1962

HUGHES TOOL COMPANY -- AIRCRAFT DIVISION
Culver City, California

FOREWORD

This report has been prepared by Hughes Tool Company -- Aircraft Division under USAF Contract AF 33(600)-30271 "Hot Cycle Pressure Jet Rotor System", D/A Project Number 9-38-01-000, Subtask 616. In fulfillment of item 9 of the contract, it summarizes the technical effort of the program, and represents completion of all work required by the contract.

For

Commander
Aeronautical Systems Division

Prepared by: S. J. Chris
S. J. Chris
Project Engineer

Approved by: J. L. Velazquez
J. L. Velazquez
Sr. Project Engineer

H. O. Nay
H. O. Nay
Manager,
Transport Helicopter Department

ACKNOWLEDGEMENTS

This report summarizes the effort and the individual reports of many at Hughes Tool Company -- Aircraft Division.

Notable contributions to this report were made by the following personnel:

K. B. Amer - Chief, Helicopter Research Section

R. A. Boudreaux - Chief, Aerodynamics Section

J. T. Doyle - Aeronautical Engineer

O. I. Plowe - Aeronautical Engineer

J. W. Rabek - Aerodynamics Specialist

S. E. Sallows - Aeronautical Engineer

C. R. Smith - Chief, Structures Analysis and Test Section

R. B. Sullivan - Helicopter Research Engineer

Hot Cycle Rotor Undergoing Whirl Test

TABLE OF CONTENTS

ILLUSTRATIONS

TABLES

1. SUMMARY

The Hot Cycle Rotor Development program summarized herein has been carried out by Hughes Tool Company - Aircraft Division under joint sponsorship of the Army, Navy and Air Force. The primary purposes of the program were to evaluate the feasibility of this concept of helicopter propulsion and to assess its potential benefits in various applications. The work accomplished under the program included comparative design studies of Hot Cycle aircraft for various applications, in addition to the design, fabrication, and testing of a full-scale rotor system.

The Hot Cycle Rotor utilizes for propulsion high pressure, high temperature gases, supplied by turbojet engine(s) mounted in the fuselage. These gases are ducted through the rotor blades to the tips, where they are exhausted tangentially to produce the thrust to drive the rotor. This system, shown schematically in Figure 1-1, provides the ultimate in helicopter propulsion simplicity. All drive gearing and shafting is eliminated, and the rotor serves as a power turbine in addition to its basic function. The tip jet drive of the Hot Cycle results in negligible torque reaction, thus eliminating the need for a second rotor - only a small jet is required at the tail for yaw control at low speeds.

The 55-foot-diameter rotor which was designed, built and tested under this program, is sized to utilize the gases supplied by two General Electric T64 gas turbine engines. The rotor incorporates a free-floating hub and three coning blades mounted on a shaft supported by an upper radial bearing and a

lower thrust bearing. The hub and control structures are conventional. The blade, on the other hand, while novel in design in order to permit passage of full temperature jet exhaust gases, is characterized by a structure which lends itself to early production with existing equipment and techniques. In addition, the structural arrangement provides protection for the primary members and allows replacement of individual components if damage does occur.

Originally the contract specified 25 hours of whirl testing as proof of feasibility. Modifications of the contract added 10 hours of whirl for demonstration of integrity under conditions of severe control and power transients and 25 additional hours of endurance-type test for study of component life. The final 25 hours were conducted with no substitution or alterations of any components whatsoever.

Structural feasibility of the Hot Cycle System was proven completely by accomplishment of the 60 hours of whirl testing with no significant problems. A sizeable portion of the testing was conducted at gas temperatures as high or higher than the maximum temperature ratings of the T64 engine. The spectrum of the whirl test conditions agrees very closely with the conditions called for in Military Specifications for rotor and engine preliminary flight rating tests. The measured loads are generally within calculated limits. The measured temperatures for all components are within predicted limits. At the completion of the tests the total leakage was measured at a very low value (about 0.2%). No dynamic problems were evidenced, in confirmation of the prediction of no resonances

in the rotor operating speed range. Post-test inspection revealed no basic mechanical or structural difficulties.

In addition to the complete proof of feasibility -- structural, mechanical and dynamic -- the lift performance of the Hot Cycle Rotor exceeded predictions, and the conversion of gas power to rotor power was better than predicted.

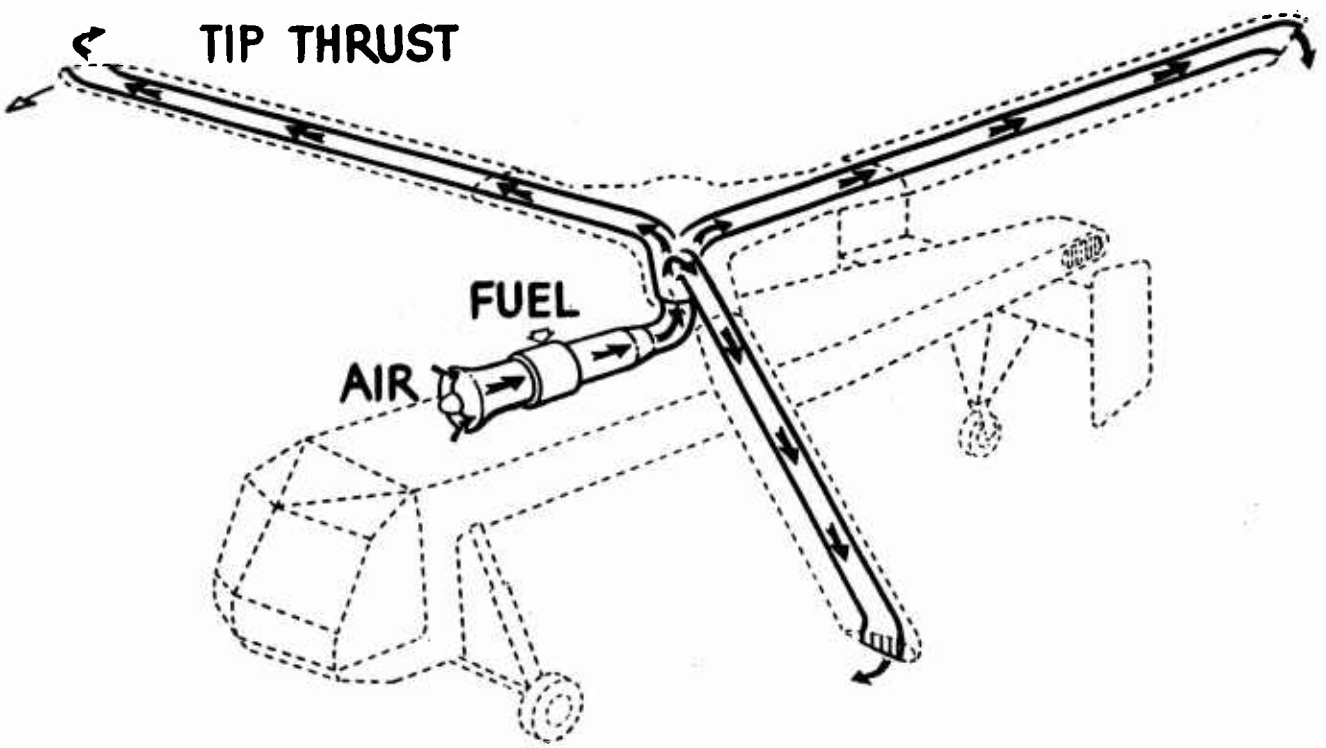

Figure 1-1 Schematic of Hot Cycle System

2. CONCLUSIONS

From the results of the rotor development work and application studies carried out on the Hot Cycle System, the following conclusions are drawn:

a. Structural and mechanical feasibility of the Hot Cycle Rotor System was proven conclusively by 60 hours of whirl testing. Conditions investigated include a full range of rotor transients and extensive operation at gas temperatures at or above the maximum T64 gas temperature.

b. Total gas leakage from the system of less than one-fifth of one percent demonstrated that the sealing problems have been adequately solved.

c. Measured lift exceeded predicted values on which application studies have been based.

d. The complete absence of instabilities, the high damping of transients, and smooth operation during testing verified the excellent dynamic characteristics predicted for the rotor.

e. Measurements during whirl testing indicated that the sound level of a Hot Cycle aircraft will be much lower than that of a typical jet or piston transport aircraft, and significantly lower than that recorded for an existing large helicopter (H-37A).

3. RECOMMENDATIONS

Based on the large improvements which the Hot Cycle System offers for both heavy lift helicopters and VTOL transports and the extremely favorable results from the development work accomplished, it is strongly recommended that further development be pursued expeditiously toward the goal of providing operational vehicles.

4. REVIEW OF PROGRAM

4.1 INTRODUCTION

The helicopter industry and the Military are continuously striving to advance the rotary wing state of the art. One area in which a great deal of effort has been expended is that of the propulsion system. The gear boxes and drive shafting normally used to transmit engine power to the rotor have been a major source of cost, weight, and maintenance. While significant advances had been made, the Hot Cycle Propulsion System promised a major advance, as shown in Figure 4.1-1. The tip drive of the Hot Cycle rotor reduces torque experienced by the fuselage to essentially support bearing friction. Thus, a very small amount of propulsion gas diverted through a nozzle at the tail gives sufficient moment to overcome this friction torque and to provide for yaw maneuvers. In contrast, the shaft driven helicopter must counteract all of the torque applied to the rotors. This is generally done by use of two rotors, either counterrotating main rotors as shown in the figure, or a single large rotor and a smaller torque reacting rotor at the tail, either system utilizing approximately the same number of parts.

Accordingly, after an industry-wide competition, Contract AF 33(600)-30271 was awarded by the Air Force to Hughes Tool Company - Aircraft Division.

The objectives of this contract were to:

a. Analyze utility of the concept as applied to helicopters, compound helicopters, and convertiplanes of various sizes.

b. Demonstrate structural feasibility by actual whirl test of a rotor for 25 hours.

As the work progressed, funding of the program was transferred to the Army Transportation Research Command, with technical and administrative cognizance still under the Air Force, Aeronautical Systems Division. At a still later date, the Navy, through BuWeps, joined in the program funding. Modifications were made to the Contract to:

a. Base the rotor design on a helicopter design gross weight of 15, 300 pounds, and to require compatibility with the full temperature output of two General Electric T64 turbine engines.

b. Further explore rotor characteristics:

1. Aerodynamic and Dynamic (additional 10 hours of whirl test)

2. Endurance-type check (additional 25 hours of whirl test)

c. Study control problems involved in gas coupled engine and rotor.

Following is an outline of the work as given by Item Number of the revised Contract:

Item 1 Design Study of the Application of the Hot Cycle Pressure Jet System to Helicopters, Compound Helicopters, and Convertiplanes of Various Sizes.

Item 2 Design Study of a Hot Cycle Powered Helicopter.

Item 3 Preliminary Design of a Hot Cycle Rotor System.

Item 4 Detail Design of the Above Rotor System.

Item 5 Fabrication of the Above Rotor System and Test Installations

Item 6 Non-rotating Tests of the Above Rotor System.

Item 7 Whirl Test of the Above Rotor System.

Item 12 Study of Engine-Rotor Control System.

A review of the effort outlined above is contained on the following pages.

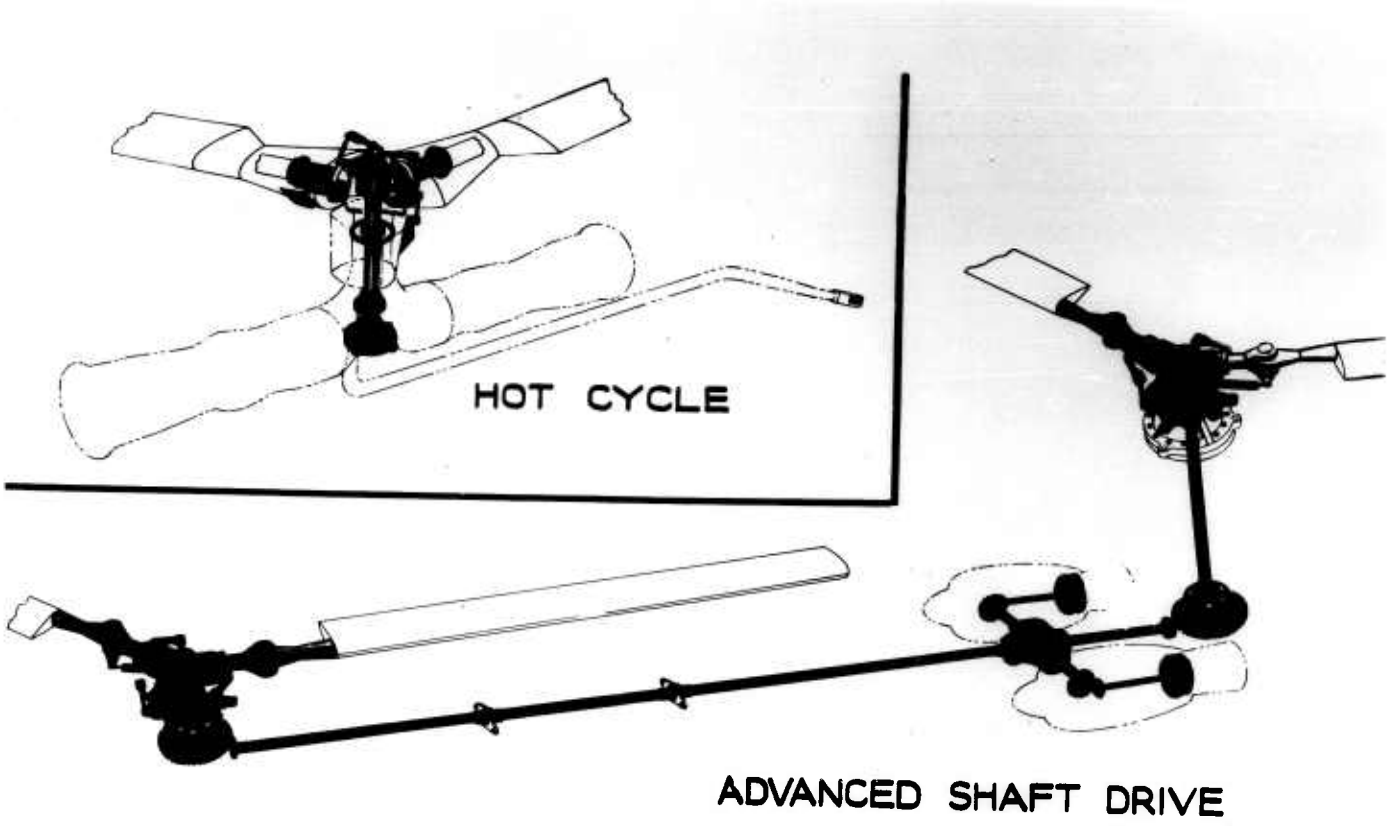

Figure 4. 1-1 Comparison of Mechanical Components of Hot Cycle and Direct Drive Systems

4.2 APPLICATIONS STUDY

Justification is required whenever a new system is proposed to replace an existing one. The Hot Cycle program therefore was initiated by studies of the efficiency of the system as applied to various types of VTOL and STOL aircraft. This detailed analysis indicated that performance would be superior to that predicted in any of the earlier studies. Results were published in Hughes Tool Company -- Aircraft Division Report 285-6 (See Appendix).

The analysis mentioned above, however, was based on use of the "Oryx" N. Or. 1 engine developed by Napier of England. This engine, a mixed flow type which combined compressed air with the exhaust gas to reduce output temperature had low output pressure. As other engine designs with higher pressure ratios became available, such as the Napier "Oryx" N. Or. 5 and Lycoming A and B gas producers, greatly improved performance of the Hot Cycle System resulted. With approval of the cognizant Government Agency, the proposed rotor was re-sized to take advantage of the newly available power and efficiency. During the accomplishment of this and other (company sponsored) effort, this Contractor discovered what became an important "breakthrough" in helicopter development. It was determined that modern turbine engines having high compressor pressure ratios produced jet exhausts at nearly ideal pressures and, when derated, temperatures sufficiently low to be used directly in the helicopter rotor blade. Thus a family of ideal "off-the-shelf" engines that could be used with little or no modification became available.

Even with the engine derated, the combination gave a system of competitive efficiency and much improved simplicity compared with shaft driven types. Finally development of high temperature metals, such as Rene' 41, eliminated the need to derate the engines, resulting in much greater efficiency and simplicity than attainable in other systems. The design and test program were therefore oriented to accept the full exhaust output of two General Electric T64 gas producers. This engine has completed its Preliminary Flight Rating Test and is currently undergoing a Flight Qualification Test. Following the above, applications studies of the vastly improved engine-rotor combination have been continued, with the following results.

4.2.1 Flying Crane Configuration

Figure 4.2-1 presents an artist's rendition of a hot cycle flying crane powered by four advanced T64 gas generators. This machine has a payload capability of approximately 20 tons at sea level. It is shown carrying the Pershing missile along with its transporter - erector - launcher, a total weight well within its capability. The predicted performance of this crane is presented below.

Figure 4.2-2 presents an over-all weight comparison between a Hot Cycle and a shaft driven crane. While weight of the Hot Cycle rotor is based on the experimental unit, that for the shaft driven rotor is from published data based on rotors which have had considerable development time. A 1.0 percent greater rotor weight thereby is indicated for the Hot Cycle and is included in the comparative figures. It can be seen that the Hot Cycle is approximately

10% of gross weight lighter than the shaft driven crane, primarily because of the elimination of the power transmission system. As a result, the ratio of useful load to empty weight of the Hot Cycle is 2.14 as compared with 1.40 for the shaft driven crane.

Figure 4.2-3 presents this data in the form of ratio of payload to empty weight versus range for a Hot Cycle and a shaft driven crane. To insure consistency, the same basic gas generator was assumed installed in both the Hot Cycle helicopter and the analytically studied shaft driven helicopter. Also, equal values of parasite area were assumed. For further comparison, data is included from a brochure put out by a manufacturer of a shaft driven crane. The crane characteristics from the manufacturer's brochure are generally inferior to those predicted in the Hughes Studies because of poorer SFC of the particular engine offered in the brochure.

The parameter payload-empty weight is used for the comparison in Figure 4.2-3 because empty weight is a primary factor in establishing initial and operating costs. It can be seen that at short ranges the Hot Cycle crane can carry over 50% more payload for a given empty weight than the shaft driven helicopter. Superiority of the Hot Cycle crane continues to a range of about 400 miles.

4.2-2 Compound Helicopter Configuration

The Hot Cycle Propulsion System also can be applied profitably to a compound helicopter configuration as shown on Figure 4.2-4 which depicts the

Figure 4.2-1 Artist's Concept of Hot Cycle Crane Delivering Pershing Missile

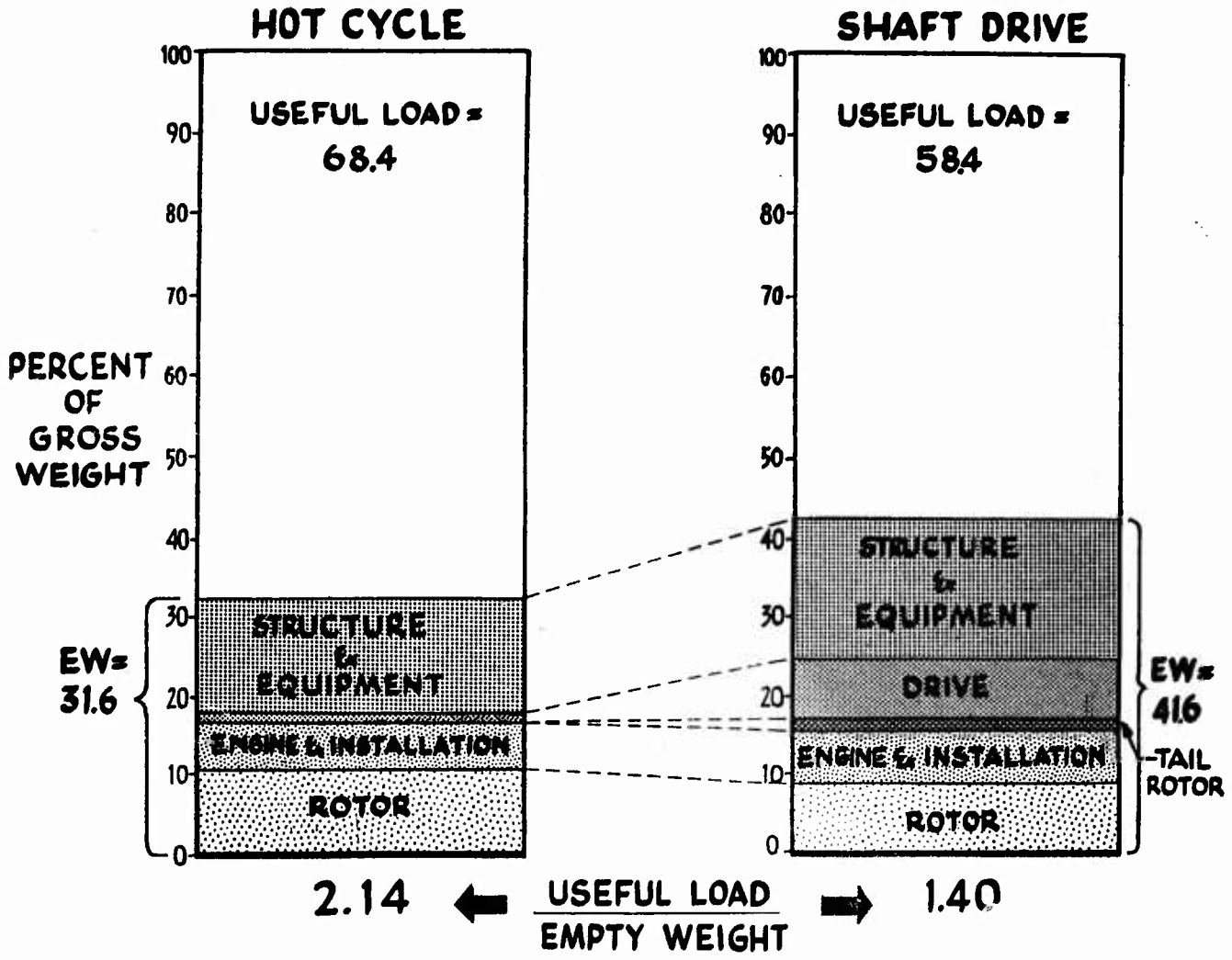

Figure 4.2-2 Weight Comparison of Hot Cycle and Shaft Driven Crane Helicopters

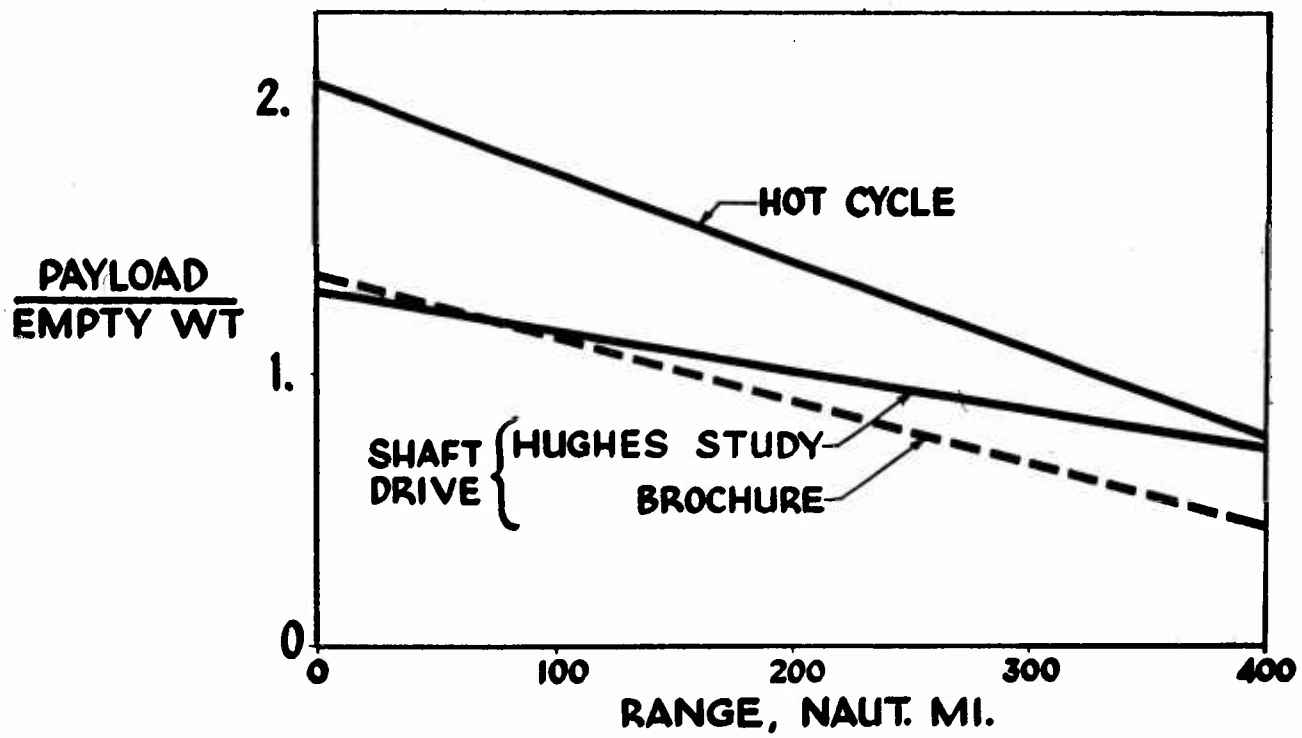

Figure 4.2-3 Payload Comparison of Hot Cycle and Shaft Driven Crane Helicopters

utility of this aircraft in combat. Figure 4.2-5 illustrates the propulsion system for such a VTOL aircraft. Two T64 gas generators power the vehicle. For vertical movement the exhaust gases are ducted to the rotor as in the Hot Cycle crane helicopter. For high speed horizontal flight the gases are ducted to the tip turbines of two horizontal thrust fans. These fans are a scaled down version of the lift fan under development by General Electric for the Army. With these ducted fans providing the propulsive thrust, the rotor autorotates and most of the lift is carried by a fixed wing. Yaw control during hovering is provided by a variable jet at the tail. Extreme mechanical simplicity of this proposed system is very obvious with the complete lack of gear boxes and shafting. The outstanding features of this Hot Cycle compound helicopter are:

a. Simplicity

b. Low Empty Weight

c. High Performance

d. Outstanding Economy

e. Low Downwash

f. Versatility

For a detailed discussion of each of these factors, refer to Reference 1.

Figure 4.2-6 presents an over-all weight comparison between Hot Cycle and shaft driven compound helicopters. As with the cranes the ratio of useful load to empty weight is considerable greater for the Hot Cycle powered vehicle. The outstanding payload performance of the Hot Cycle Compound Helicopter is

presented in Table 4.2-1 below, which lists payload for 4 different type missions. Payload for a single mission in comparison with that of a shaft driven compound helicopter is shown in Figure 4.2-7. Initial take-off is STOL but hovering is required at the midpoint of the mission. It can be seen that the ratio of payload to empty weight for the Hot Cycle Compound Helicopter is approximately 70% higher than its nearest competitor. This superiority is primarily due to the low empty weight of the Hot Cycle Compound Helicopter which, in turn, is due to the very low propulsion system weight.

TABLE 4.2-1

HOT CYCLE COMPOUND MISSION CAPABILITIES

	Payload (Lb.)	Radius (N. Miles)
STOL	9,800	500
(Hover at Midpoint)	12,300	200
VTOL	9,000	300
Crane	14,000	25

Figure 4.2-4 Hughes Hot Cycle VTOL Transport in Combat Operation

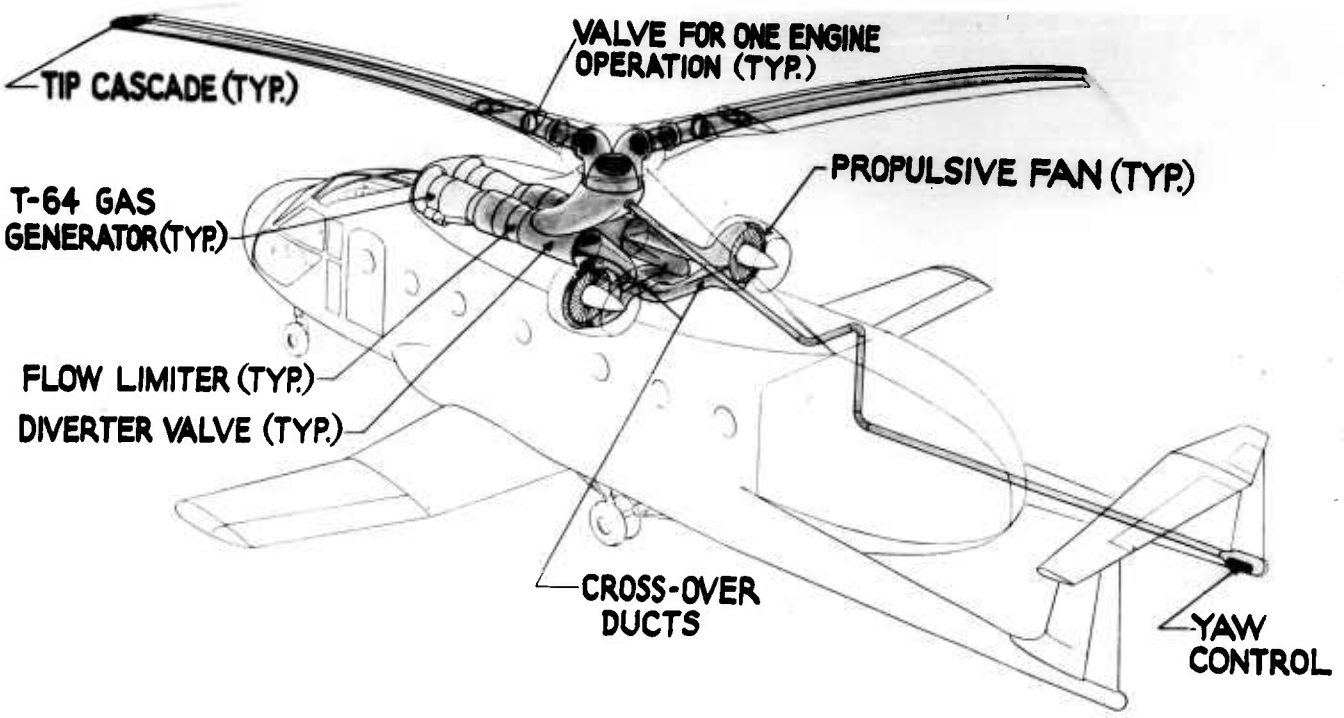

Figure 4.2-5 Propulsion System Schematic - Hot Cycle Compound Helicopter

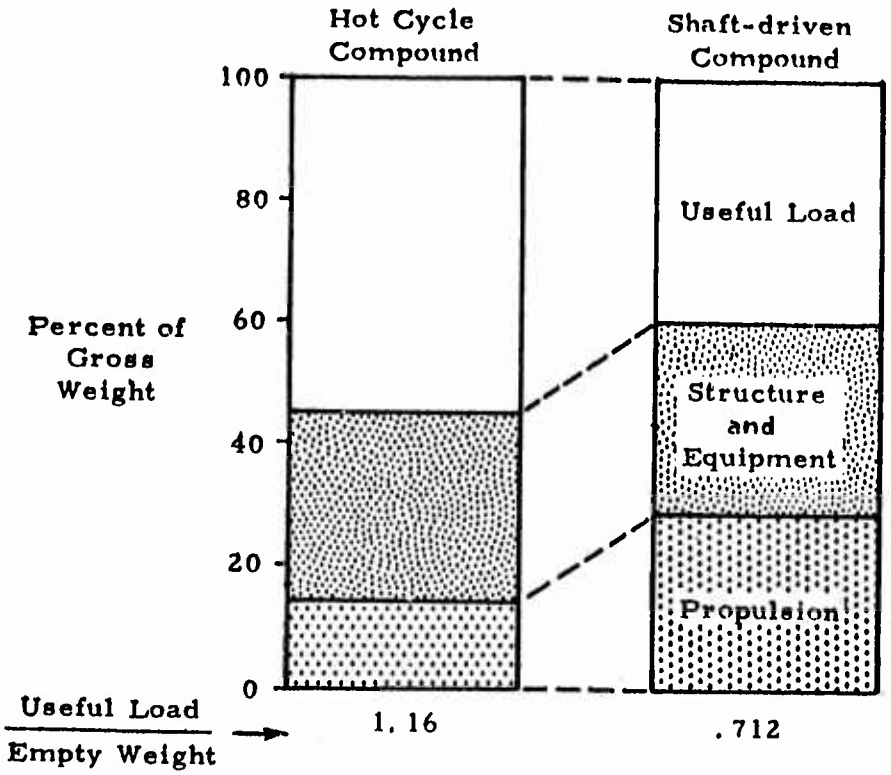

Figure 4.2-6. Weight Comparison of Hot Cycle and Shaft Driven Compound Helicopters.

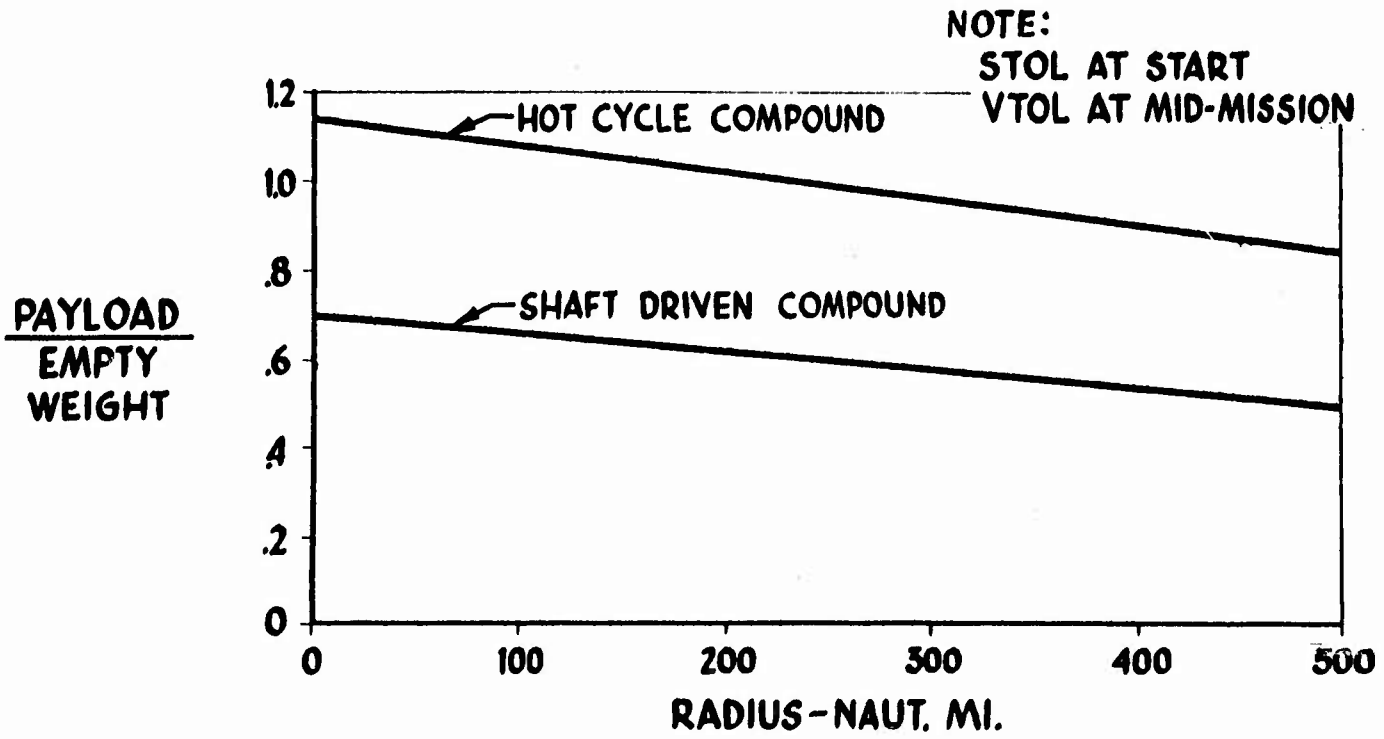

Figure 4.2-7 Payload Comparison for Compound Helicopters

4. 3 DEVELOPMENT PROGRAM

As noted in the introduction to Section 4, the contract specified that a rotor be designed, fabricated, and tested to prove feasibility of a Hot Cycle structure and to evaluate performance of the system. The necessity of carrying 1200°F degree gases through the rotor required use of a high temperature duct material to contain the full turbojet temperature with acceptable weight, and a unique blade structural design to limit fatigue in hot parts, to provide for thermal expansion, and to be dynamically suitable. The program therefore resulted in advances in the state of the art in regard to large non-lubricated seals and bearings, brazing and spot welding processes, and the rolling of previously unavailable lengths of Titanium Alloy. Features of this rotor will be discussed in detail in Section 5.

A design tool, other than a very elaborate layout on paper, was required to permit study of the kinematics of the tilting hub, coning blade and fixed duct combination. Such a tool consisted of a wood mock-up of one-third of the hub and one blade root from the strap attachment inboard. Only basic structure was duplicated, and secondary items were added only when the location was critical for clearance. This mock-up reduced the over-all cost and elapsed time for the program inasmuch as it narrowed the paper studies to a few spot layouts and minimized possibilities of later changes in hardware which might have resulted from an inadvertent error or omission during the layout study. Photographs of the mock-up are shown in Figures 4. 3-1 and 4. 3-2.

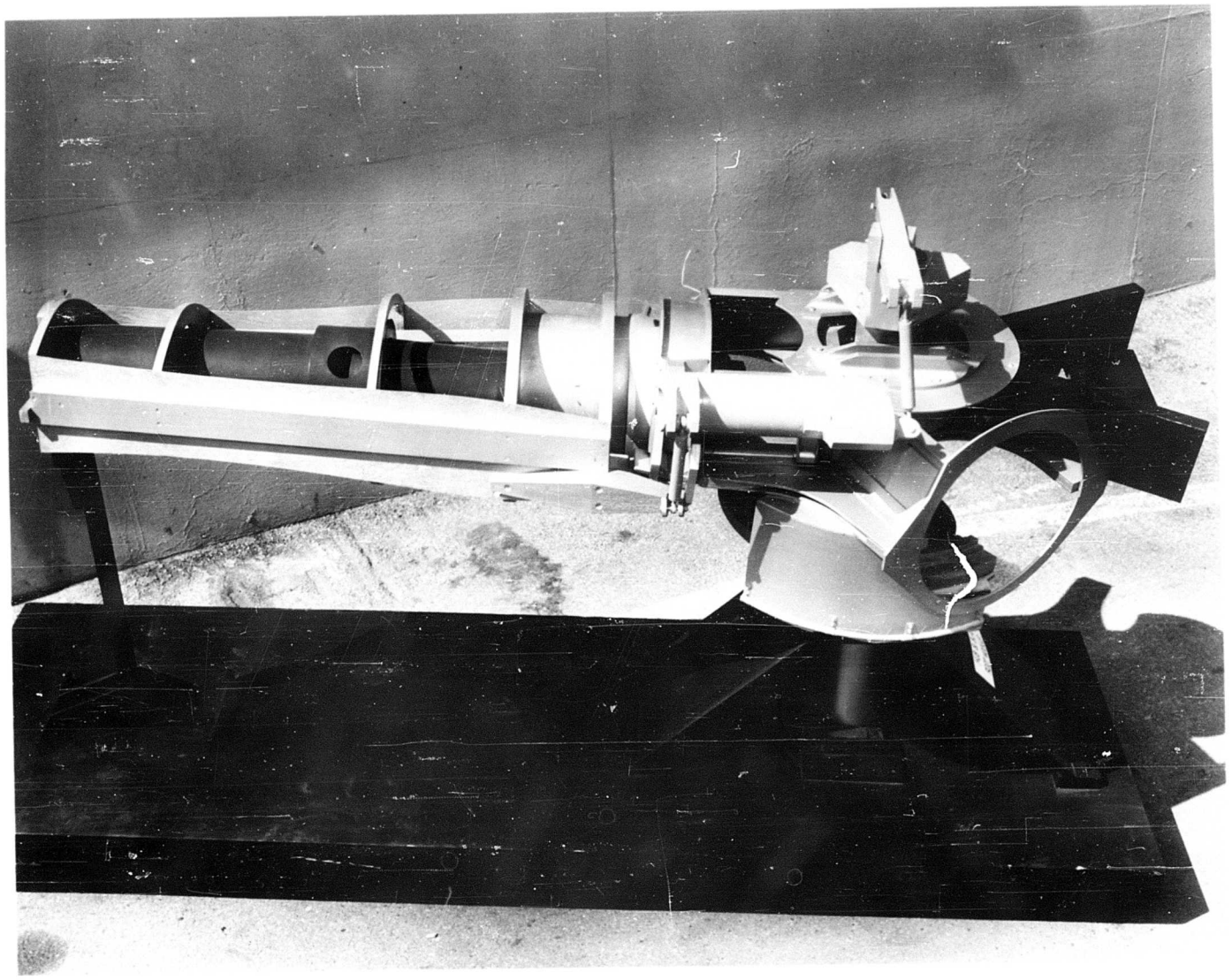

Figure 4. 3-1 Partial Mock-up of Hub and Blade Root

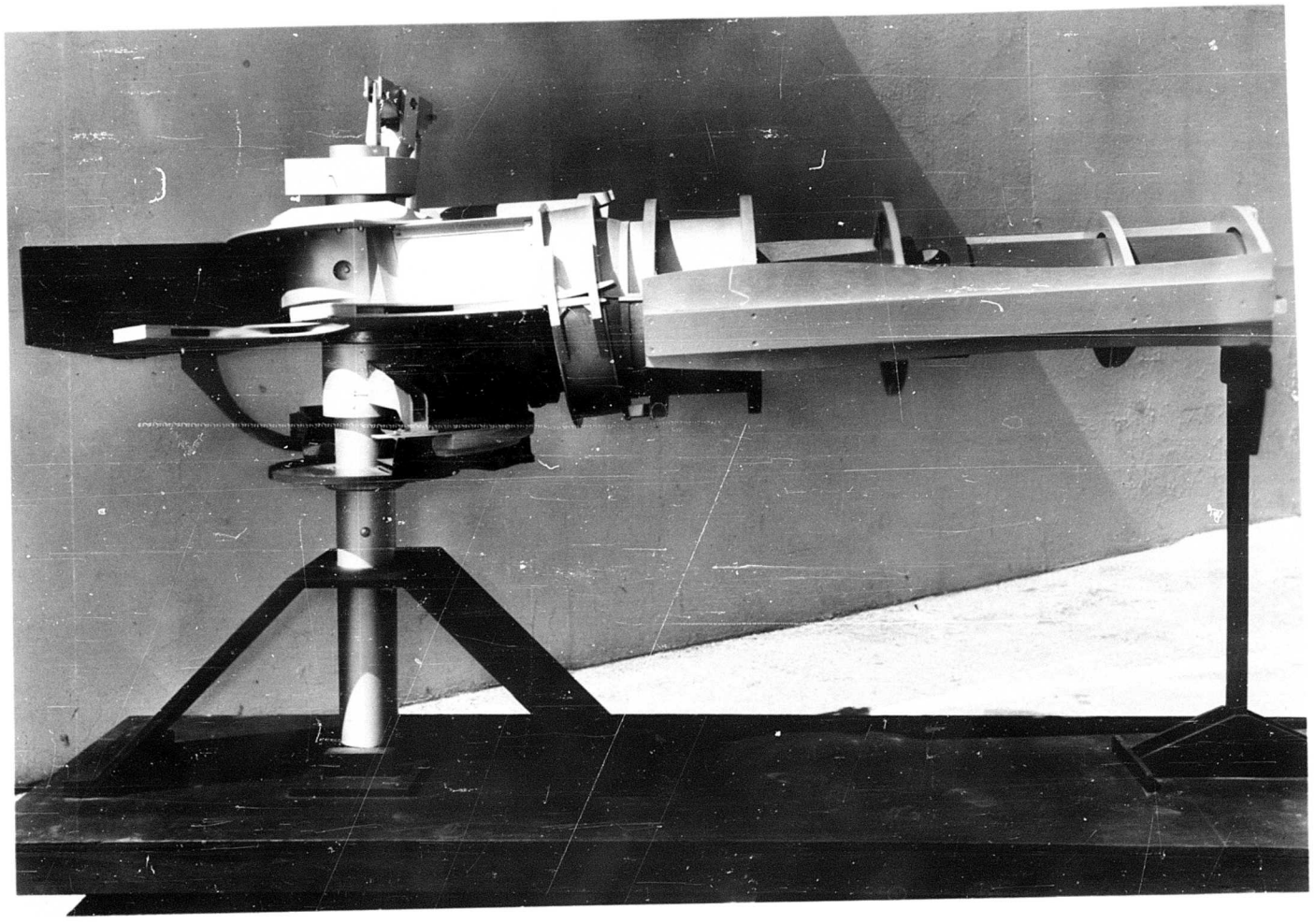

Figure 4. 3-2 Partial Mock-up of Hub and Blade Root

4.4 TESTS

Development of a unique rotor structure involved tests both to define the structure and configuration, and to evaluate the design chosen. The first group included development tests of potentially useful materials, flow distribution studies, and the blade screening fatigue test. The second group included tests of seals and bearings, a tether test to determine tip nozzle coefficients and blade duct losses, a fatigue test of a full scale blade specimen, and a whirl test of the complete rotor.

4.4.1 Material Tests

Material tests, static and fatigue at ambient or operating temperatures as required, were conducted on electroformed pure nickel, 6Al-4v Titanium Alloy, Armalon[1], Fabroid[2], RTV601 Silastic[3], Rene' 41 nickel alloy, and on brazed and pokewelded 17-7 PH corrosion resistant steel. A flow distribution study was made on a plaster mock-up of the hub upper tri-duct in order to determine if the contour established required changes of shape or the installation of vanes. These tests are discussed in detail in the reports listed under Item 6C of Appendix B.

---

[1] Armalon is a teflon impregnated glass cloth fabric manufactured by E. I. duPont de Nemours and Company, Incorporated, Wilmington 98, Delaware.

[2] Fabroid is a fabric woven of teflon monofilament and fiberglas thread, manufactured by Micro-Precision Division of Micromatic Hone Company, Los Angeles 32, California.

[3] RTV601 Silastic is a high temperature silicone potting compound manufactured by Dow Corning Corporation, Midland, Michigan.

The major test made to define the structure is that labeled "Screening Fatigue Test". Development of the fabrication technique for the blade segments had previously resulted in five available single duct segments, each fabricated by varying methods and/or more than one source. In order to aid in finalization of the fabrication technique, the method of attachment of the segment to the spar and other significant design details, these 5 segments were mounted on dummy spars and fatigue tested for over 6,000,000 cycles and over 400 equivalent flight hours. The specimen is shown in Figure 4.4-1. A complete resume of this test is given in Report 285-9-5.

4.4.2 Tests to Evaluate the Design

Component tests to evaluate the design prior to whirl test included life tests of the feathering-flapping bearing (see Figure 4.4-2) and the articulate duct outboard seal (see Figure 4.4-3). Discussions of these tests are contained in Report 285-9-8.

4.4.2.1 Tether Test

Upon installation of the rotor on the tower (shown in the Frontispiece), a test was conducted with the rotor tethered. This test was to determine tip thrust, duct pressure loss, and tip nozzle coefficients, as well as the characteristics of the hub and blade root cooling system. Flow was allowed in one blade only, by sealing the remaining two. A hand directed water spray cooling system was utilized to reduce external blade temperatures. The test blade was attached to a gin pole by a cable in series with a tension load cell. Calibrated

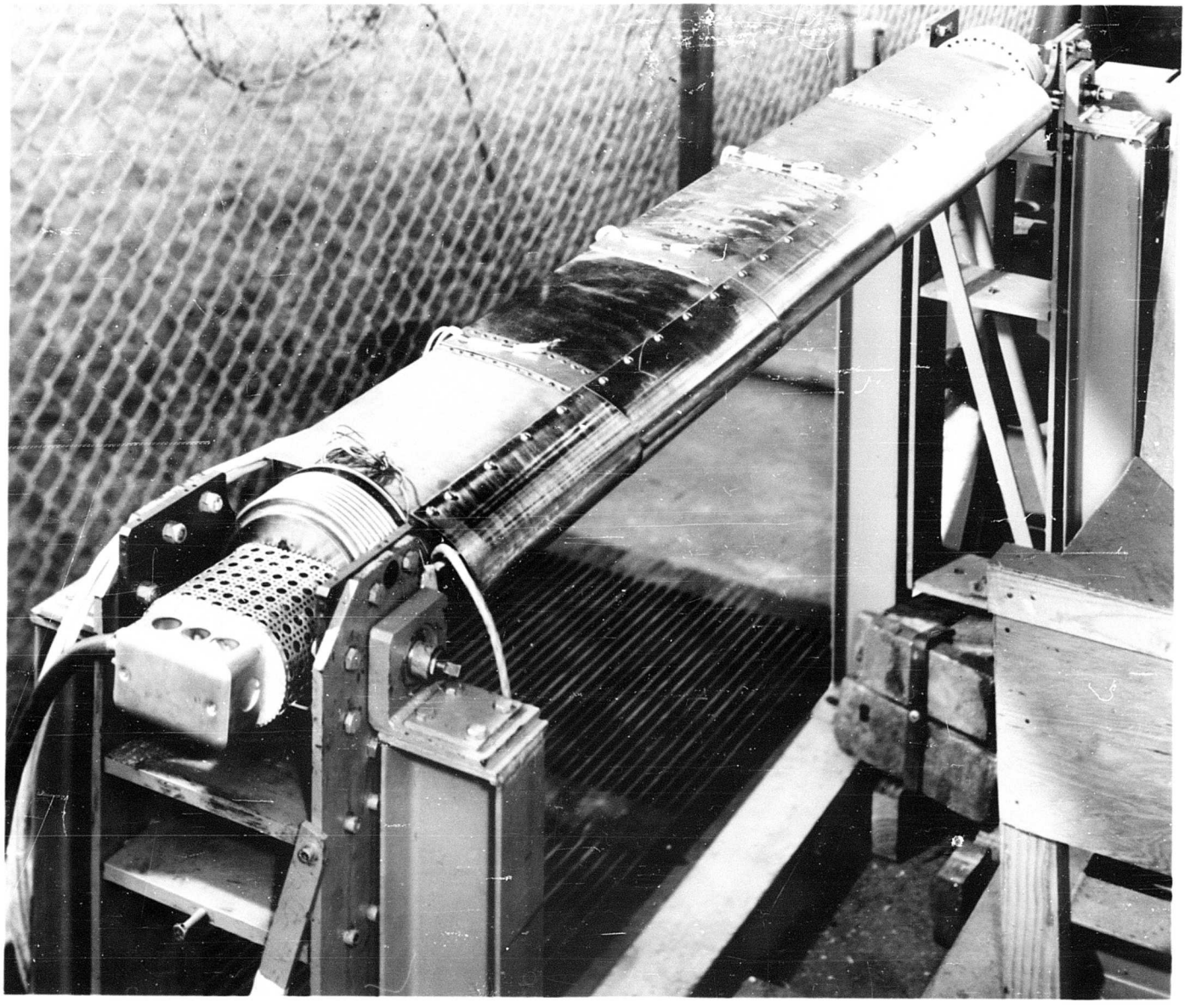

Figure 4.4-1 Screening Fatigue Test Specimen in Test Jig

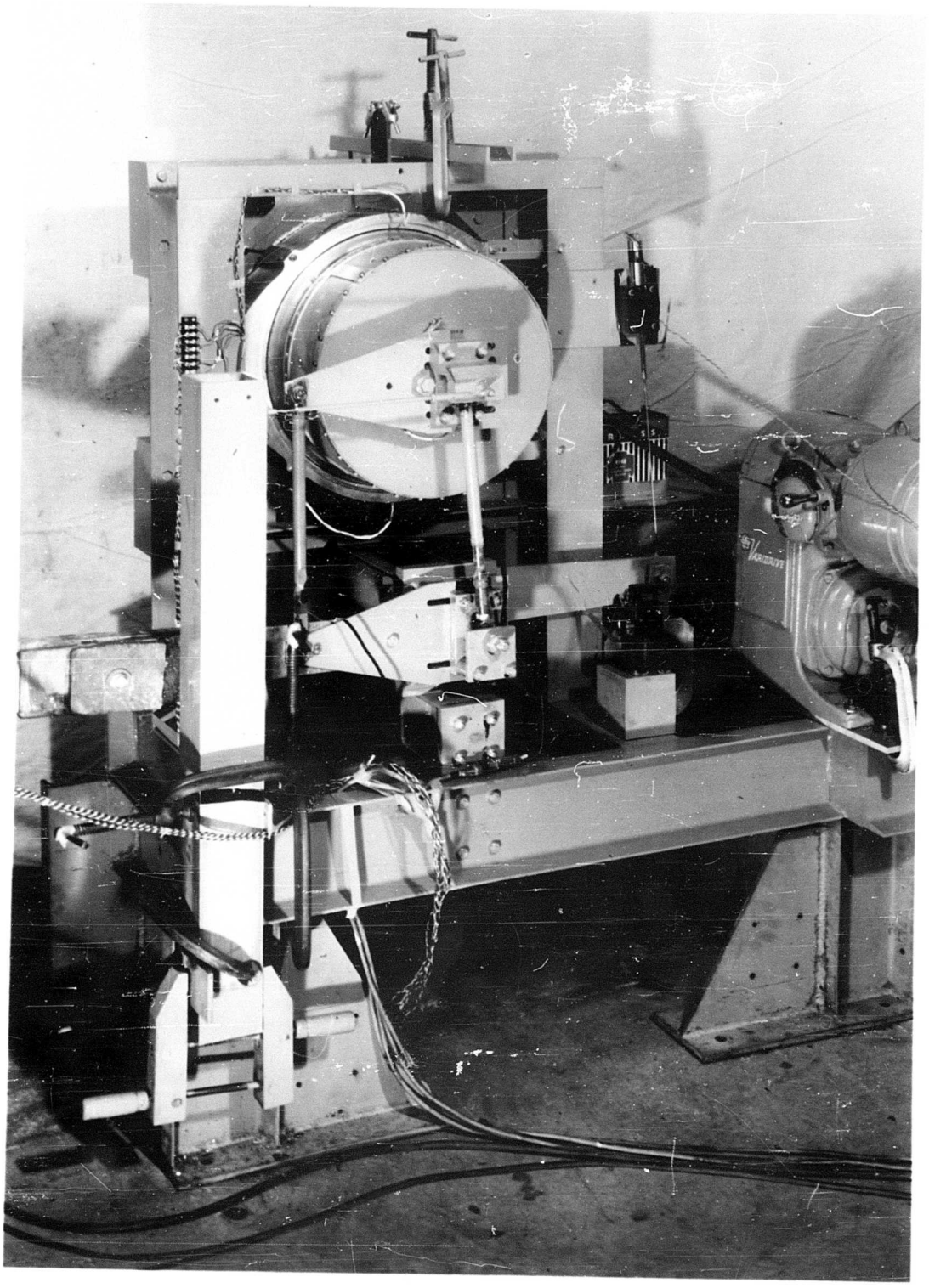

Figure 4.4-2 Blade Feathering-Flapping Bearing Test

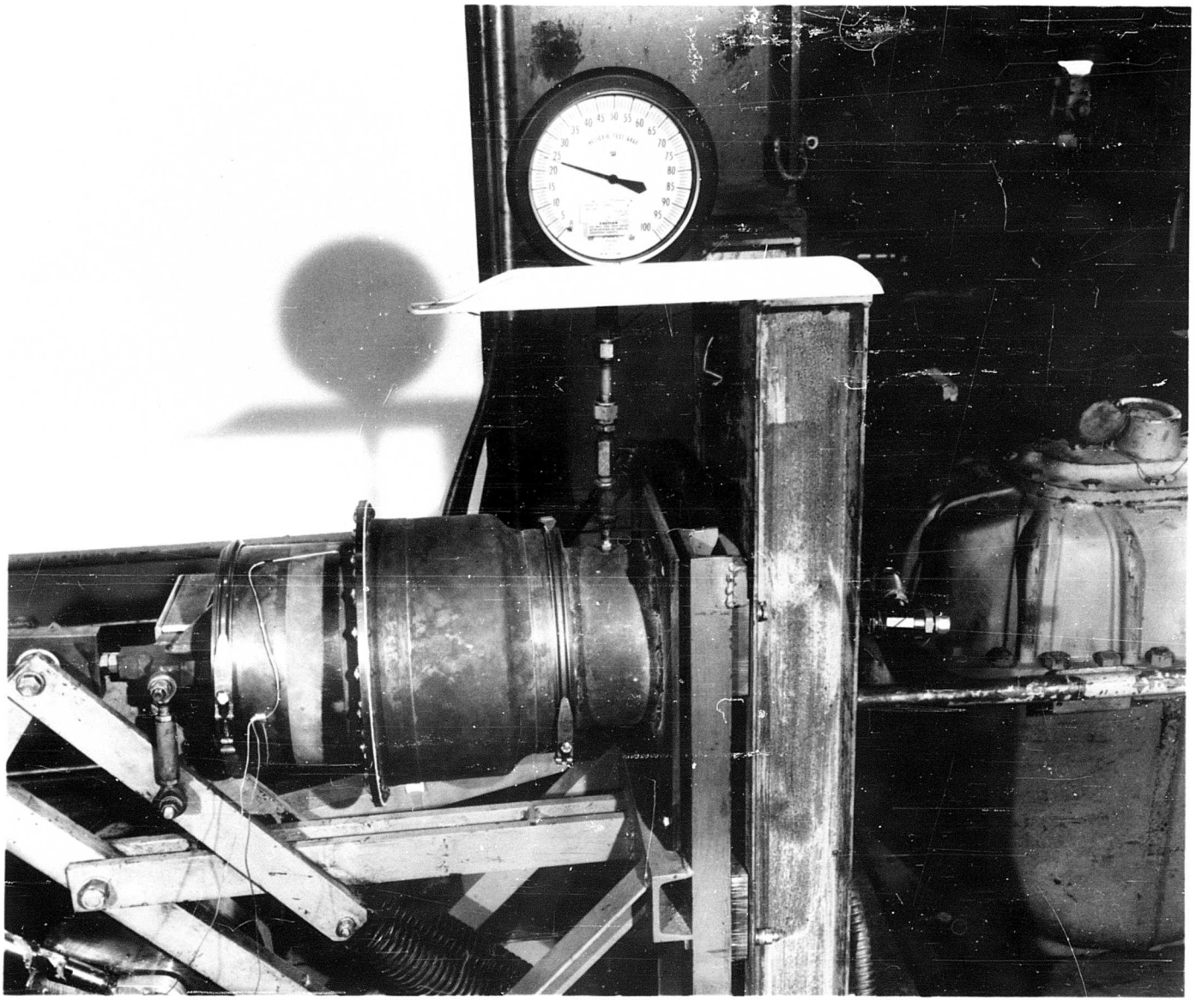

Figure 4.4-3 Duct Outboard Seal Test (Heat Retention Blanket Removed)

stresses in the load cell then permitted a direct measurement of the thrust of one blade. In general, agreement between predicted and measured valued of duct losses, nozzle coefficients, and tip thrust was realized. Most significant, the tip nozzle effective velocity coefficient, which is directly proportional to tip thrust, was measured to be 0.98, 2.5% better than predicted. Details of this test are given in Report 285-9-7.

4.4.2.2 Full Scale Fatigue Test

Another major test to evaluate the design was that of the fatigue test of a full scale blade specimen. This specimen included all of the blade root and 5' of constant blade section. The test blade assembly was mounted in the test fixture as a hinged beam with axial tension simulating centrifugal force. The fixture consisted of an I-beam base 40 ft. long which supported load reaction structures on each end. Figure 4.4-4 is a photograph of the specimen mounted in the test fixture. Flapwise bending was produced by excitation in the flapwise direction utilizing a 5 HP varidrive eccentric of adjustable stroke located at the approximate center of the tension beam. Torsion was induced by a 4-bar linkage arrangement at this same station. Internal heat and external cooling closely simulating predicted flight temperatures were applied while the specimen was excited at calculated weighted fatigue deflections.

The initial test showed that a reinforcement of the blade rear spar was necessary where this spar bends at approximately station 73. Following the installation of this reinforcement, the test program was completed with

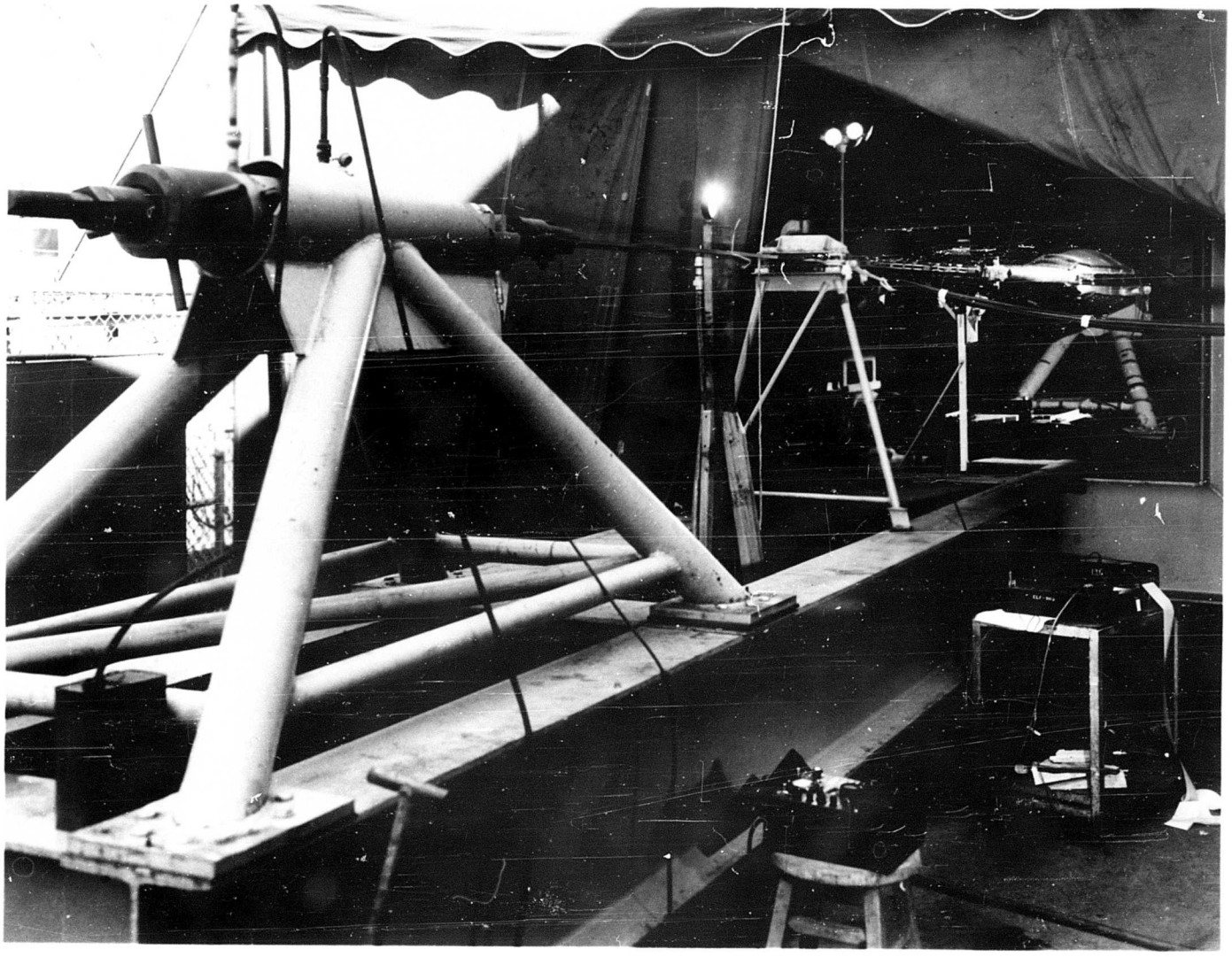

Figure 4.4-4 Blade Full Scale Fatigue Test Setup, View Looking Inboard At Leading Edge

no further requirements for modifications. A total of 2,000,000 cycles was accumulated. A complete discussion of this test is contained in Report 285-9-8.

4.4.3 Whirl Test

The whirl test was the climax in the development of the Hot Cycle system. Testing was conducted on the Hughes Tool Company -- Aircraft Division site shown on Figure 4.4-5. The tower is approximately 30 feet high, is built of large-diameter steel tubes, and is secured at its base to a reinforced concrete pad. A hydraulically operated permanent work platform, long enough to service an entire blade, is attached to the tower.

Rotor power is supplied by a Pratt and Whitney J57 engine located at the base of the tower with intake and excess-exhaust noise suppressors. Approximately one-third of the J57 exhaust flow was used to power the rotor and the surplus flow was exhausted directly to the atmosphere. Control of the flow directed to the rotor was obtained by a butterfly valve located in the vertical duct, while a second butterfly valve located in the overflow line was adjusted to keep the engine back pressure in accordance with standard tail pipe conditions. Accessories such as engine starter, power generator, fuel trailer, lubricating oil pump and air compressor are grouped around the tower as close to the point of application as applicable, as shown in Figures 4.4-5 and 4.4-6.

Control of the rotor and all equipment was performed remotely from a

van located 72 feet from the tower in such a manner as to give a clear view of the tower and surrounding area. Housed within the van are rotor controls, engine controls, and instrumentation equipment. Interior views of the van showing the pilot's rotor and engineer's stations, and the temperature, pressure and strain recording instrumentation are given in Figures 4.4-7 and 4.4-8 respectively.

The program was, in general, conducted in accordance with Report 285-8-3SR, "Proposed Whirl Tower Program", dated November 1961. A summary of hours of test conducted at various temperature levels is given in Table 4.4-1. Also shown in the table are the exhaust temperatures of both the current and advanced versions (ST129) of the T64 gas generator. It can be seen that a total of 5.5 hours were run at temperatures of 1200° to 1275°F, which is equivalent to the Take-Off Rating (5 minute rating) of the ST129. A total of 14.8 hours were run at engine discharge temperatures of 1100° to 1200°F which is equivalent to the Take-Off Rating of the standard T64 and the Military Rating of both the current and ST129 versions of the T64.

A comparison of the hours run at Take-Off and Military power temperature levels with the hours of running required by Military Specifications is given in Table 4.4-2. Inasmuch as the Hot Cycle rotor is both a rotor and a portion of an engine, both rotor and engine 50 hour specifications are presented.

It can be seen that the hours at the Take-Off temperature level are approximately twice those called for in the Specifications, while the hours at the Military temperature level are 3 to 5 times the values in the Military Specifications. Also noted is the number of power transients performed during the whirl test program compared to those called for in the Military Specifications, showing that the number of transients performed is approximately equal to the average of the two specifications.

In addition to the power transients noted above, the tests included a considerable number of control transients; that is, rapid movements of the cyclic and collective controls. These were performed in various combinations to explore potential resonances and natural damping.

The whirl test specimen is discussed in Section 5 following, while the whirl test results are summarized in Section 6.

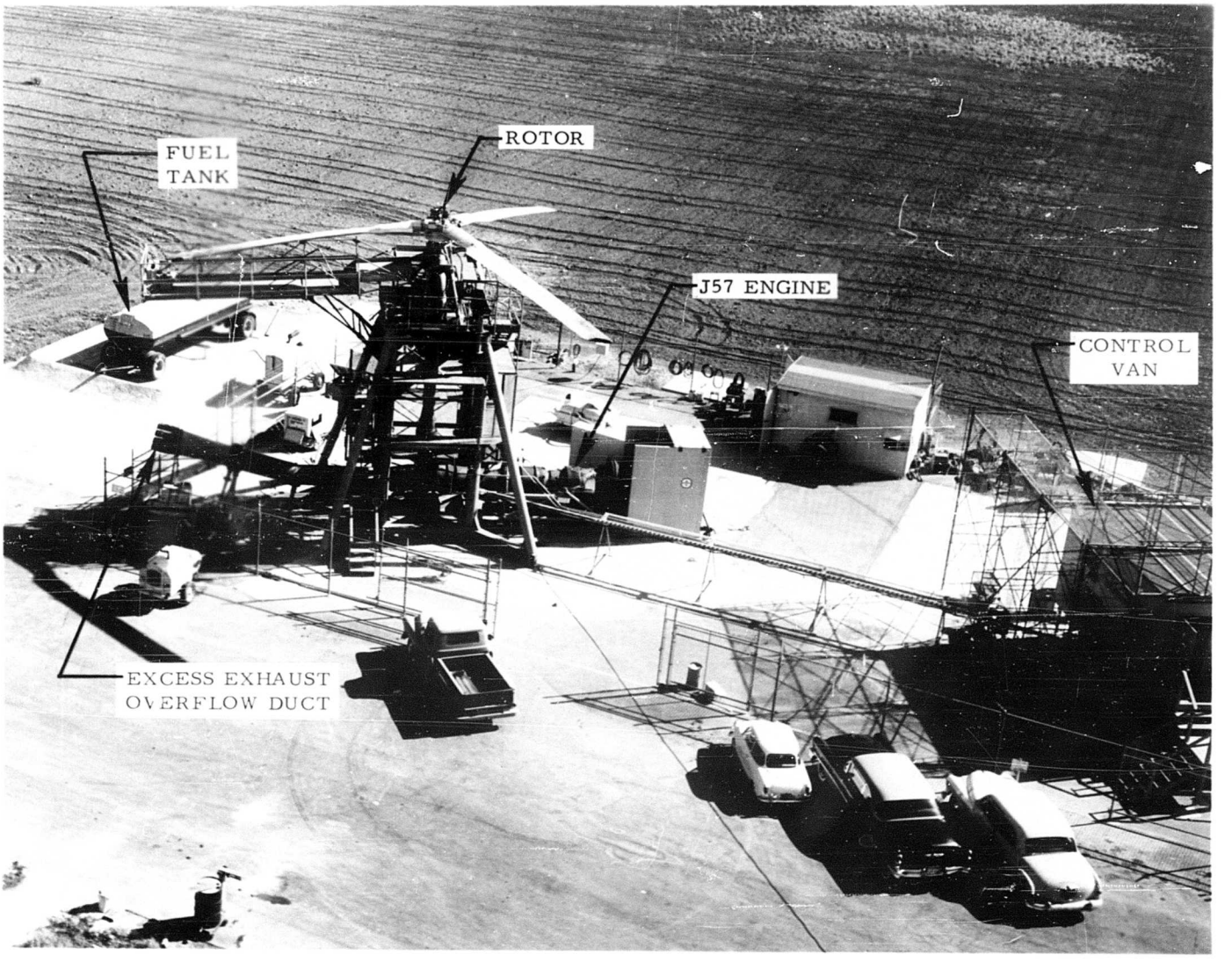

Figure 4.4-5 Whirl Test Site Area

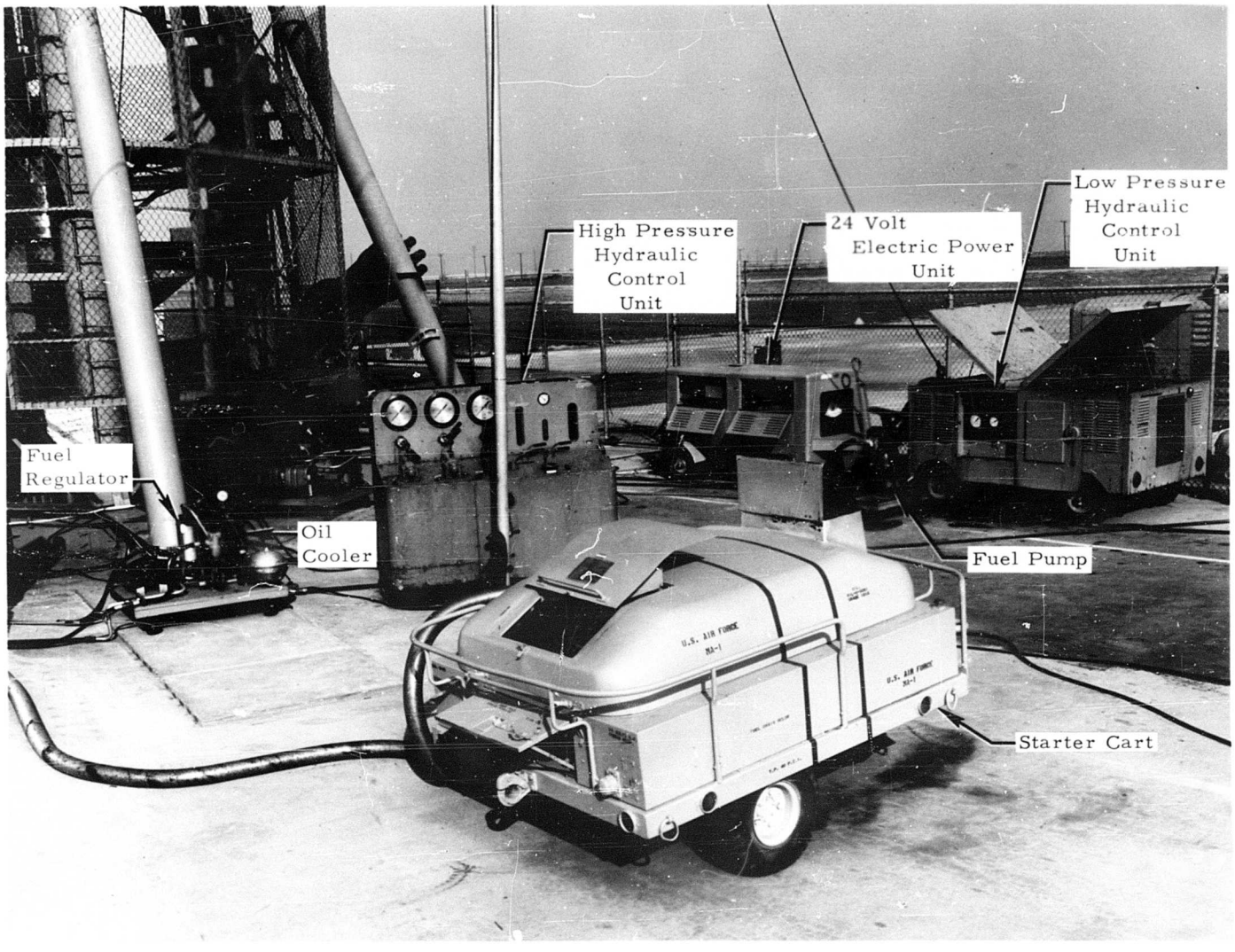

Figure 4.4-6 Whirl Site Support Equipment

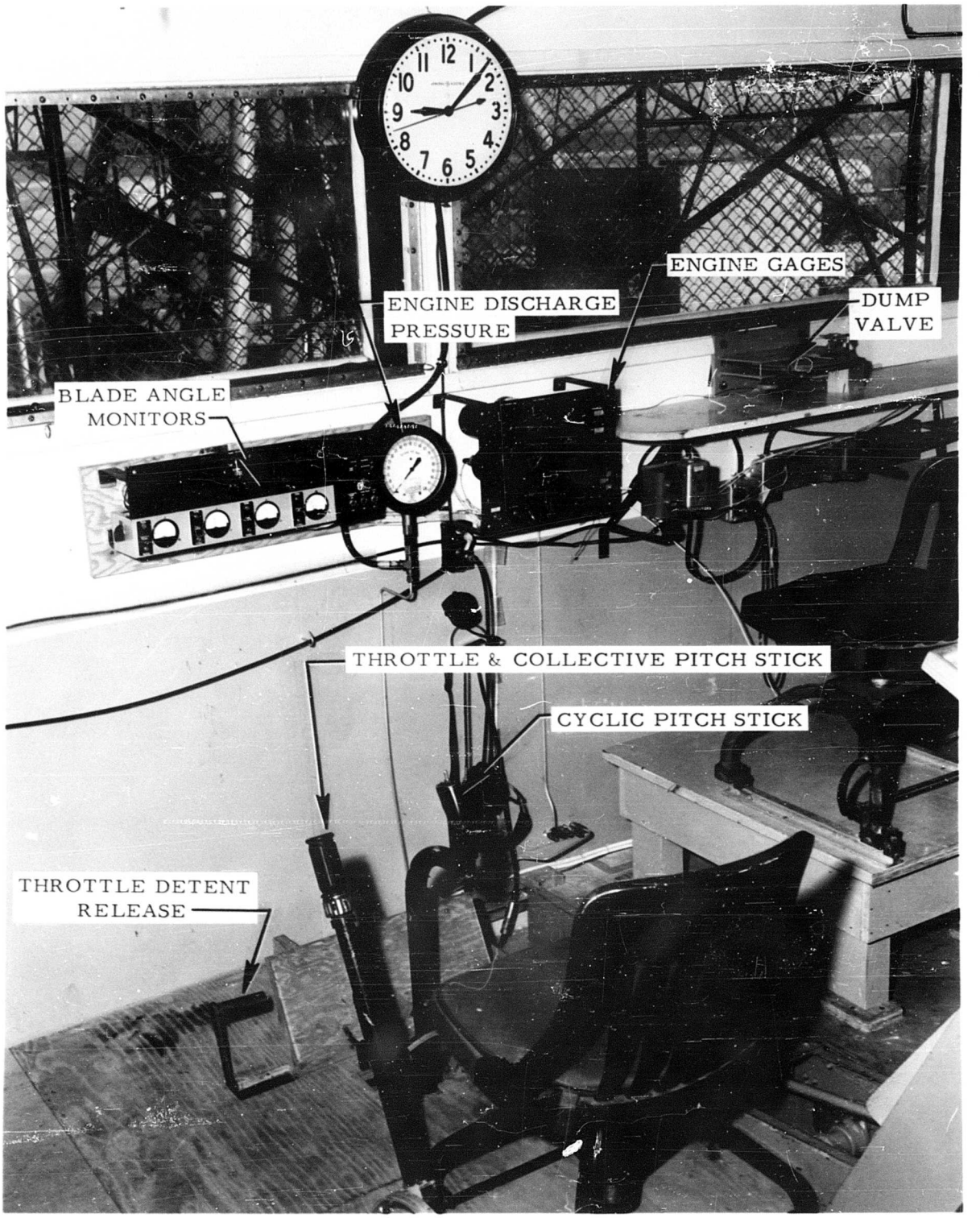

Figure 4. 4-7 Internal View of Control Van; Rotor and Engine Controls

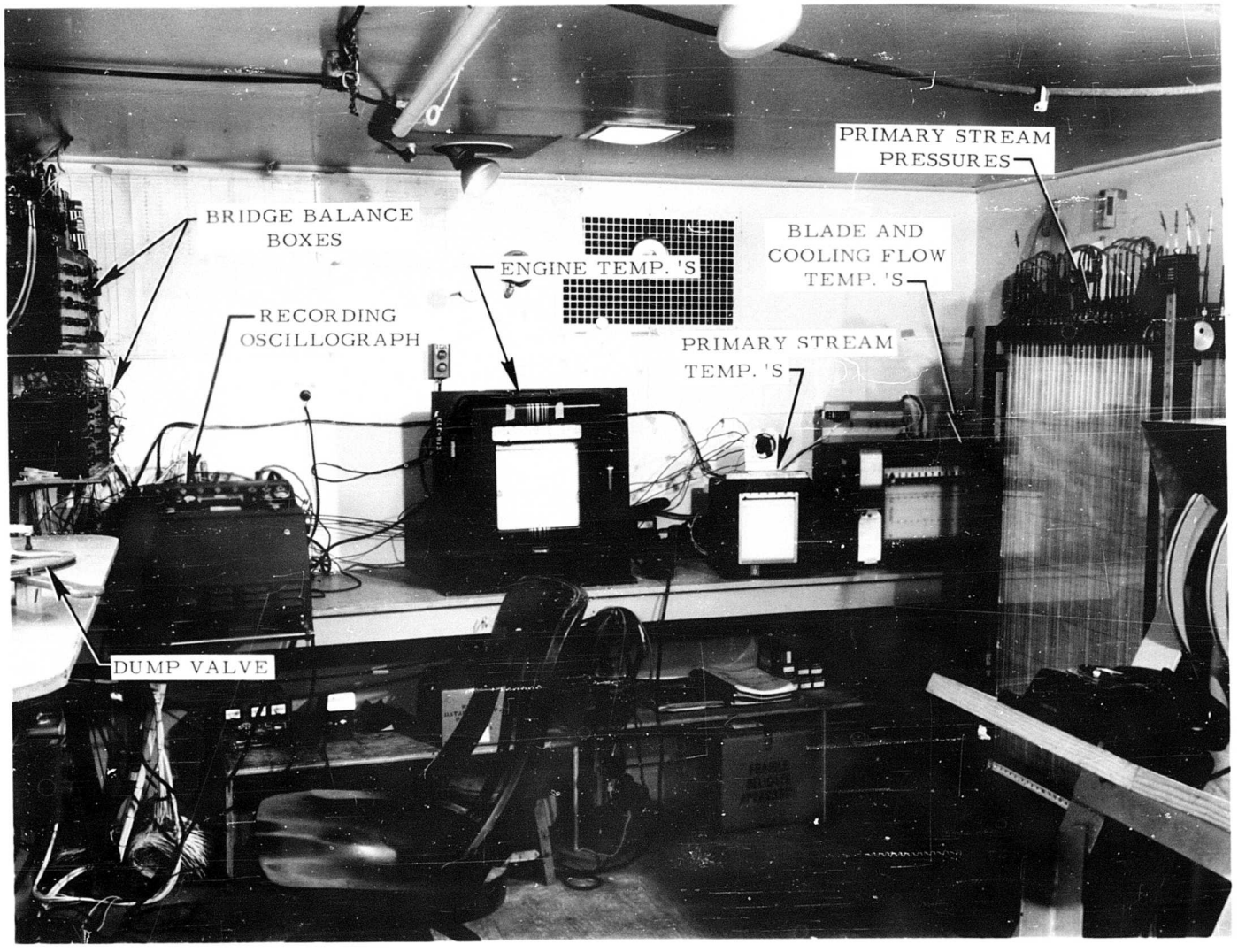

Figure 4.4-8 Internal View of Control Van Showing Temperature, Pressure and Strain Recording Instruments

TABLE 4.4-1

HOT CYCLE ROTOR WHIRL TEST

TEMPERATURE LOG

T_T °F 7 Engine Discharge	Equivalent T-64 Engine Rating	Time at Temperature		
		0-35 Hours Whirl Test	35-60 Hours Whirl Test (No Change of Components)	Total
1200-1275	Take-off, ST129: 1225	3.2	2.3	5.5
1100-1200	Military, ST129: 1180 Take-off, Std: 1180 Military, Std: 1150	6.9	7.9	14.8
900-110	NRP, Std. and ST129: 1100 75% NRP, Std. and ST129: 1010	5.8	2.6	8.4
900		19.1	12.2	31.3
TOTALS		35.0	25.0	60.0

TABLE 4.4-2

COMPARISON OF WHIRL TEST WITH

MILITARY SPECIFICATIONS

Power Condition	Hot Cycle Whirl Test	MIL T 8679 50 Hour Rotor Ground Endurance	MIL E 8597 Engine PFRT
Take-Off (hours)	5.5	2.5	2.7
Military (hours)	14.8	2.5	4.0
Number of Transients	37.0	30.0	48.0

5. KEY ASPECTS OF ROTOR DESIGN

5.1 DESIGN PHILOSOPHY

Experimental programs such as the one under consideration are sometimes allowed to become interlocked with other experimental and perhaps secondary programs. Thus, if any one part of the over-all program flounders or fails, solutions for the basic problem may not reach fruition. For this reason it was decided at the outset that the Hot Cycle Program should not be dependent on materials, processes, or equipment not yet matured, the development of which might require considerable work on the part of others or might ultimately reach a stalemate. The rotor evolved therefore relied on only a reasonable advance in existing production technologies for its realization. It did not require the development of entirely new fabrication methods or the building of new production and/or processing equipment.

As a result of the above philosophy the rotor blade consists of a relatively few parts duplicated many times. These are fabricated and assembled by equipment now in existance. By the same reasoning, the hub and control system structural members are conventional. As a result, this rotor could be placed in production with minimum cost and delay.

This section of the report covers the detail structural and mechanical design of the Hot Cycle Rotor System. The design was initiated by an analysis of temperatures, loads, and control movements which are reported in Appendix 1

of Report 285-12. The System designed was based on a helicopter of 15, 300 pounds gross weight with a load factor of 2. 5, and was made capable of accepting the full output of two General Electric T64 eingines. As shown schematically on the perspective sketch in Figure 5. 1-1, the rotor consists of a free-floating hub and three coning blades mounted on a shaft supported by an upper radial bearing and a lower thrust bearing. These bearings are positioned above the whirl tower (or fuselage) by a steel tubular truss. Photographs of the completed rotor are presented in Figures 4. 4-5 and 5. 1-2. Complete accounts of the rotor design and fabrication are contained in Reports 285-12 and 285-15.

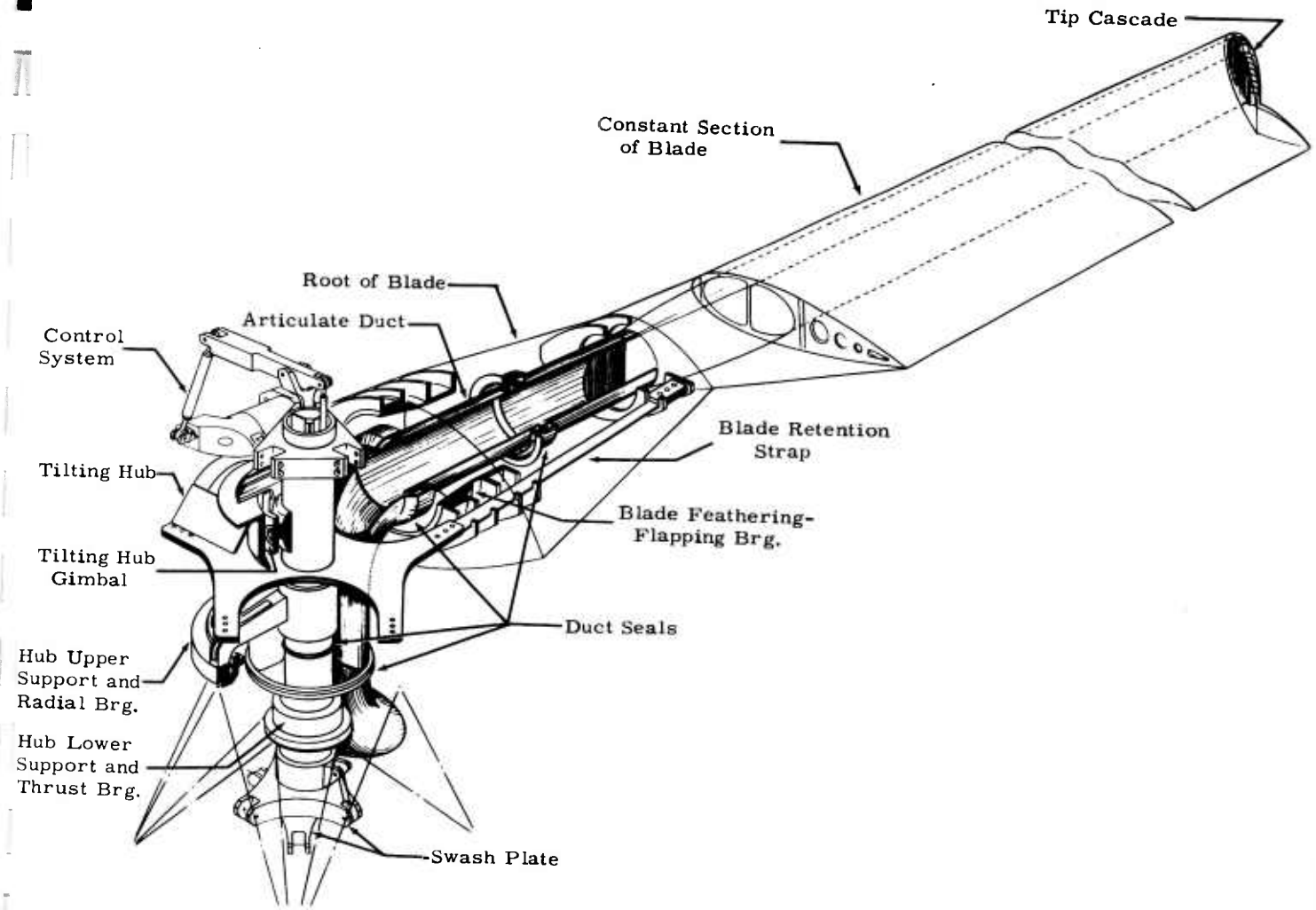

Figure 5.1-1 Perspective Sketch of Hot Cycle Rotor

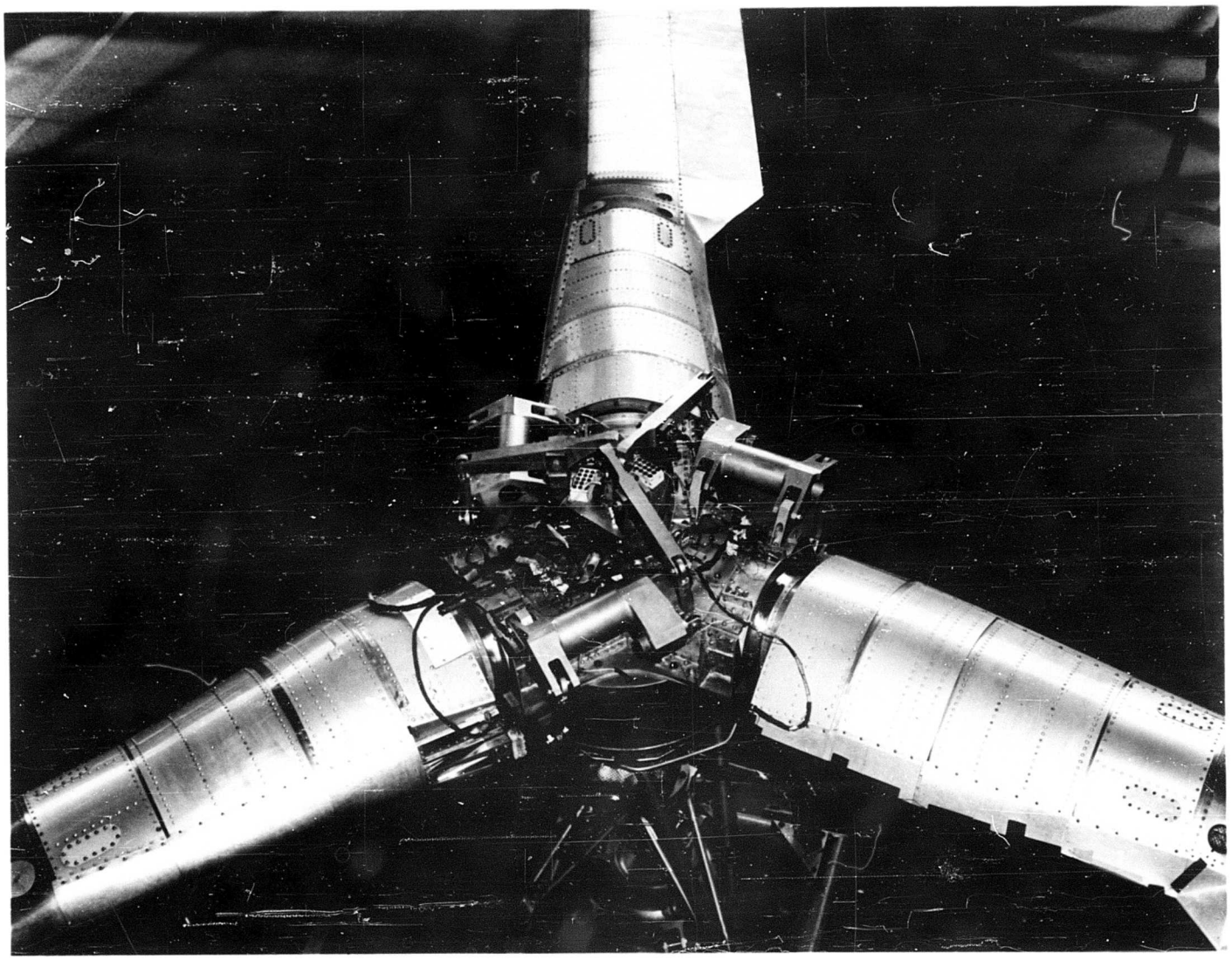

Figure 5. 1-2 Hot Cycle Rotor Assembly

5.2 BLADE SIGNIFICANT DETAILS (Drawing 285-0100, Figure 5.2-1)

5.2.1 The blade design incorporates two machined titanium alloy spars that comprise the only continuous members running from the blade root to the tip. The spars are separated fifteen inches chordwise by eighteen identical sheet-metal segments 12.50 inches long, made up of two ducts contained within nine ribs and an outer cover. A typical cross-section is shown on Figure 5.2-2. The segments are bolted to the spars and are joined together by bellows-type flexible couplings riveted to the outer cover. The ducts and skins of adjacent segments are slip-jointed. An exploded view of the blade exposing the typical breakdown into easily handled components is presented in Figure 5.2-3.

In this structural arrangement the spars are the only members that react blade bending and centrifugal loads. Torsional and chordwise shear loads are carried by the assembly of segments. Advantages of this arrangement are:

(a) The principal load carrying elements of the structure are insulated from the hot gas transfer system by a dead air space between the ducts and outer cover of the segments.

(b) Loads produced by thermal expansion differences between the segments and spars are minimized by the slip-jointed and flexibly-coupled assembly of the segments.

(c) Blade natural frequencies in bending can readily be kept within a safe range by control of the spar depth.

(d) Ground resonance is avoided by means of high chordwise bending stiffness resulting from the spar chordwise spacing, and by tuning of the blade by a change in area and/or modulus of the retention strap pack.

(e) Repair of punctured or otherwise damaged skins and ducts could be accomplished by replacing one or more of the interchangeable segment sections.

5.2.2 The front and rear spars are milled from flat-rolled bar stock of 6AL-4V titanium alloy, purchased in lengths sufficient to make the spars without splicing. It is believed that these are the longest bars of this material ever produced for a specific purpose.[1] To maintain the strength properties of the spars, they are air cooled during rotor operation by the inherent centrifugal pumping action of the rotor. A cooling tunnel is provided for the front spar by the leading edge cap, while the forward face of the trailing edge fairings completes a tunnel for the rear spar. A shim of low friction material is installed between the spars and blade segments to prevent fretting by avoiding contact of the surfaces.

5.2.3 The blade segments are identical sheet metal assemblies consisting of two ducts contained within nine ribs and an outer cover. Each segment is 12.50 inches spanwise and 15.00 inches chordwise. The ribs are die-formed with flanges matching the airfoil and duct contours. On the basis of experience gained from the Flexural Fatigue and Screening Test (refer to Section 4.5 of this report), the segments are assembled entirely by spot and

---

1. Furnished by Reactive Metals, Niles, Ohio.

seam welding. The extreme simplicity of the components which comprise a blade segment is apparent in Figure 5.2-4.

The ducts and the inner edges of the ribs are subjected to the full gas temperature of the power system. Rene' 41 alloy sheet was chosen for these parts because of its outstanding strength at high temperatures and excellent corrosion resistance. The ribs and ducts were formed and spot-welded together as a sub-assembly while in the solution treated condition to gain advantage of the superior joints obtained between Rene' 41 parts when welding is performed prior to age hardening. This sub-assembly was then age hardened for maximum strength and the segment was completed by spot welding outer covers of type 301 corrosion resistant steel sheet.

5.2.4 A bellows-type flexible coupling is riveted to the outer cover at each joint between segments of the rotor blade. This coupling performs a number of functions. It provides a pressure tight enclosure around the duct slip joints, it absorbs the thermal expansion and centrifugal load deflection differences between the segments and the spars, it transfers torsional and chordwise shear loads from segment to segment, and it incorporates a high degree of flexibility into the assembly of segments so that no appreciable blade bending loads are carried by any part of the structure other than the spars. This last feature is an important factor in controlling the stiffnesses of the blade to hold the natural frequencies within the required limits. The coupling is made up of two identical die stampings of Inconel X welded

together at the center line of the blade, the point of minimum cyclic stress. The welded assembly is heat treated and glass peened for maximum fatigue strength. A typical coupling is shown on Figure 5.2-3. As stated above, the coupling forms the joining member between segments, and is riveted to each by blind monel rivets, as shown in the sketch of Figure 5.2-5.

5.2.5 The tip cascade (Figure 5.2-6) is a welded assembly of contoured sheet metal parts, consisting of two elbow ducts faired into the ducts of the blade segments, four hollow airfoil-section turning vanes in each duct, and an outer cover faired into the skins of the blade. The leading and trailing edges of the assembly each incorporate a discharge orifice for the centrifugally pumped air used to cool the spars during rotor operation. The components of the cascade are joined by heliarc and spot welding.

Conventional production forming tools would be applicable to all elements of this design, but since only three cascade assemblies were needed for the whirl test, the detail parts were designed so that they could be shaped with hand tools and simple form blocks. Haynes Alloy 25 cobalt base sheet was chosen as material for the tip cascades because of its strength and dimensional stability at high temperatures, its high corrosion resistance and good welding properties.

5.2.6 Aft segments of the blade are conventional interchangeable sheet-metal assemblies consisting of four ribs, a single skin and a channel joined by adhesive bonding. The channel section also functions as one wall of a tunnel

for air flow to cool the blade rear spar during rotor operation. The ribs are identical flanged die-stampings. Skins of adjacent segments are slip jointed with the skin-laps designed so that any one segment may be removed or replaced by loosening the fastenings of not more than two adjacent segments. As true of the forward segments, the extremely small number of differently shaped pieces is obvious in Figure 5.2-7.

5.2.7 Blade root design, in general, consists of conventional structure of ribs, frames, webs and skins, bolted to the spars. As in the outer blade, the distinctive feature of the blade root design is that the spars are the only members reacting bending loads, and therefore the blade natural frequency is readily controlled by selection of spar stiffness. This effect was accomplished by dividing the sheet metal structure into seven sections joined together by six frames with hat-type cross sections that open and close as the blade deflects, without reacting the bending loads. Torsional and chordwise shear loads are carried by the flexible frames from section to section.

1

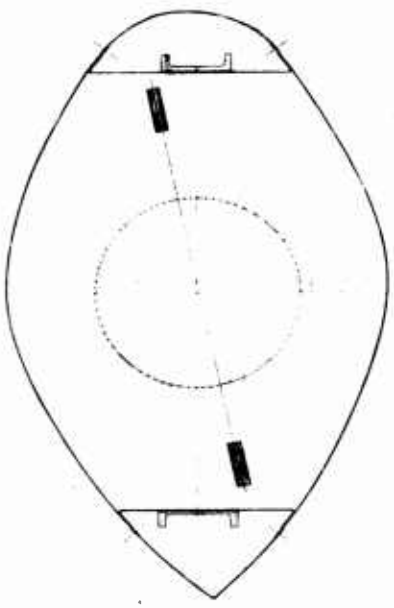

SECTION B B

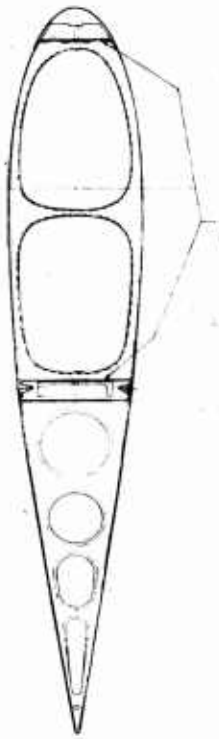

SECTION - A A

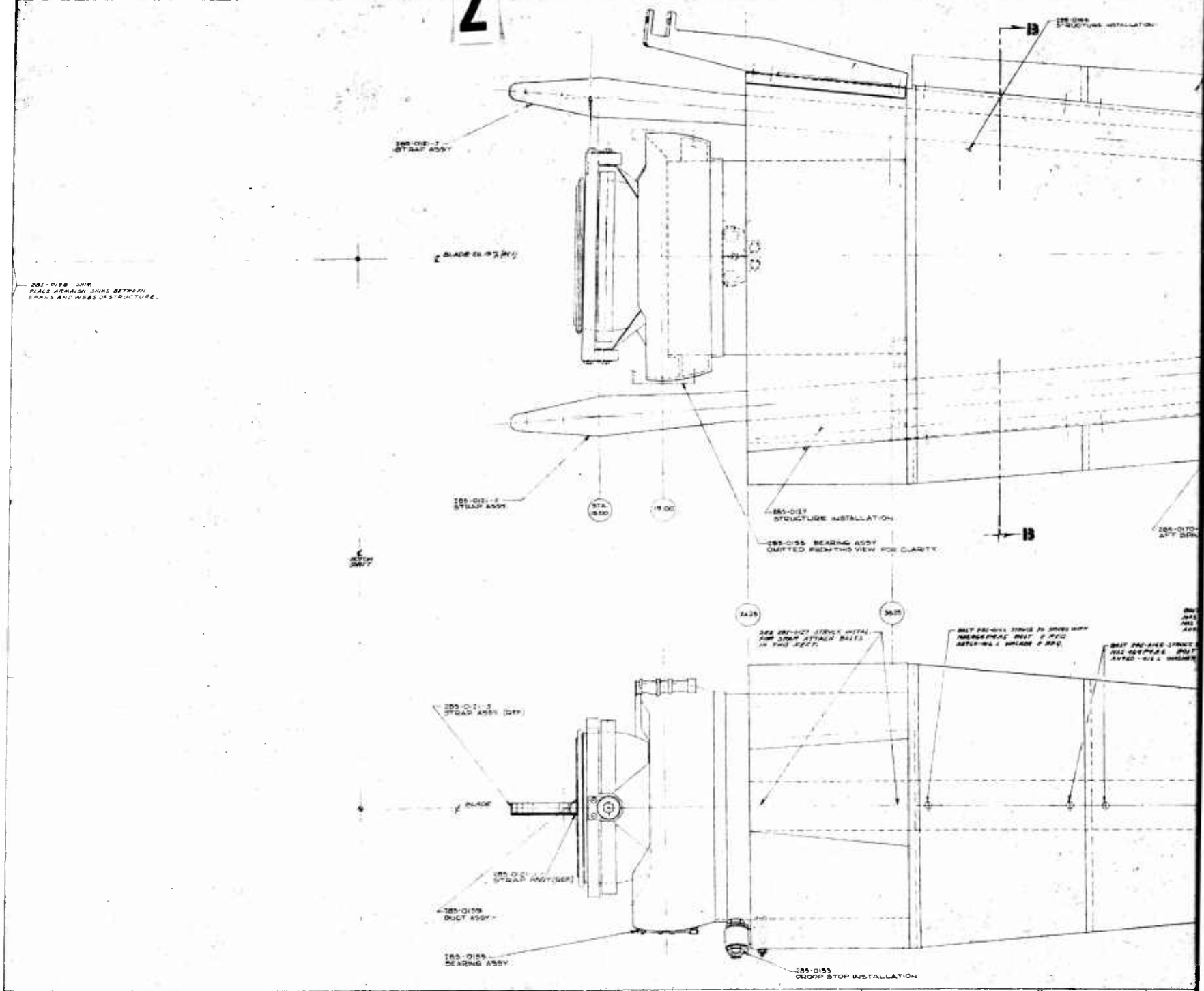
285-0198 SHIM
PLACE ARMALON SHIMS BETWEEN SPARS AND WEBS OF STRUCTURE.
285-0121-1 STRAP ASSY
285-0121-5 STRAP ASSY
STA 8.00
19.00
285-0157 STRUCTURE INSTALLATION
285-0155 BEARING ASSY OMITTED FROM THIS VIEW FOR CLARITY
B
B
285-0121-5 STRAP ASSY (OFF)
285-0121-3 STRAP ASSY (OFF)
285-0159 DUCT ASSY
285-0155 BEARING ASSY
285-0153 DROOP STOP INSTALLATION

3
285-0125
FAIRING INSTALLATION-
INBOARD AFT
A
A
7
6
5

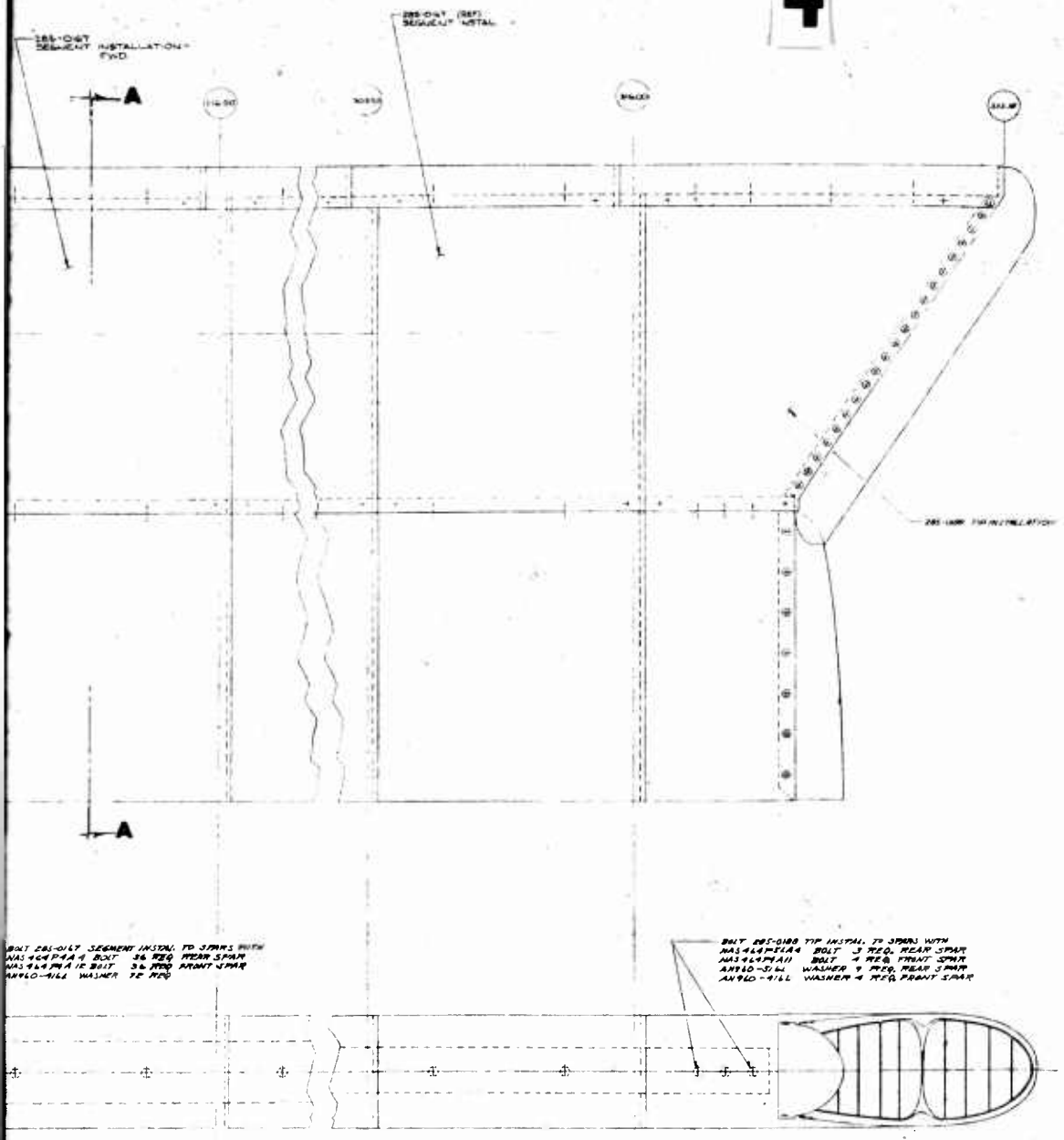

BOLT 285-0167 SEGMENT INSTAL TO SPARS WITH
NAS464P4A4 BOLT 36 REQ REAR SPAR
NAS464P4A12 BOLT 36 REQ FRONT SPAR
AN960-416L WASHER 72 REQ

BOLT 285-0168 TIP INSTAL TO SPARS WITH
NAS464P5A4 BOLT 3 REQ. REAR SPAR
NAS464P4A11 BOLT 4 REQ. FRONT SPAR
AN960-516L WASHER 9 REQ. REAR SPAR
AN960-416L WASHER 4 REQ. FRONT SPAR

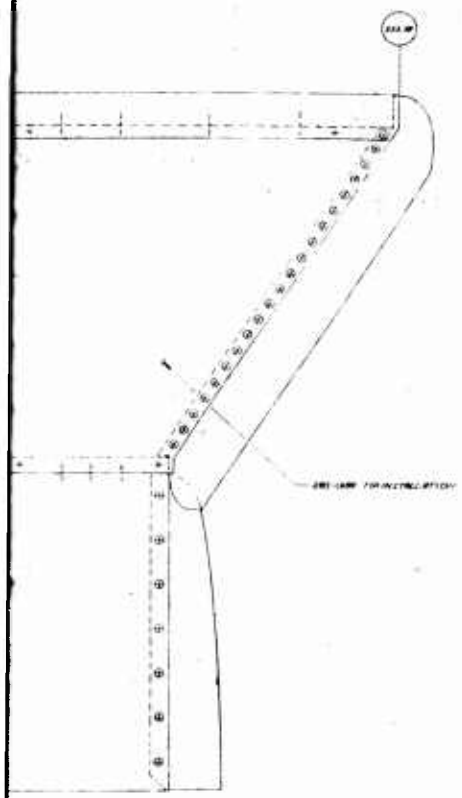

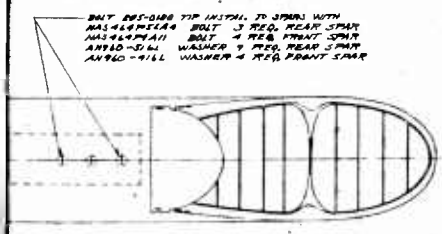
BOLT 285-0188 TIP INSTAL. TO SPARS WITH
MS4649M5AA BOLT 3 REQ. REAR SPAR
MS4649M5A11 BOLT 4 REQ. FRONT SPAR
AN960-516L WASHER 7 REQ. REAR SPAR
AN960-416L WASHER 4 REQ. FRONT SPAR

Figure 5.2-1

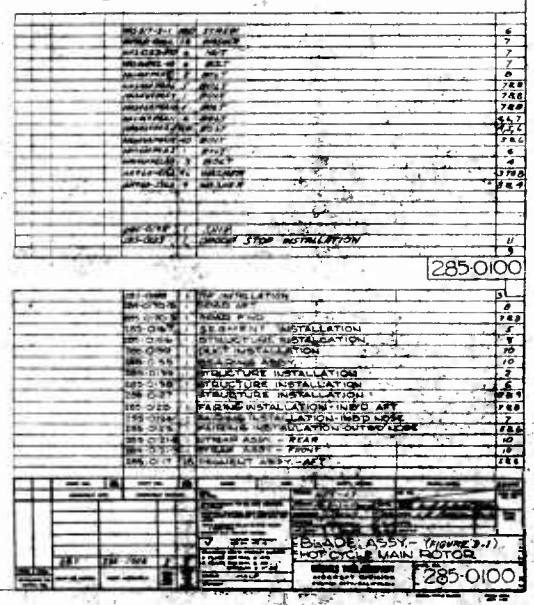
285-0100
BLADE ASSY. (FIGURE 5-1)
HOT CYCLE MAIN ROTOR
285-0100

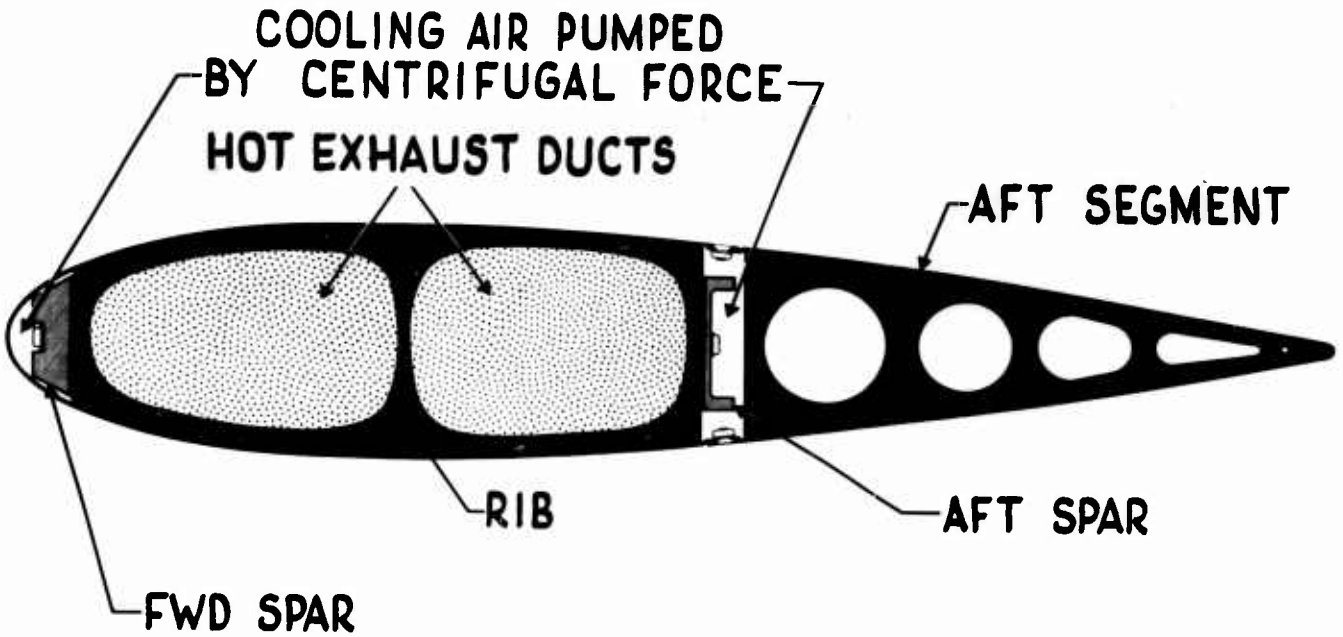

Figure 5.2-2 Blade Cross Section

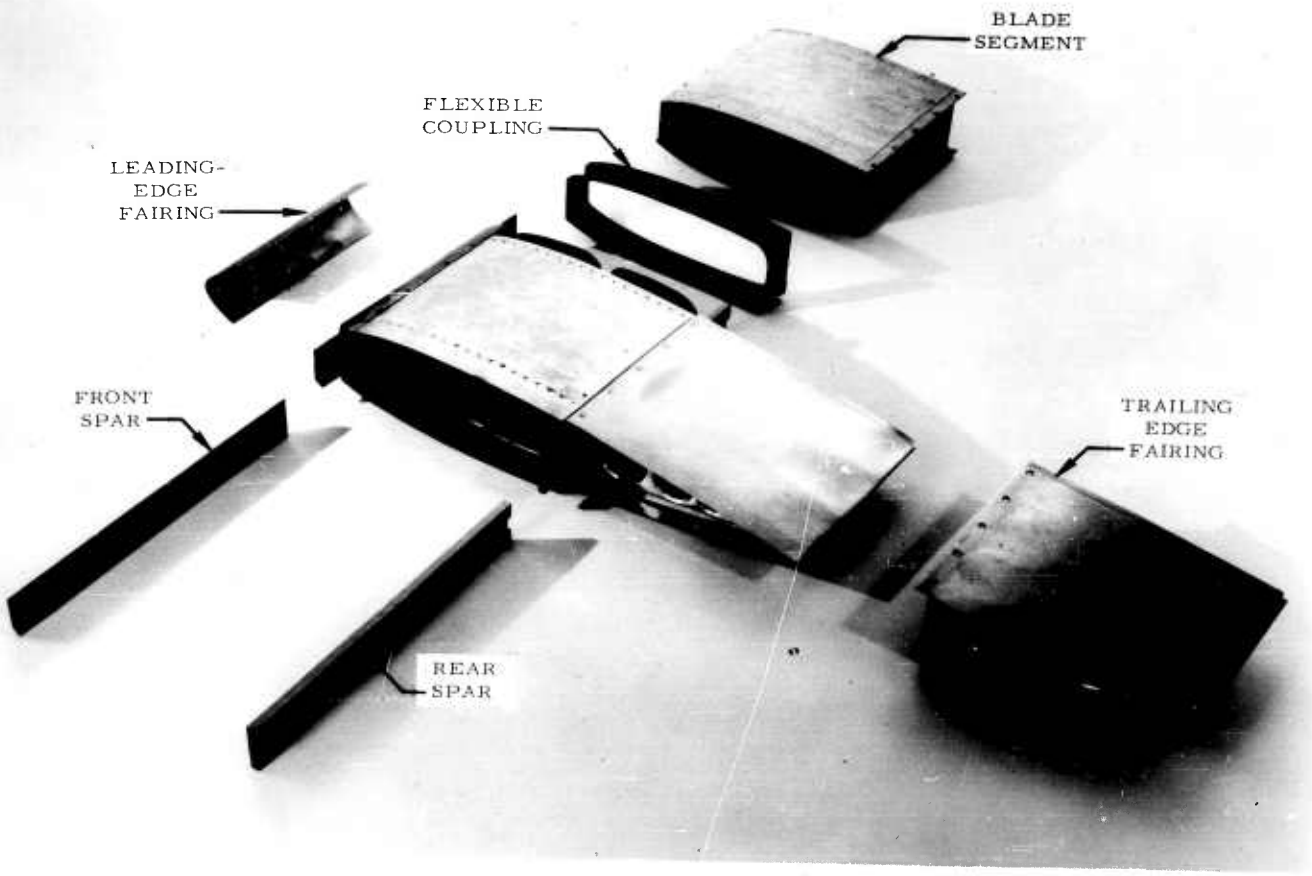

Figure 5.2-3 Typical Segment Length of Blade and Its Components, Showing Breakdown to Fundamental Elements

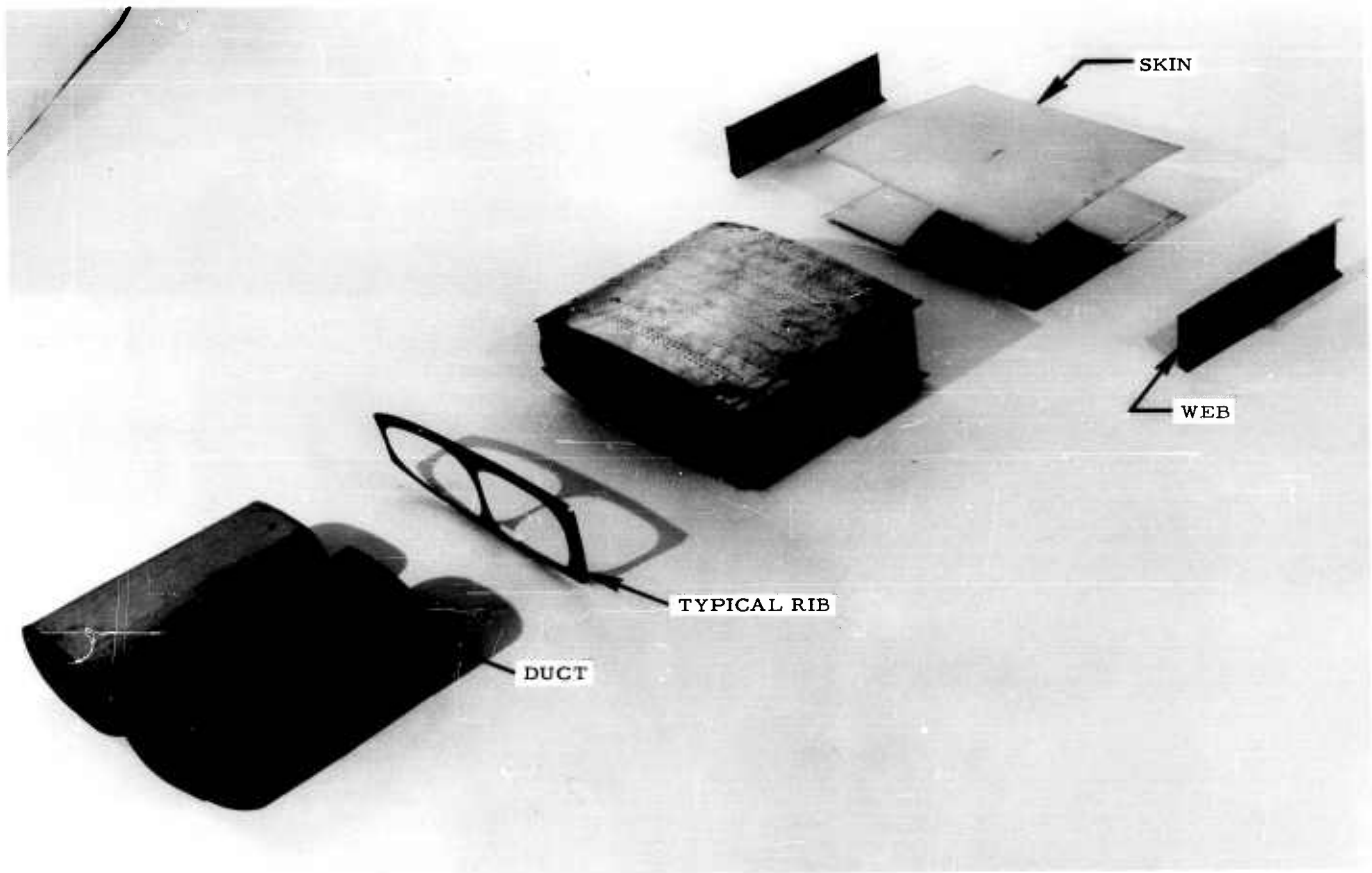

Figure 5.2-4 Blade Forward Segment and Its Detail Parts Showing Small Number and Simple Nature of Components

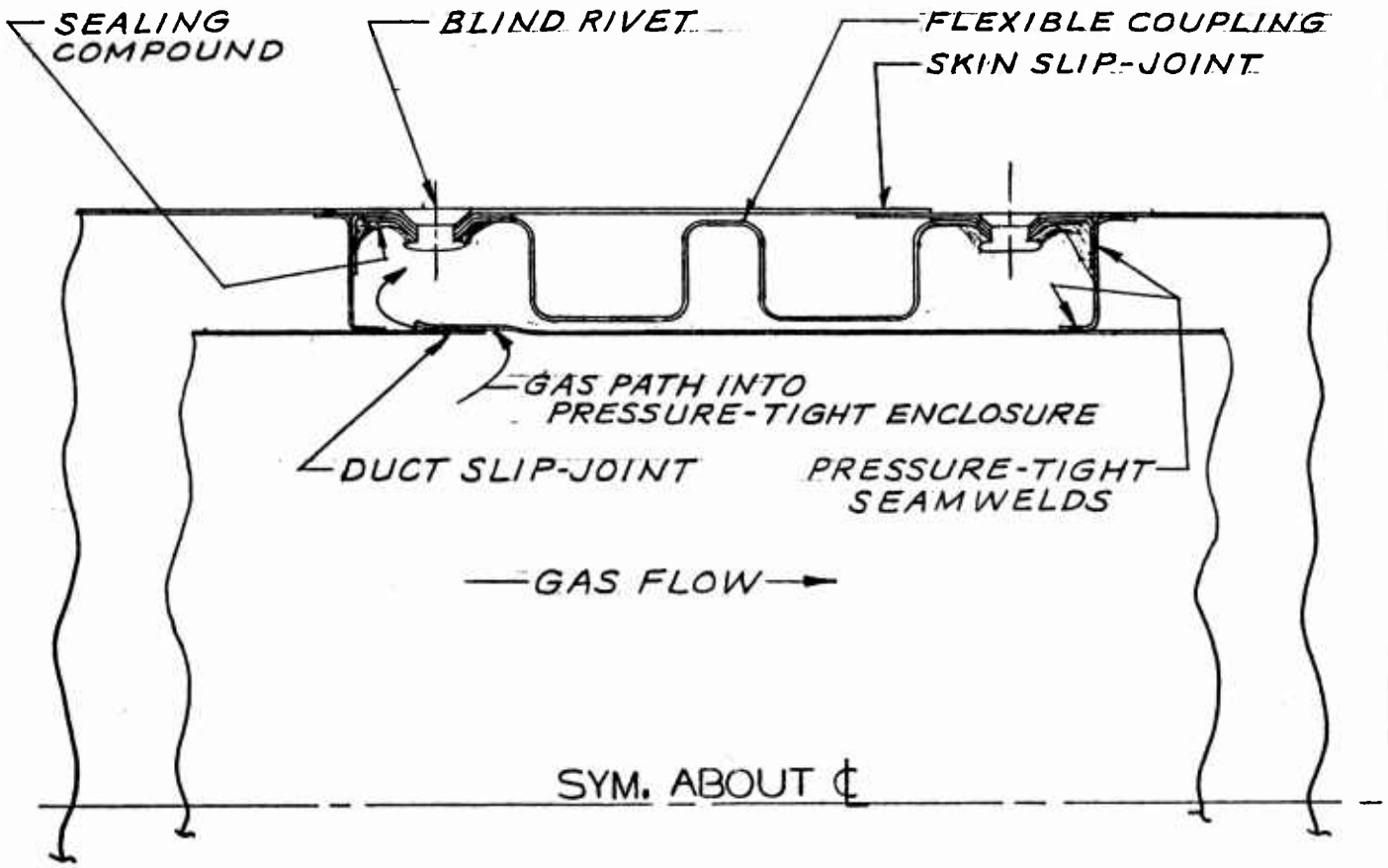

Figure 5.2-5 Typical Blade Segment Joint

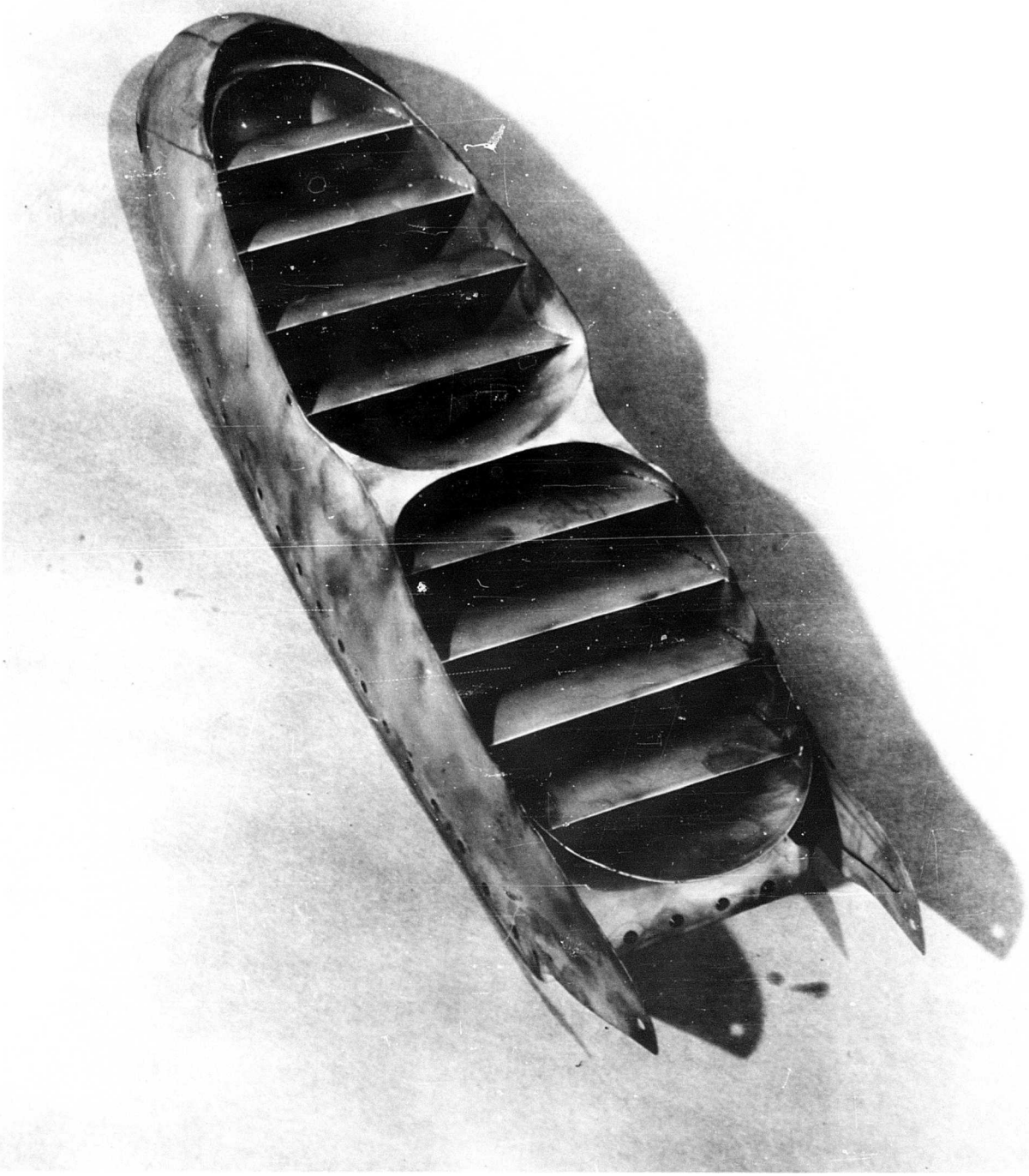

Figure 5.2-6 Tip Cascade - Viewed From Outboard

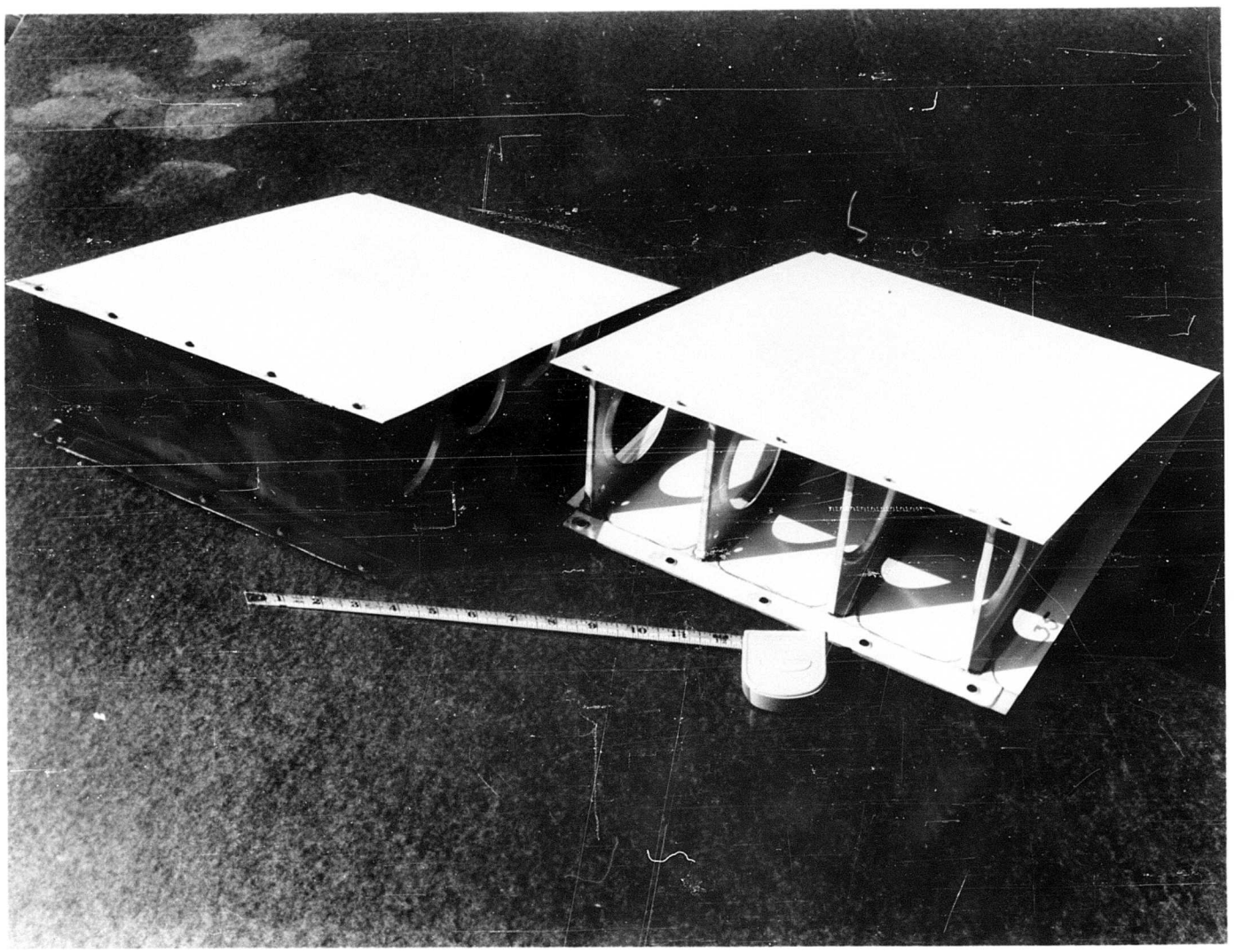

Figure 5.2-7 Blade Constant Section Aft (Trailing Edge) segments; Note the Few Components Required

5.3 HUB SIGNIFICANT DETAILS (Drawing 285-0500, Figure 5.3-1)

5.3.1 The hub structure and rotor blade retention consists of a free-floating hub supporting three coning blades with converging tension straps tying the blades to the hub. Schematically, this is shown on Figure 5.3-2. The free-floating hub ties the rotor blades together and transfers their loads to the mast and then through two bearing systems to the supporting trusses. Clearance is provided between this hub and the ducts which transfer the propulsion gases from below the hub to the three blades. The over-all hub structure also provides support for the control system.

5.3.2 The free-floating hub structure (shown schematically on Figure 5.3-3) is composed of a central hexagonal box with two vertical parallel beams extending from the hexagon to support each feathering bearing housing and a pair of blade retention strap shoe fittings. The radial strap loads from the three blades are balanced across the lower surface of the floating hub structure by two parallel plates. Vertical components of the strap loads are transferred from the shoe fittings through the parallel beams to the hexagonal box. Most of these loads are balanced across the box by similar loads from opposing blades. The free-floating hub is universally mounted at the upper end of a rotating mast by a gimbal system. A hub tilt stop is incorporated at the top of the hub, providing a one-degree tilt for low rpm and ground handling, and ten degrees for the normal flight operation.

5.3.3 Two bearing assemblies support the rotating mast. (See Figure 5.3-2)

A lower bearing (tapered roller) resists all of the vertical or thrust load while the moments are resisted by radial reactions on this same lower bearing and by an upper bearing (straight roller) which is free to float vertically. A circulating oil system was provided in order to insure optimum lubrication and maximum cooling in case bearing temperatures proved to be higher than anticipated.

The upper bearing outer housing is supported by three radial spokes attached to the mast. The inner housing of this same bearing is attached to a supporting truss attached to the whirl tower (or a fuselage). The lower bearing housing is likewise attached to a concentric and similar supporting truss. These two trusses, of welded steel tubing, meet at four panel points at the fuselage level.

1

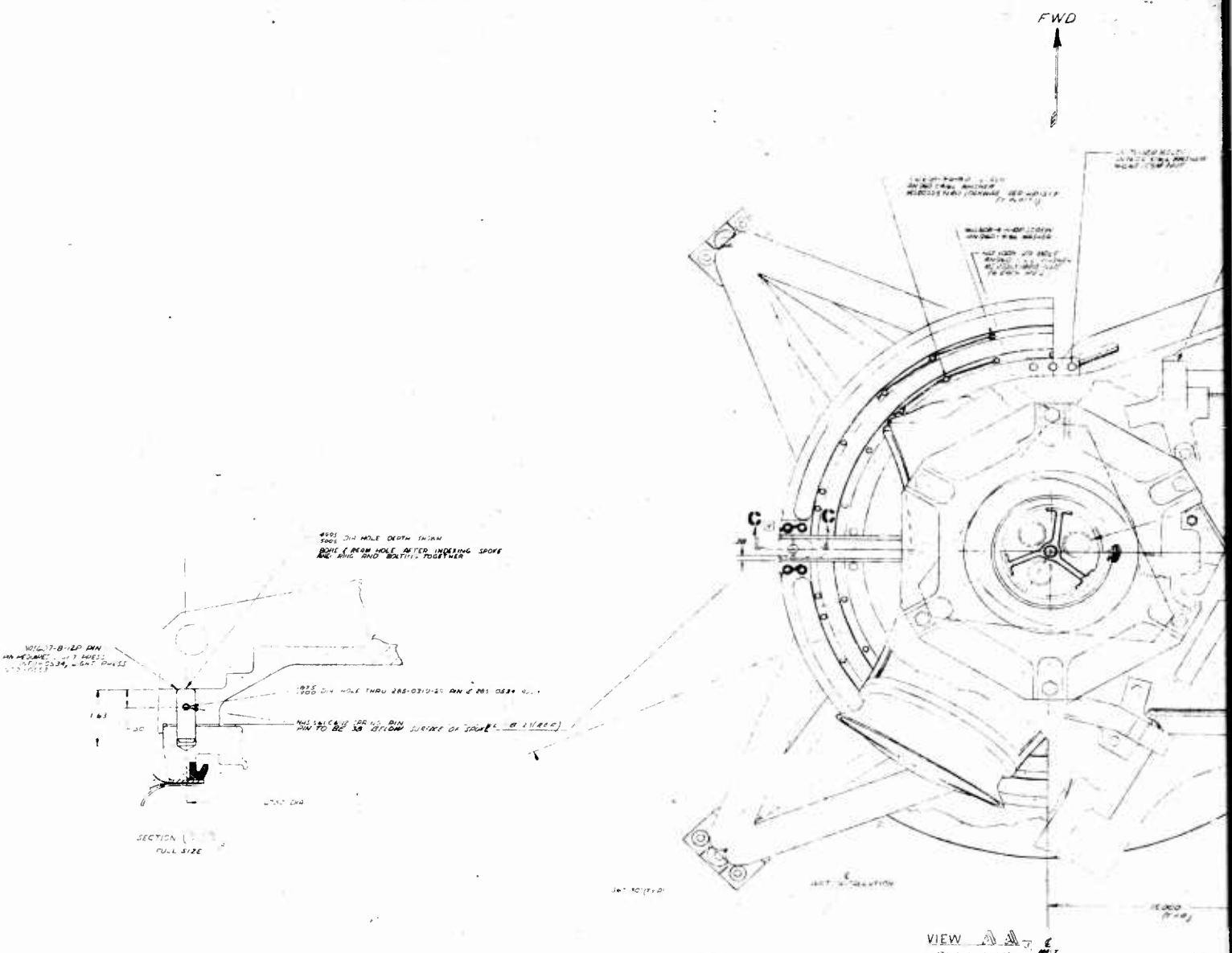

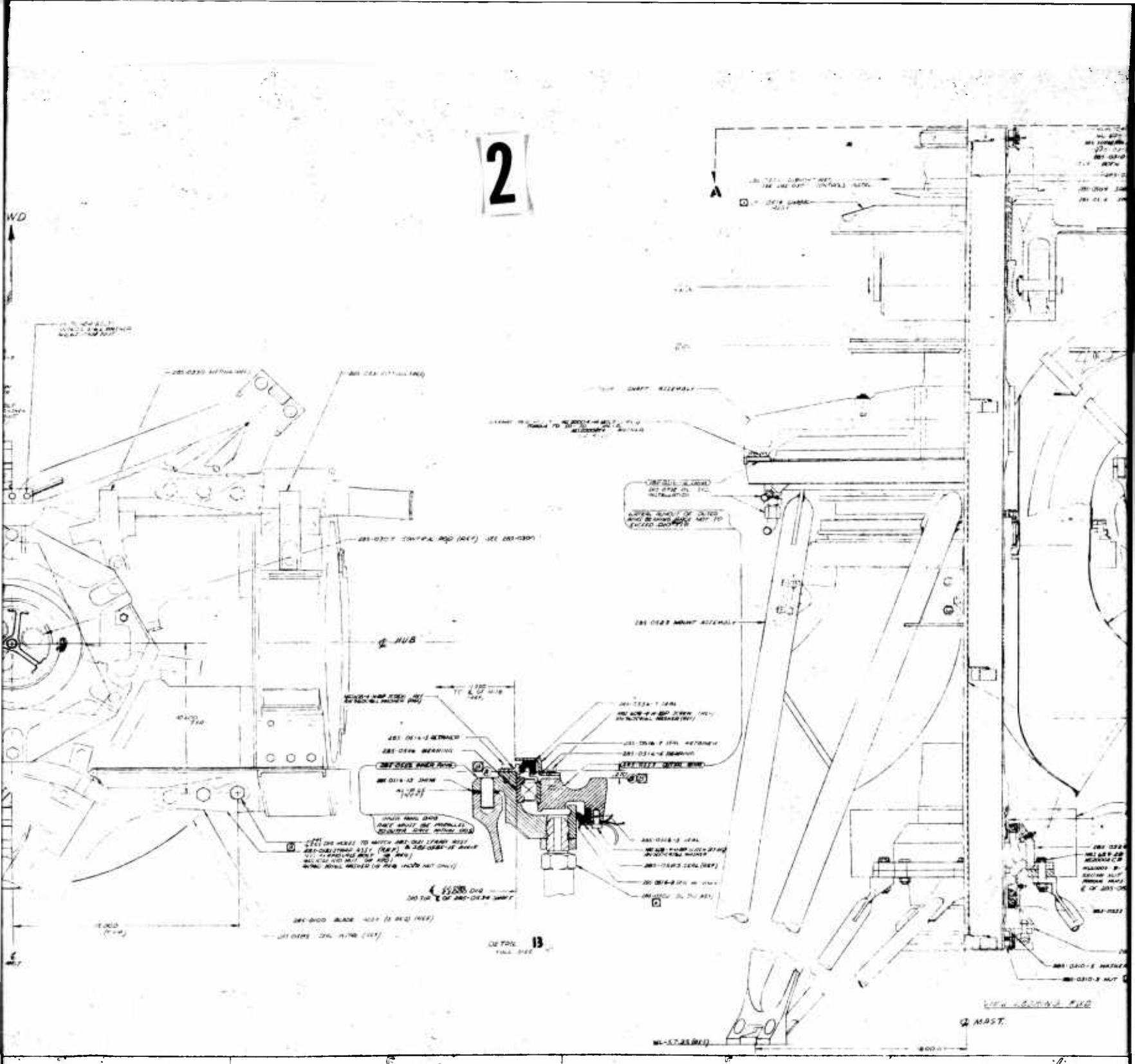
2
A
WD
℄ HUB
DETAIL 13
℄ MAST.

3

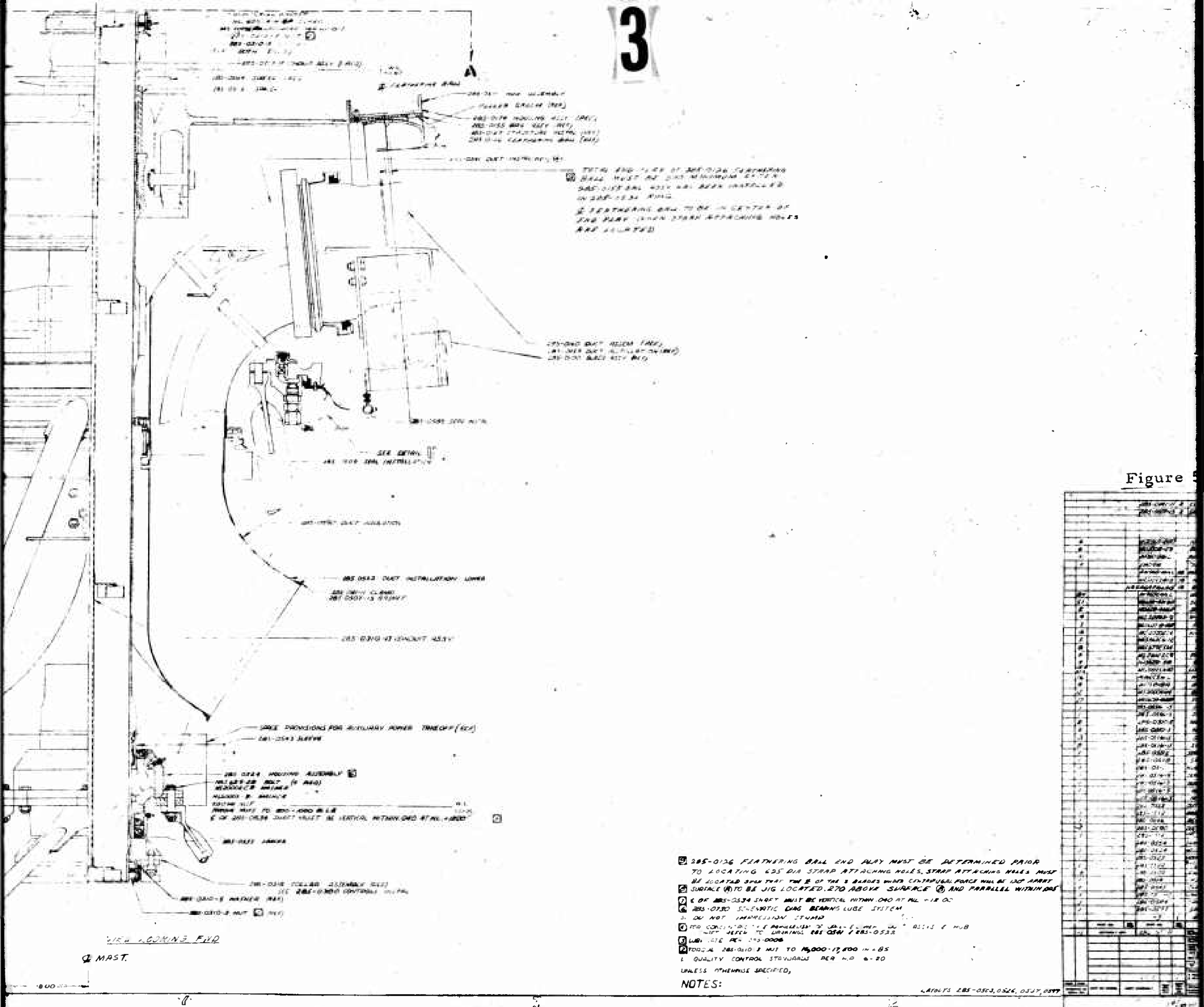

Figure 5

Report 285-17

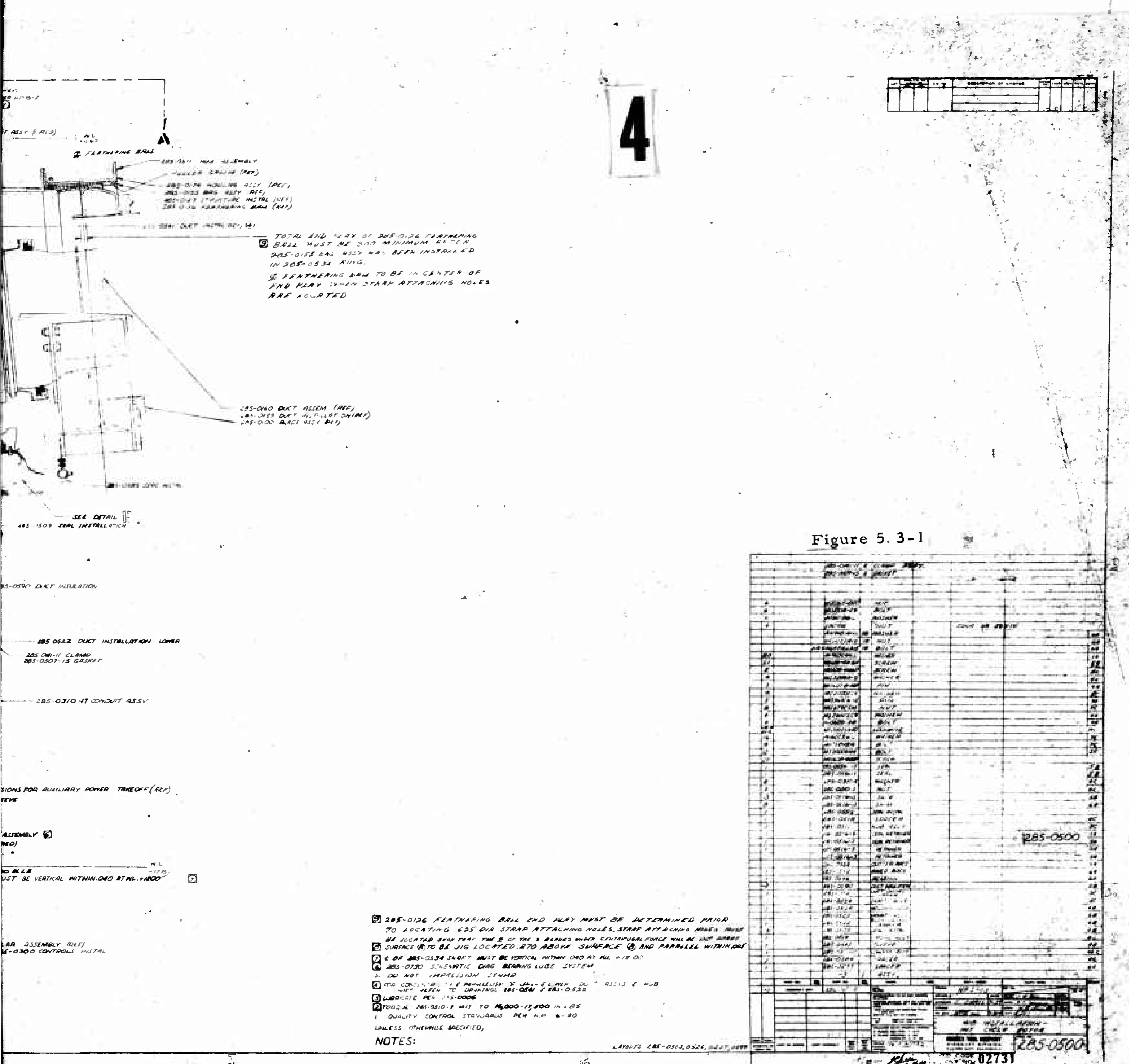
4
TOTAL END PLAY OF 285-0126 FEATHERING BALL MUST BE .300 MINIMUM AFTER 285-0155 BRG ASSY HAS BEEN INSTALLED IN 285-0534 RING.
℄ FEATHERING BRG TO BE IN CENTER OF END PLAY WHEN STRAP ATTACHING HOLES ARE LOCATED
285-0160 DUCT ASSEM (REF)
SEE DETAIL
285-0590 DUCT INSULATION
285 0522 DUCT INSTALLATION LOWER
285 0411-11 CLAMP
285-0507-15 GASKET
285-0310-47 CONDUIT ASSY
285-0126 FEATHERING BALL END PLAY MUST BE DETERMINED PRIOR TO LOCATING .625 DIA STRAP ATTACHING HOLES.
SURFACE Ⓐ TO BE JIG LOCATED .270 ABOVE SURFACE Ⓑ AND PARALLEL WITHIN .005
285-0730 SCHEMATIC DIAG BEARING LUBE SYSTEM
DO NOT IMPRESSION STAMP
UNLESS OTHERWISE SPECIFIED,
NOTES:
285-0500
02731

Figure 5. 3-1

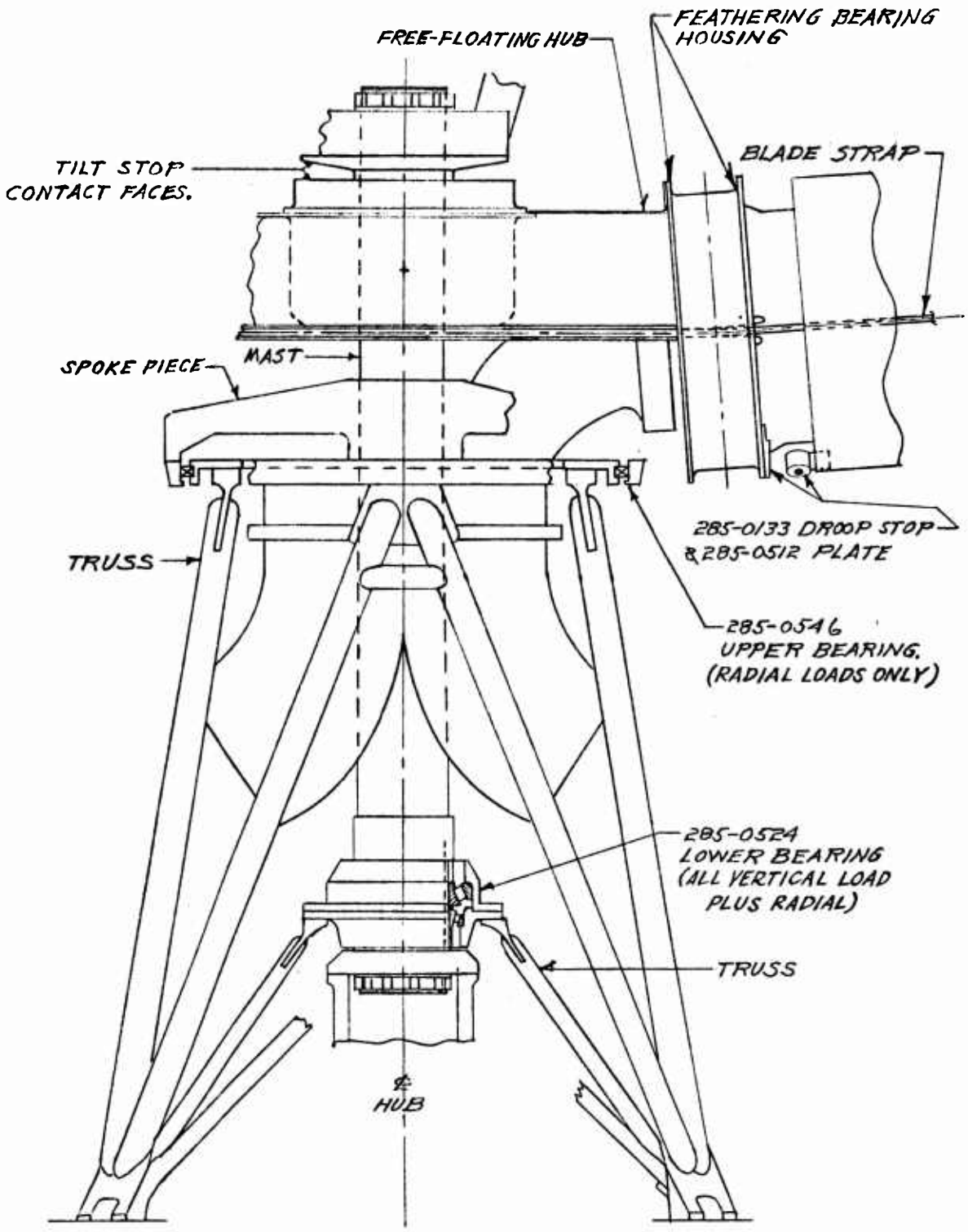

Figure 5.3-2 Schematic of Hub Support Structure

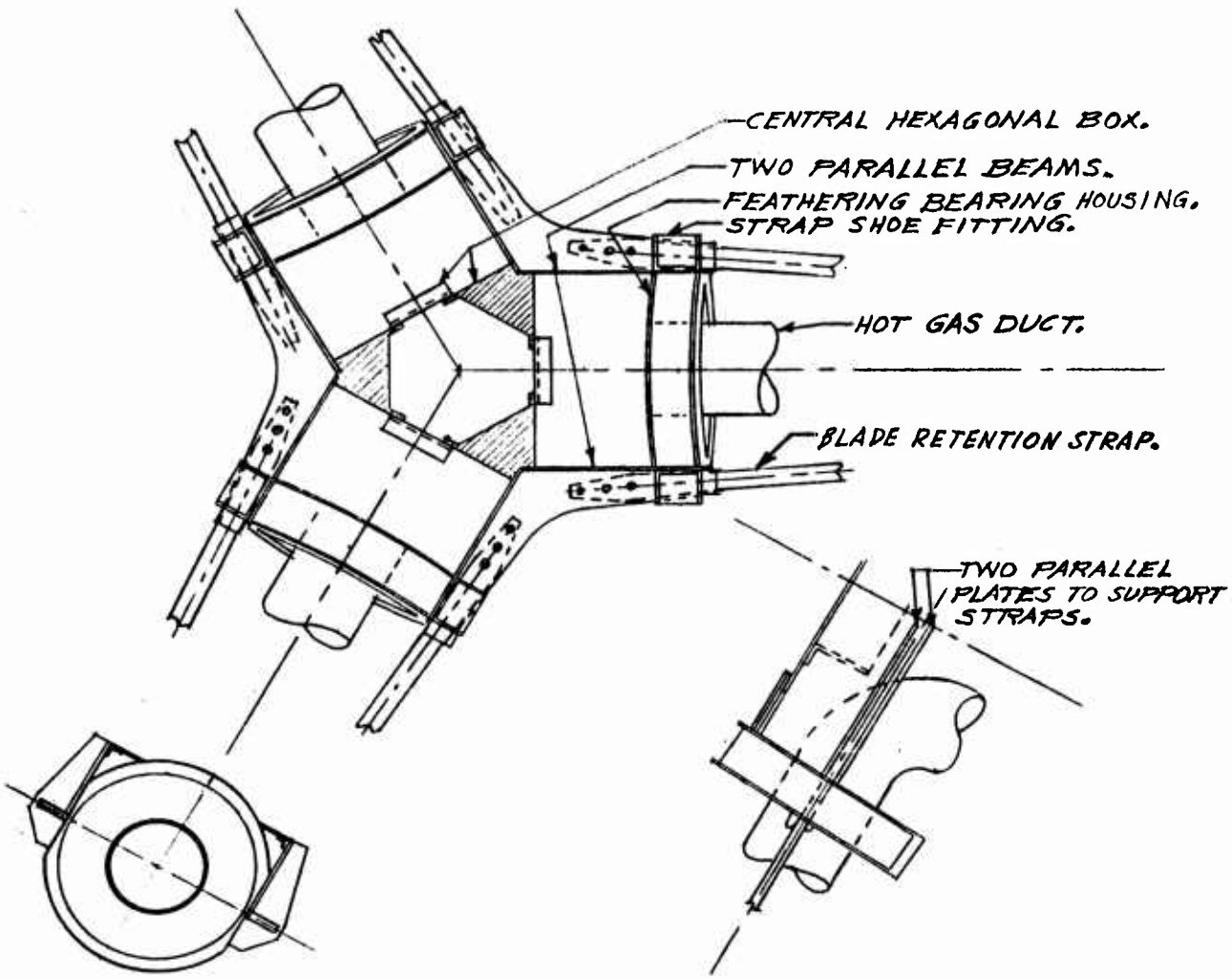

Figure 5. 3-3 Basic Free-Floating Hub Structure

5.4 CONTROL SYSTEM DETAILS (Drawing 285-0300, Figure 5.4-1)

In designing the controls an attempt was made to make the system as conventional and trouble-free as possible. The various components were located so as to keep them small in size and relatively cool. Corrosion protection, lubrication of bearings and ease of access to all parts were given careful attention.

The system utilizes a small swashplate located at the lower end of the hub shaft since this location permits use of relatively small standard bearings, and keeps control components away from the hot ducts. This is shown schematically for one blade in Figure 5.4-2. Geometry of the control system has been laid out so that hub float or blade coning do not appreciably change the blade pitch angle.

Self-aligning type roller bearings[1] were used in all but one location. For correlation, actual experimental data were available with this type bearing on other helicopters of approximately the same size as the Hot Cycle Rotor. Reduced clearance, high quality bearings were specified for all locations. Bearing forks have been oriented to minimize misalignment. This practice increases bearing life and permits the use of standard $\pm$ 10° misaligning bearings in most places. With the configuration chosen none of the bearings operate at over 200°F. For this reason, conventional helicopter bearing greases are used.

The configuration of the components has been designed to meet actual

---

[1] Manufactured by Shafer Division of Chain Belt Company, Downers Grove, Ill.

flight conditions. Since this rotor system was intended primarily as a ground whirl test model, however, fabrication costs were reduced by minimizing coring-type machine operations, sometimes adding considerably to component weight.

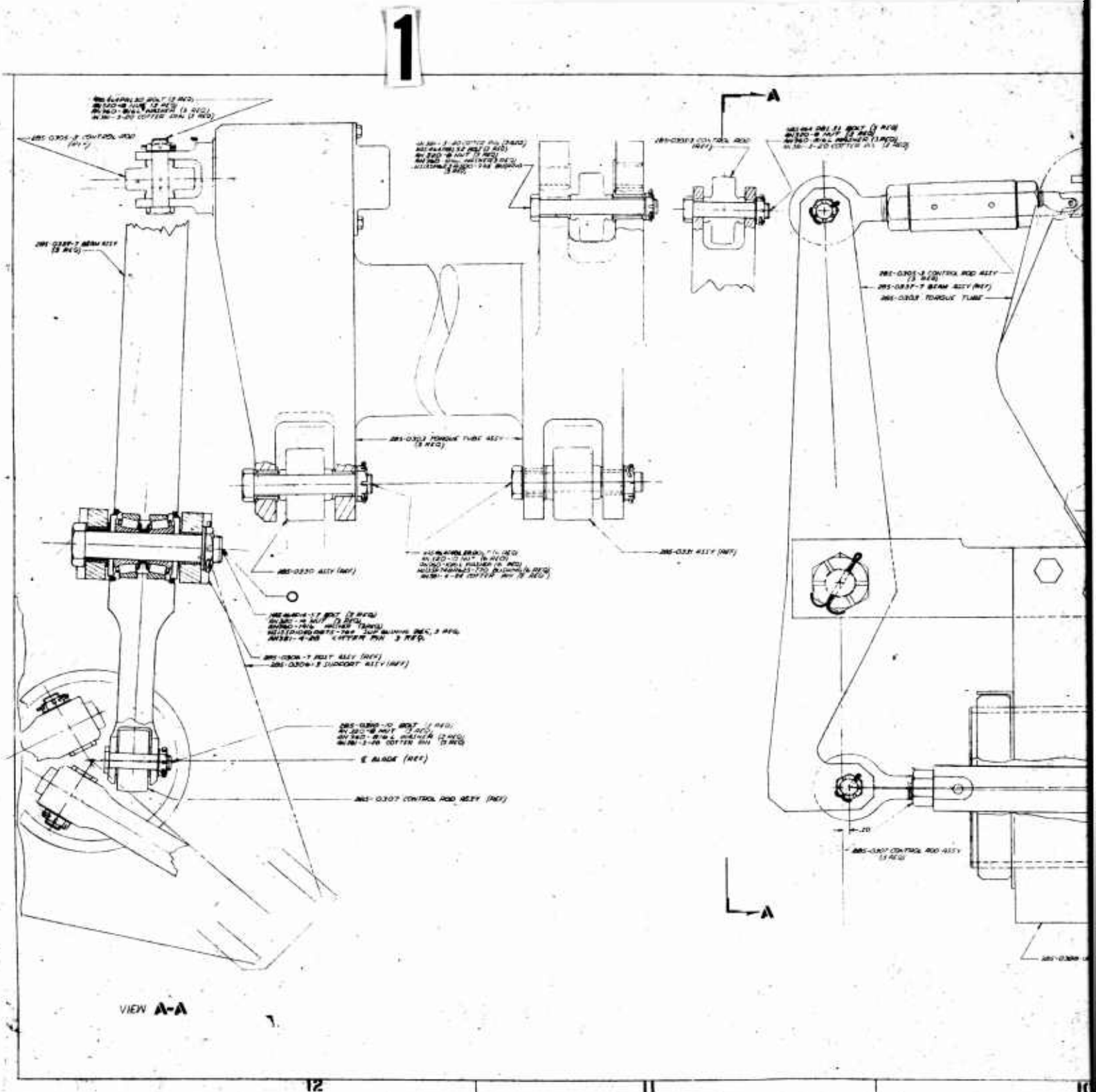
A
A
VIEW A-A
12
11

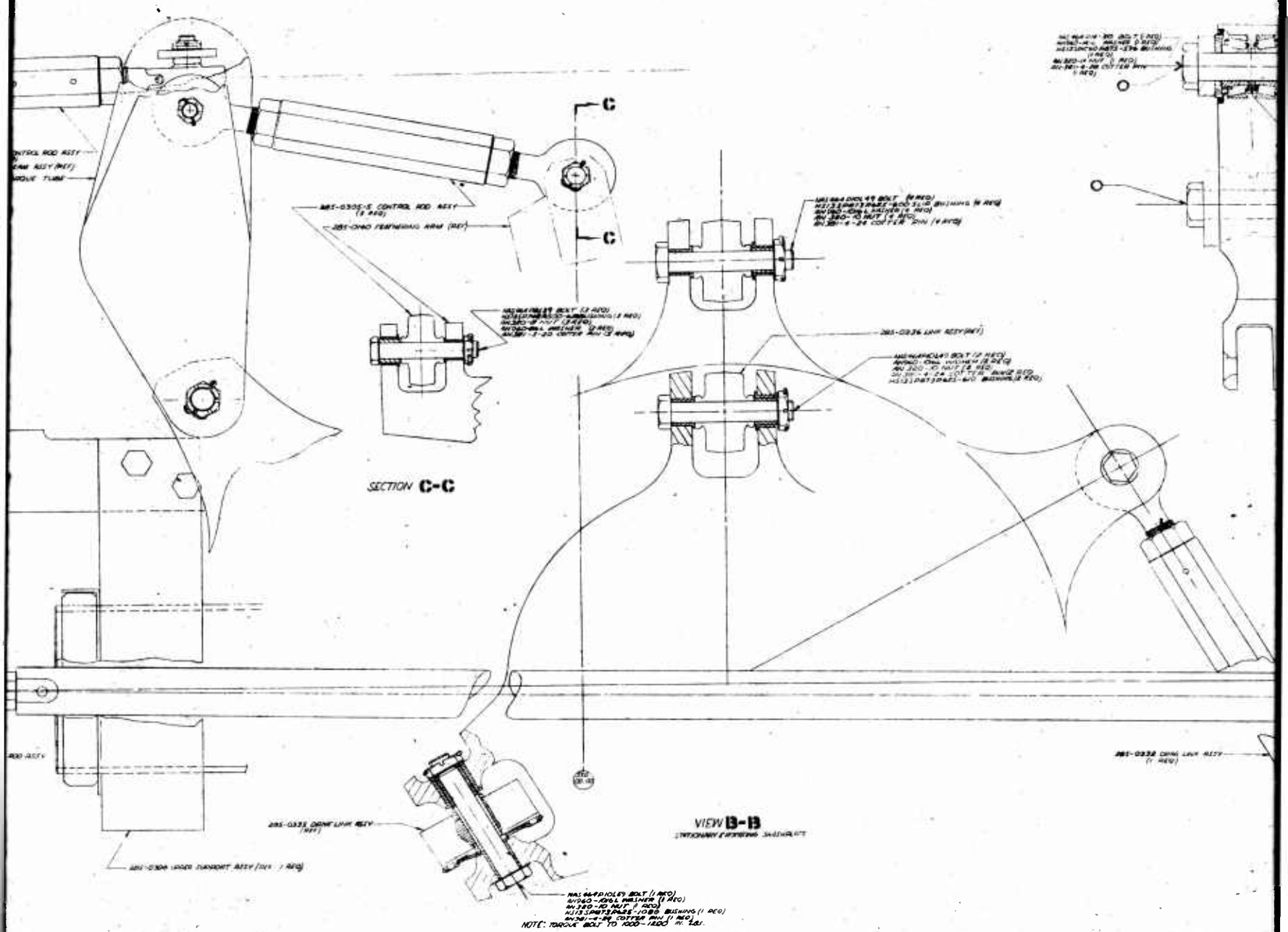
C
C
SECTION C-C
VIEW B-B

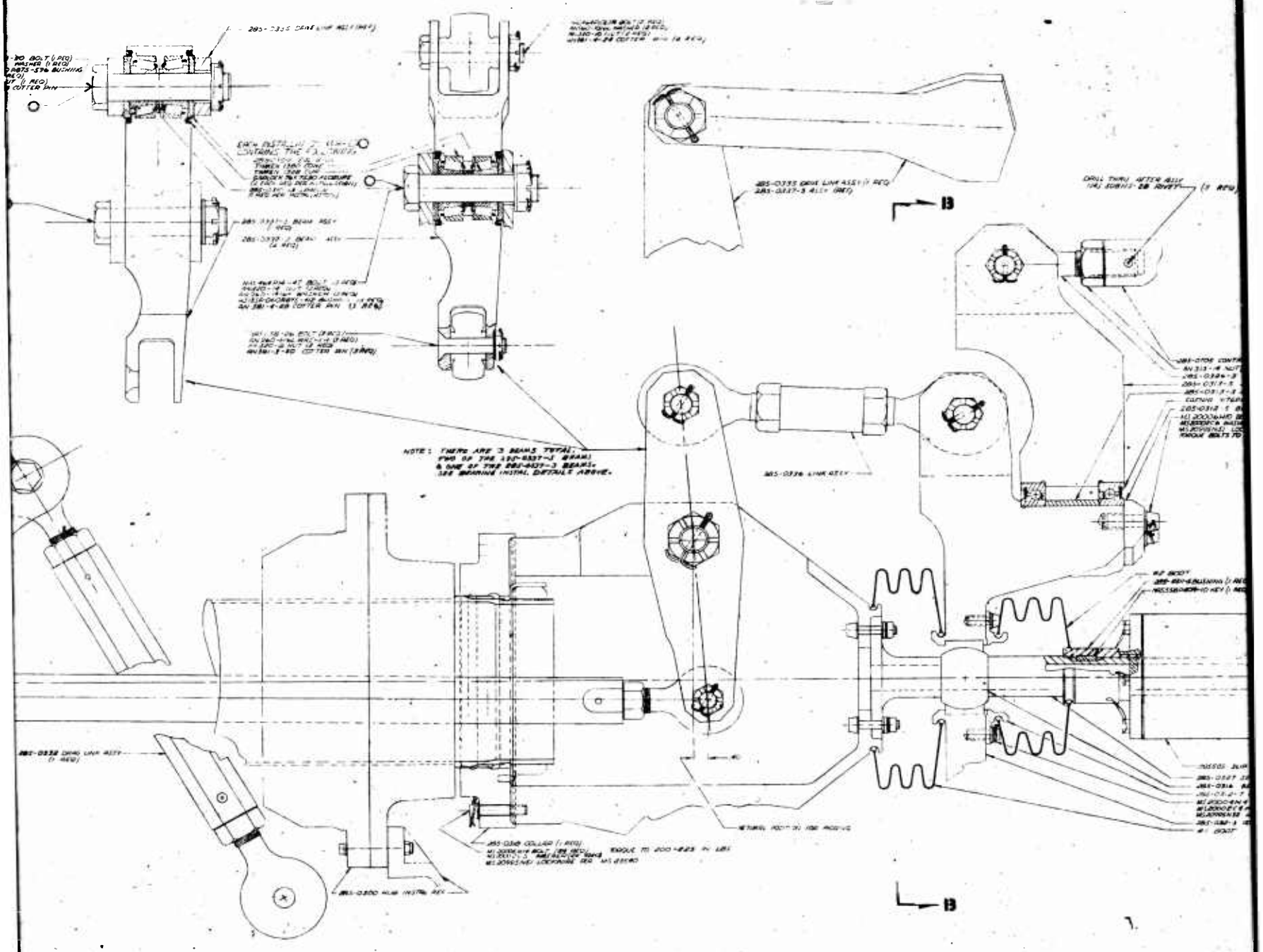
B
B
NOTE: THERE ARE 3 BEAMS TYPAL
TWO OF TYPE 285-0337-1 BEAM
& ONE OF TYPE 285-0337-3 BEAM.
SEE BEARING INSTAL DETAILS ABOVE.

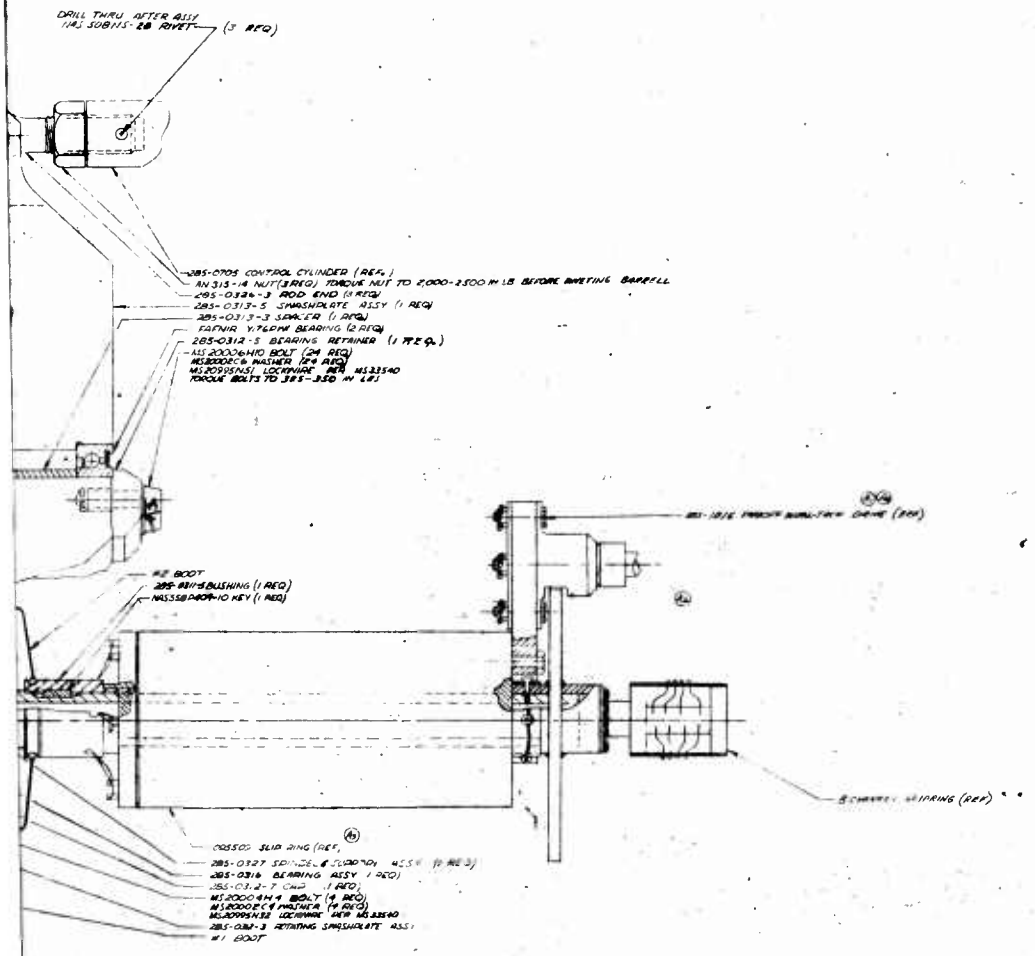

NOTES: UNLESS OTHERWISE SPECIFIED:

1. CONTROLS ARE SHOWN IN THE NEUTRAL POSITION: ZERO STRAP TWIST.
2. CARLOCK "CLOSURES" ARE TO BE FURNISHED WITH CAD PLATED STL CASES.
3. BOLT TORQUES PER NOTE 3 UNLESS OTHERWISE NOTED.

Figure 5. 4-1

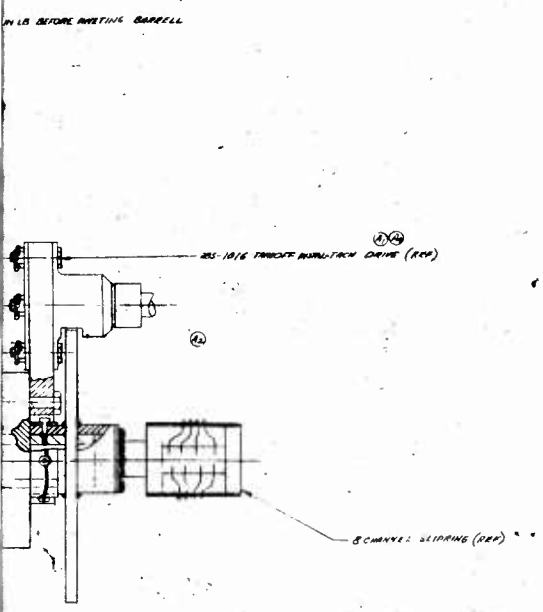

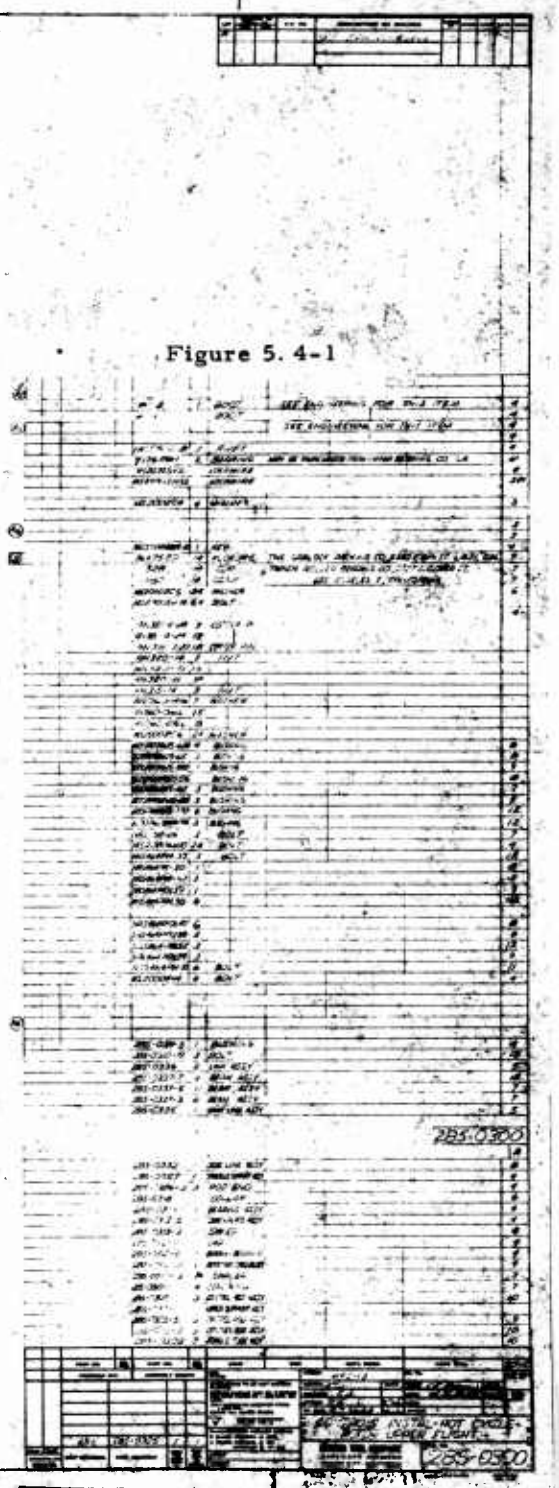

NOTES: UNLESS OTHERWISE SPECIFIED:
1. BOLT TORQUES PER NO. 3 UNLESS OTHERWISE NOTED.
2. GARLOCK KLOZURES ARE TO BE BURNISHED WITH CAD PLATED STL CASES
3. CONTROLS ARE SHOWN IN THE NEUTRAL POSITION: ZERO STRAP TWIST

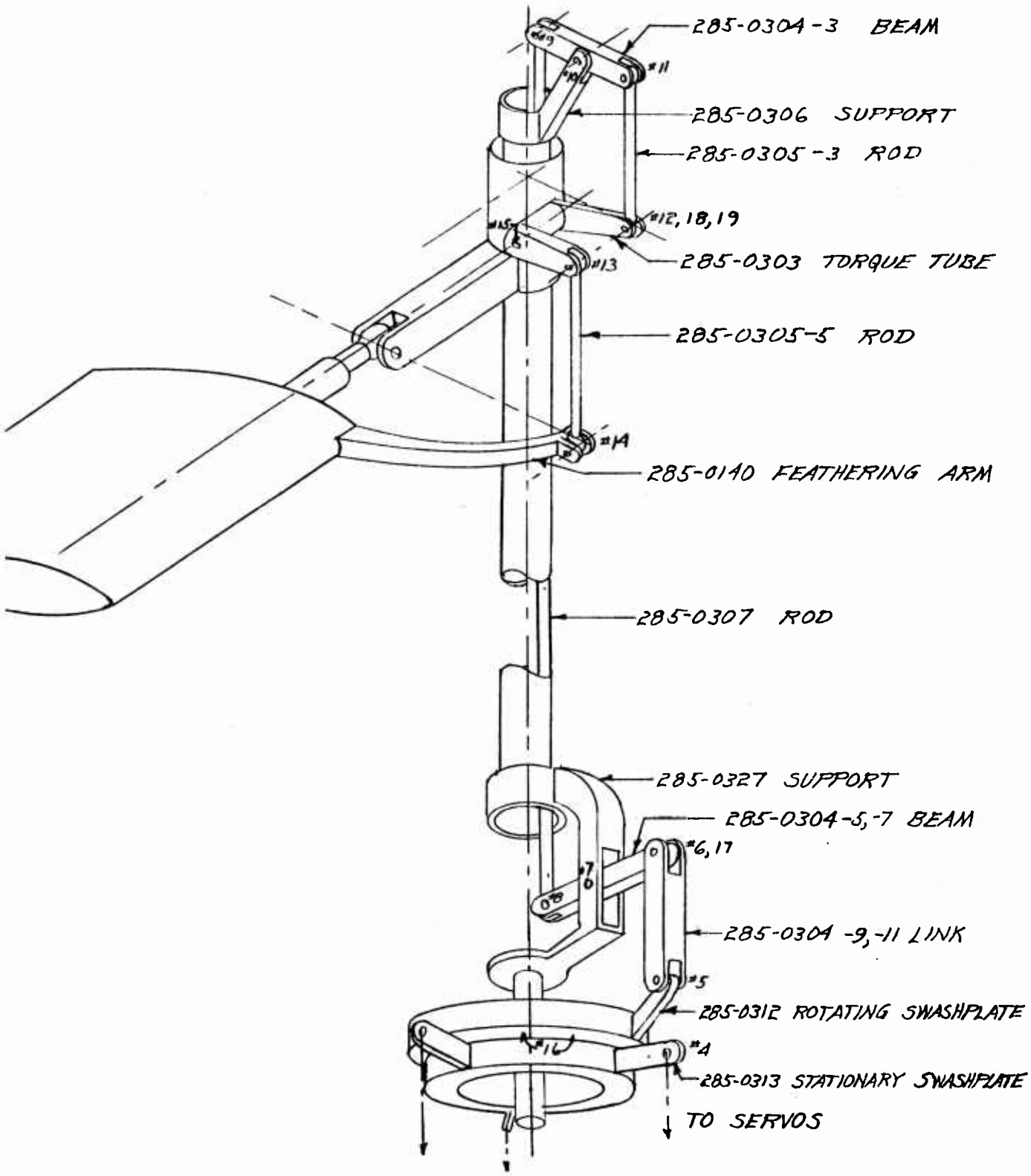

Figure 5.4-2 Schematic of Control System

5.5 DUCT AND SEAL DETAILS

5.5.1 Basically, the purpose of the ducts is to receive up to 1200°F exhaust gas from the engines and to provide an avenue for it through the hub, then along the entire length of the blade to the tip cascades. A schematic of the duct system is shown on Figure 5.5-1. The hub two-branch stationary and three-branch rotating ducts are fabricated of type 347 corrosion resistant steel, with the basic ducts formed on a drop hammer. From the articulate duct inboard seal to station 60.50 the duct is circular in shape, of type 321 or 347 corrosion resistant steel. Each duct joint is identical in cross section and consists of lightweight machined flanges, an asbestos gasket, and a V-band clamp.

From station 60.50 to 91.00 a transition exists which starts with a circular shape at the inboard end and progresses to two roughly-elliptical openings at the outboard end. Due to the non-circular shape, a relatively high strength alloy, Inconel "X", is used for this duct.

The duct from station 15.50 to 42.50 is articulated to allow for hub float, blade coning, and blade pitch change. At the inboard end of this duct a mechanism for allowing freedom of motion in two directions is required. Therefore, a gimbal is incorporated utilizing Fabroid[1] bearings for the coning motion and flexures for the chordwise motion. At the outboard end of the

---

[1] Micro-Precision Division of Micromatic Hone Company, Los Angeles, California.

duct even greater freedom of motion is required and the design at that point is discussed later in Section 5. 5. 3.

5. 5. 2 Carbon seals, with no supplemental lubrication, are used in the hub ducts. These seals are shown schematically on Figure 5. 5-2. The carbon has been impregnated to improve its operation at high operating temperatures.

In the hub duct outer seal, two rows of carbon segments are held against the rotating duct by two garter springs, while a wave spring holds the carbon segments against the surface of the seal housing. Gas pressure aids the springs in maintaining a tight seal.

The hub duct inner seal utilizes a carbon face seal at the rotating face, and two rows of carbon segments supported by garter springs and a wave spring for the static seal, as shown in the sketch of Figure 5. 5-2. This seal allows $\pm$ 0. 090 inch of relative movement between the upper (rotating) and the lower (stationary) duct without separation occurring at the face seal.

The articulate duct inboard seal (Figure 5. 5-1) is approximately the same as the hub duct outer seal described above.

5. 5. 3 At the articulate duct outboard seal (Figure 5. 5-1) a different set of conditions exist. The seal at this point must seal against axial movement (due to hub float and blade coning), rotation (due to blade feathering), misalignment (due to hub float and blade coning), and transverse loading.

A more malleable material than carbon is required here because of the necessity to withstand reversal of transverse loading.

This seal, sketched on Figure 5.5-3, consists of a nest of three slotted-lip laminations riding on a tungsten-carbide coated cylinder. Each lamination is formed from 0.010 Rene' 41 alloy. Slots in the laminations are staggered to eliminate continuous paths through which gas could leak. In addition to the three laminated lips, two overload leaves (0.020 thick) were added at the top and bottom only. All lip laminations and the cylinder are coated with Electrofilm 1000X[1] to reduce friction.

---

[1] Electrofilm, Inc., North Hollywood, California

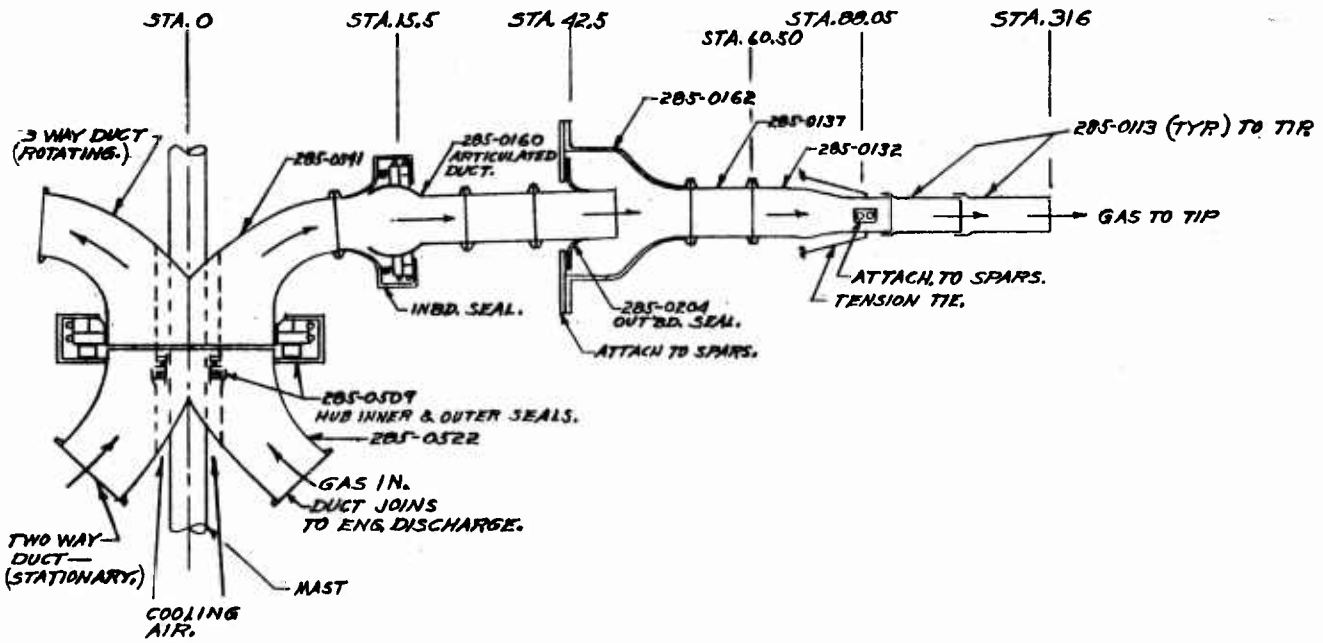

Figure 5.5-1 Hub and Blade Duct System With Seal Sizes Enlarged

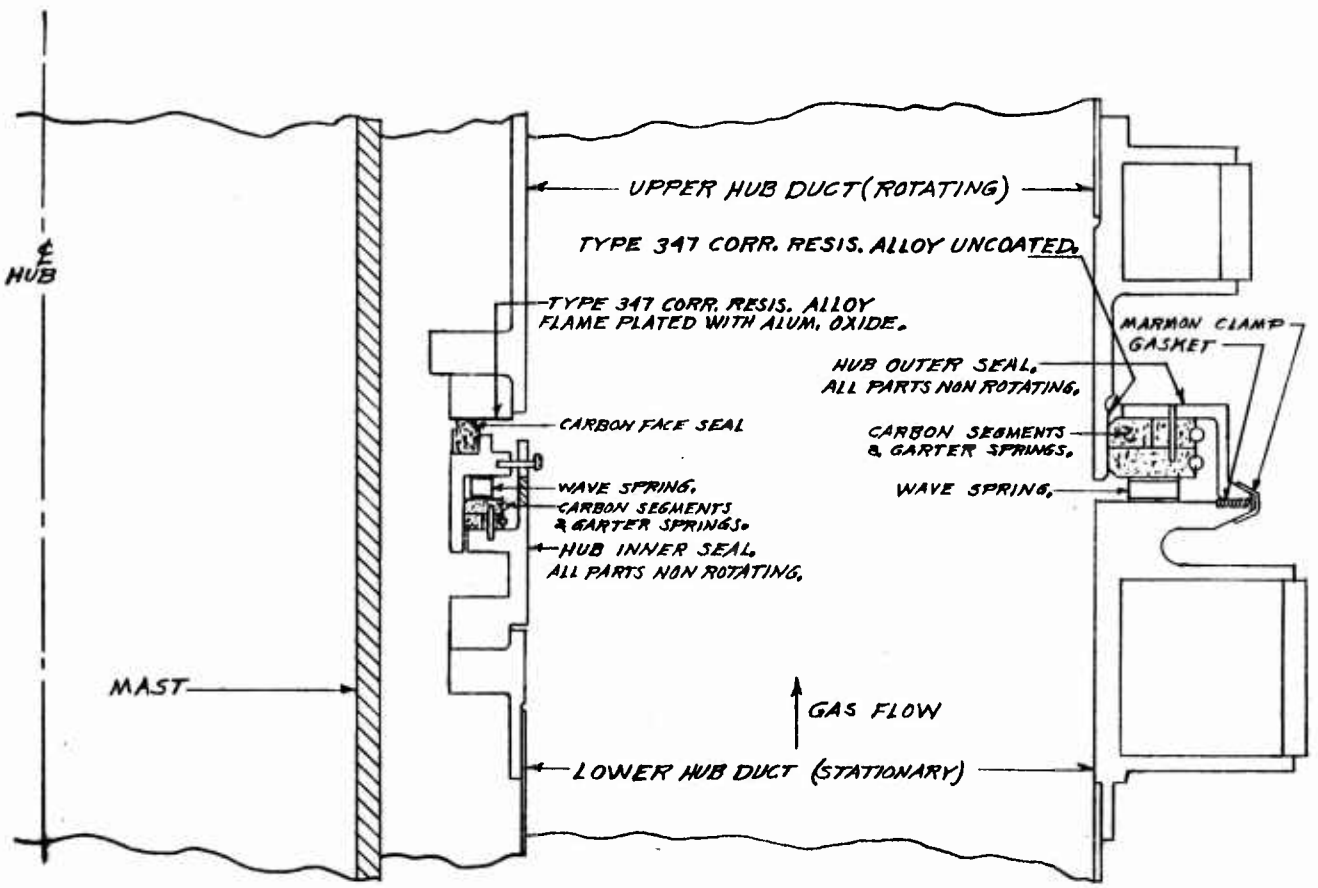

Figure 5.5-2 Hub Inner and Outer Seals

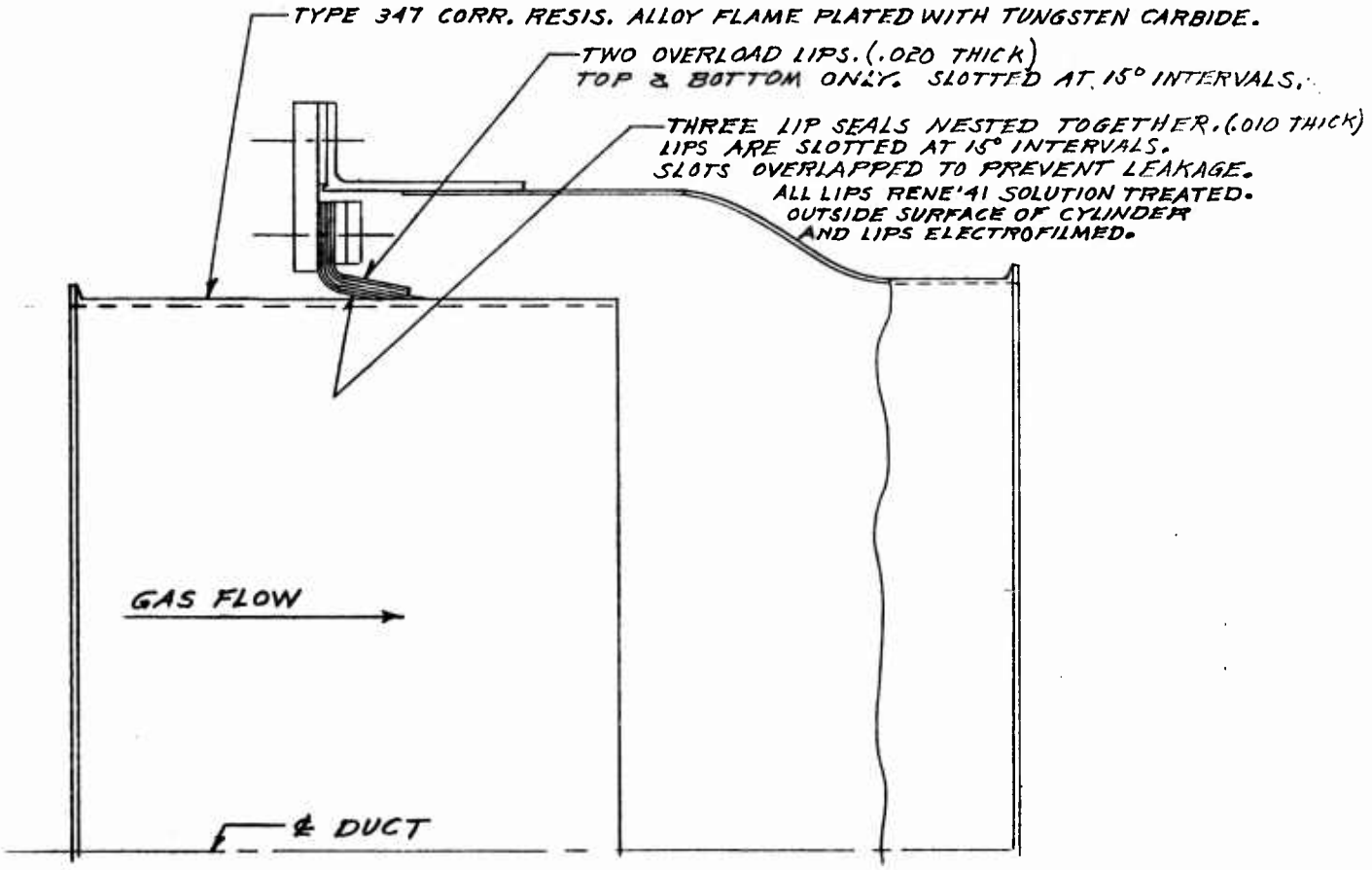

Figure 5.5-3 Articulate Duct Outboard Seal

5.6 COOLING OF COMPONENT PARTS

A simple, effective method of cooling the various parts of the hub structure was achieved and is sketched schematically on Figure 5.6-1. Because the ducts surround the mast and are located in close proximity to the gimbal assembly, upper support assembly and free-floating hub, the temperature of these parts without cooling would rise beyond a value permitting use of standard bearings and conventional materials. By installing an air seal between the floating hub and the rotating race of the upper bearing, air is drawn through the hub in a controlled manner by centrifugal pumping of the rotating blades. This air moves through the hub from three directions (down through the gimbal assembly, up between the mast and duct, and up inside the upper bearing stationary race), and flows outward through the feathering bearings, over the articulate ducts, and is exhausted at approximately blade station 60.00. By this means, the maximum temperature of these important components is maintained at values permitting use of conventional parts and material.

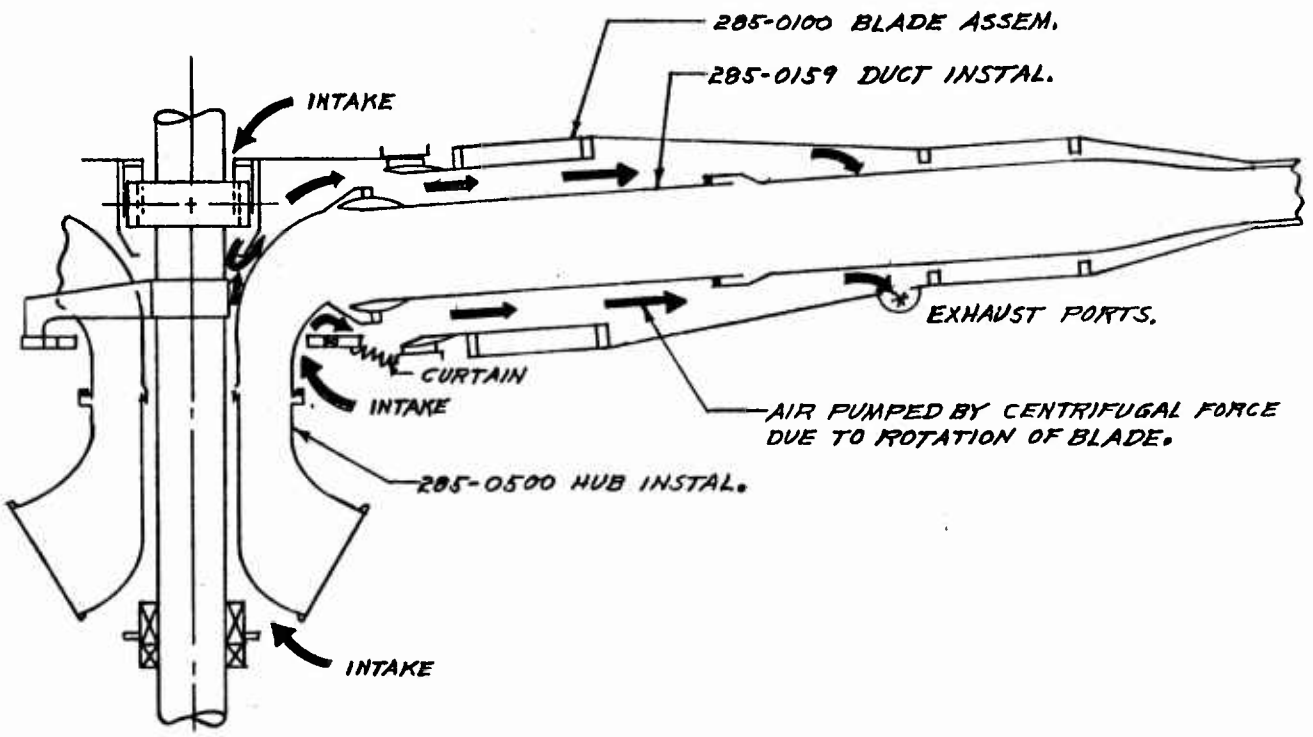

Figure 5.6-1 Cooling of Hub and Blade Root

5.7 ROTOR WEIGHT

Realistic predictions of payload capability require reliable predictions of empty weight. The actual weight of the current Hot Cycle Rotor is 2530 pounds. During the design and fabrication of the Hot Cycle Rotor, weight penalties were accepted, particularly in the hub, in order to save cost. It is estimated that this excess weight is approximately 280 pounds. It is therefore believed that a flight version of the current hot cycle rotor would weight 2250 pounds. Dividing this weight by the rotor blade area results in a value of 10.4 pounds of rotor weight per square foot of blade area.

HOT CYCLE:

ACTUAL WEIGHT	2530 LB
LESS SURPLUS WEIGHT	-280 LB
NET FLIGHT WEIGHT	2250 LB

BLADE AREA (b × c × R) = 217 SQ.FT.

WT/SQ.FT. = 10.4 LB/SQ.FT.

Figure 5.7-1 Rotor Weight

6. RESULTS OF ANALYSES AND TESTS

6.1 STRUCTURAL CONSIDERATIONS

6.1.1 Blade Stresses

Measurements made during the whirl test indicate the following:

(a) All of the measured cyclic pitch arm loads fall well below the design limit.

(b) Maximum blade flapwise cyclic bending moments (measured at Stations 53.5 and 73.4) versus wind speed were below the design allowable limit, with the exception of one point at each station. A few cycles at this one amplitude occurred and probably resulted from severe wind gusts.

(c) Maximum axial cyclic loads in the rear spar at Station 103 inches, and in the front spar at Station 83.3 were measured versus wind speed. Three points for the rear spar and nine points for the front spar fell above the endurance limit. It is believed that the spar axial cyclic loads (chordwise cyclic bending) were aggravated by gusty wind conditions. It is estimated that this small number of cycles used but a negligible percentage of the service life of the blade.

6.1.2 Thermal Effects on Structural Components

A comparison of design and measured temperatures for the Hot Cycle rotor shows that predicted values used in design were reasonably accurate for

critical components. From an over-all standpoint, inspection of the rotor subsequent to completion of the whirl tests show no deleterious effects of temperature on the structure.

Several components have been singled out and analyzed for the thermal effects of the measured temperatures, as follows:

(a) Blade forward segment ribs have the possibility of 11 percent higher thermal stresses. Post test inspections of the duct walls however, showed no evidence of permanent set.

(b) Blade spar measured temperatures (all below 230°F) were well below predicted temperatures. At these low temperatures, effect on the material properties of titanium is negligible.

(c) Blade flexures in the initial design were made of electro-formed nickel. However, due to a procurement problem with the nickel parts, the basic flexure was changed to Inconel "X" which proved to be superior from both a fatigue and temperature standpoint. The Inconel "X" parts were used throughout with the exception of the three flexures nearest the tip, where cyclic deflections are a minimum. A comparison of predicted and measured temperatures is given below. Post test inspection showed no damage to either type flexure.

Flexure	Predicted Temp.	Measured Temp.
Electroformed Nickel	600°F	510°F
Inconel "X"	600°F	660°F*

(d) Rotor hub and shaft measured temperatures are below predicted temperatures for all structural components.

6.1.3 Gimbal Lug Stresses

The hub is attached to the gimbal ring through two pairs of lugs that extend down from the 285-0529 fitting, each of which straddle a bearing. The critical design condition is a side load which produces bending in the lugs. A comparison of design and measured loads (H_c) and critical stresses (at Section B-B) is given below.

	Design (Weighted Fatigue)	Measured During Whirl Test	Allowable
Load	± 1050#	± 700 to ± 1600# (Normal) ± 3340# (Maximum)	
Stress (Cyclic Part Only)	± 6580 psi	± 21,000 psi	± 26,000 psi

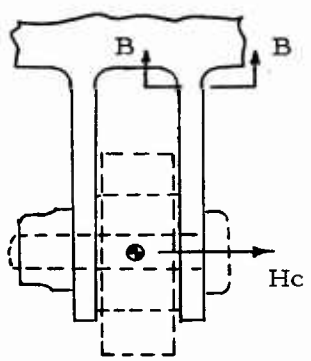

*Inconel "X" retains its strength to approximately 1000°F

Although this calculated cyclic stress is acceptable, there are certain unknowns involved such as the load distribution between lugs. In view of this, a modification was made at the 35 hour inspection period to increase the rigidity and strength of the side load path. Set screws were added in the wall of the hub surrounding the gimbal to bear directly against the lug-to-ring attach bolts. For application to a flight article a minor design change to strengthen the lugs would be in order.

6.2 TEMPERATURE MEASUREMENTS

Table 6.2-1 compares predicted and measured component temperatures. No correction is made to account for the difference in ambient conditions. The analysis of all data leads to the following conclusions:

(a) The temperatures of the duct and flexures are as predicted.

(b) All remaining components operate at temperatures considerably lower than predicted. Spars, outer skin, and hub temperatures compared with the estimates are more than 40% or 50% cooler. These low thermocouple readings are confirmed by indications of temperature sensitive tape checked at corresponding locations.

Figures 6.2-1 through 6.2-4 show temperatures measured for what originally were considered some of the more critical locations throughout the rotor. These are given for various power (exhaust temperature) levels.

Figure 6.2-1 shows a plot of transient temperatures during acceleration runs. It is interesting to note that the outer skin temperatures change little between idling and the maximum power. The differential temperature between the duct and the skin is largest at steady state. Transient runs did not disclose the existence of any critical thermal conditions in the blade.

Figure 6.2-2 shows temperatures prevailing in the hub of the rotor. Two hot runs are presented, with exhaust gas temperatures of 1176°F and 1152°F. It can be seen that the hub assembly temperatures are considerably lower than predicted.

Figures 6.2-3 and 6.2-4 show the relation between the temperature of pertinent rotor components and the turbine discharge temperature T_{T_7}. It is interesting to note that most of the component temperatures are almost directly proportional to T_{T_7}. The data of Figures 6.2-3 and 6.2-4 represent 13 test runs taken at various rotor rpm and engine temperature levels.

TABLE 6.2-1

COMPONENT TEMPERATURES

COMPONENT	Predicted at 1200°F Gas Temp.	Corrected for 1176°F Gas Temp.	Measured	Estimated Absolute Error*	Actual Error	Component Temp. % of Estimated
Duct 3/8" from chord line BS-1-13	1177	1153	1105	-50, +30	+48	4.2% Cooler
Duct top, BS-18-4 Blade Radial Station	1105	1083	1070	-50, +30	+13	1.2% Cooler
Outer Skin on the Rib, BS-18-7	465	457	272	-60, +100	+185	41% Cooler
Rear Spar BRS-3	430	423	240	-60, +100	+183	42% Cooler
Flexure BC_2 (Aver.)	645	633	640	- 0, +200	-7	1% Hotter

*ERROR = Measured - Predicted

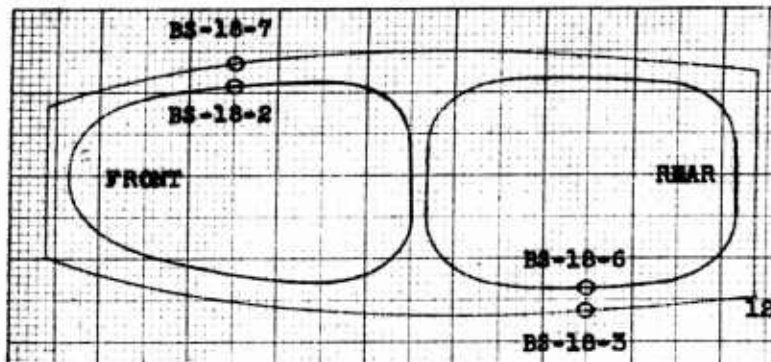

SEGMENT NO. 18

LOCATION OF THERMOCOUPLES
BETWEEN RIBS

NOTE:

READINGS OF DUCT WALL TEMPERATURE BS-18-2 and BS-18-6 WERE ALMOST IDENTICAL

READINGS OF OUTER SKIN TEMPERATURE BS-18-7 and BS-18-9 WERE WITHIN ± 5% FROM THEIR AVERAGE VALUE.

HEAVY LINES REPRESENT PLOT OF AVERAGE TEMPERATURE OF DUCT WALL OR OUTER SKIN.

TRANSIENT TEMPERATURES:

——— Test on Dec. 13-1951 at 1230° Eng. Disch. Temp.

—·—·— Test on Dec. 11-1951 at 1170° Eng. Disch. Temp.

– – – – Predicted at 1200° Dust Gas. Temp.

STEADY STATE:

——·——·—— Test Run No. 6 on Dec. 1-1961 at highest recorded gas temp. (1176°F) (spar thermocouples not at No. 18 segment)

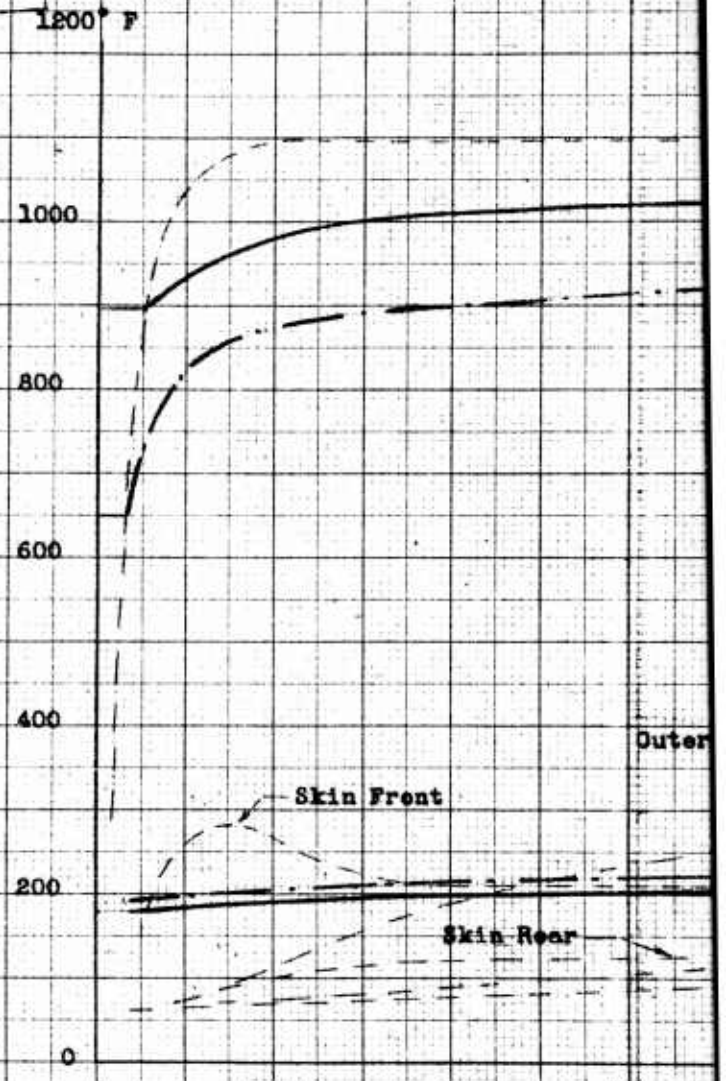

Figure 6.2
Transient Tempe
Predicted and Me

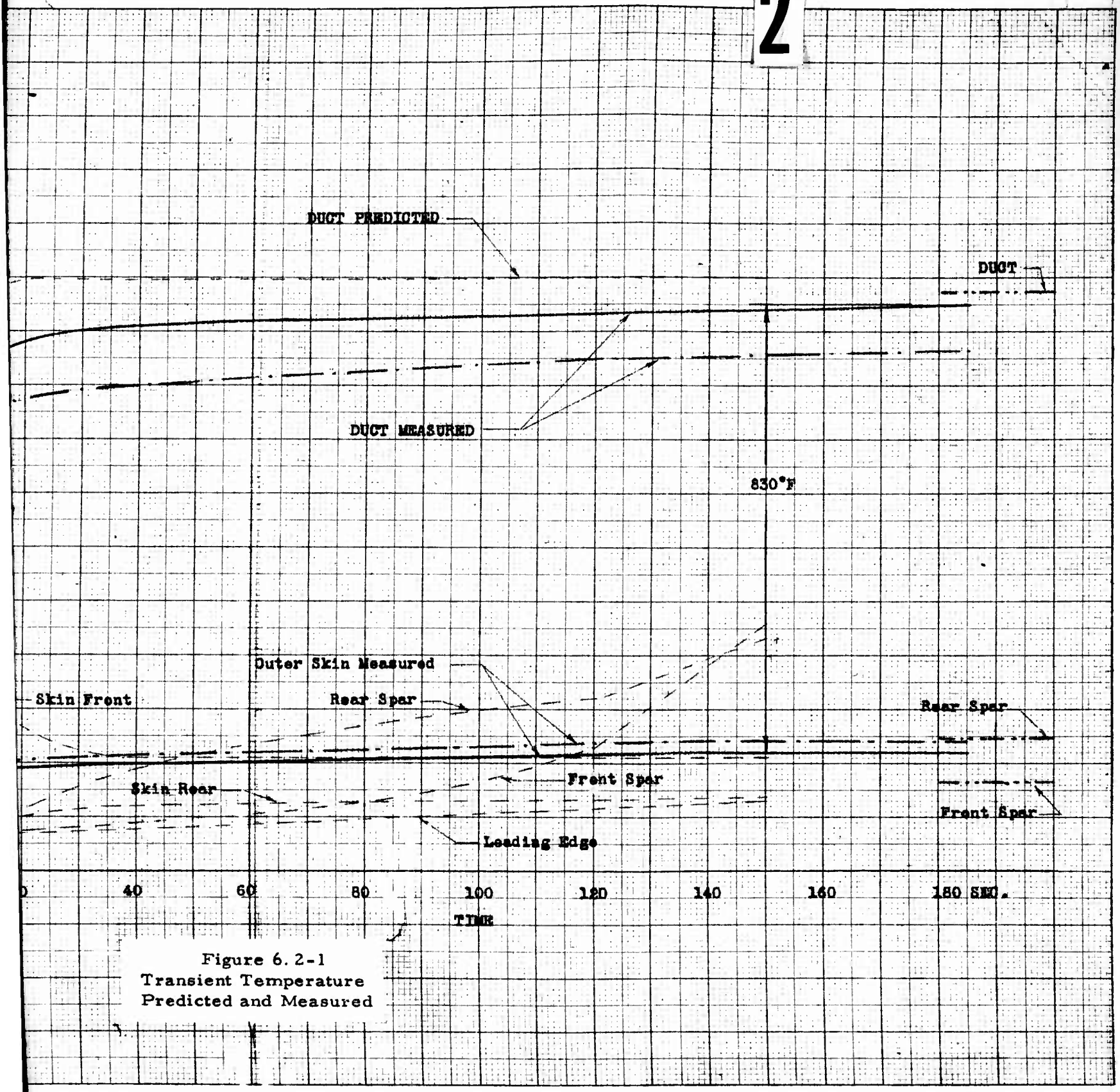

Figure 6.2-1
Transient Temperature
Predicted and Measured

NOTE:

1. Temperatures indicated by upper numbers at each thermocouple represent measurements from Run No. 11 (Oct. 27-61) at 1152°F gas temperature.

2. Temperatures indicated by intermediate numbers represent measurements from Run No. 66 (Dec. 1-61) at 1176°F gas temperature.

3. Bottom Numbers (in parentheses) are predicted values.

4. Thermocouples No. 3, 4 and 8 were inactive.

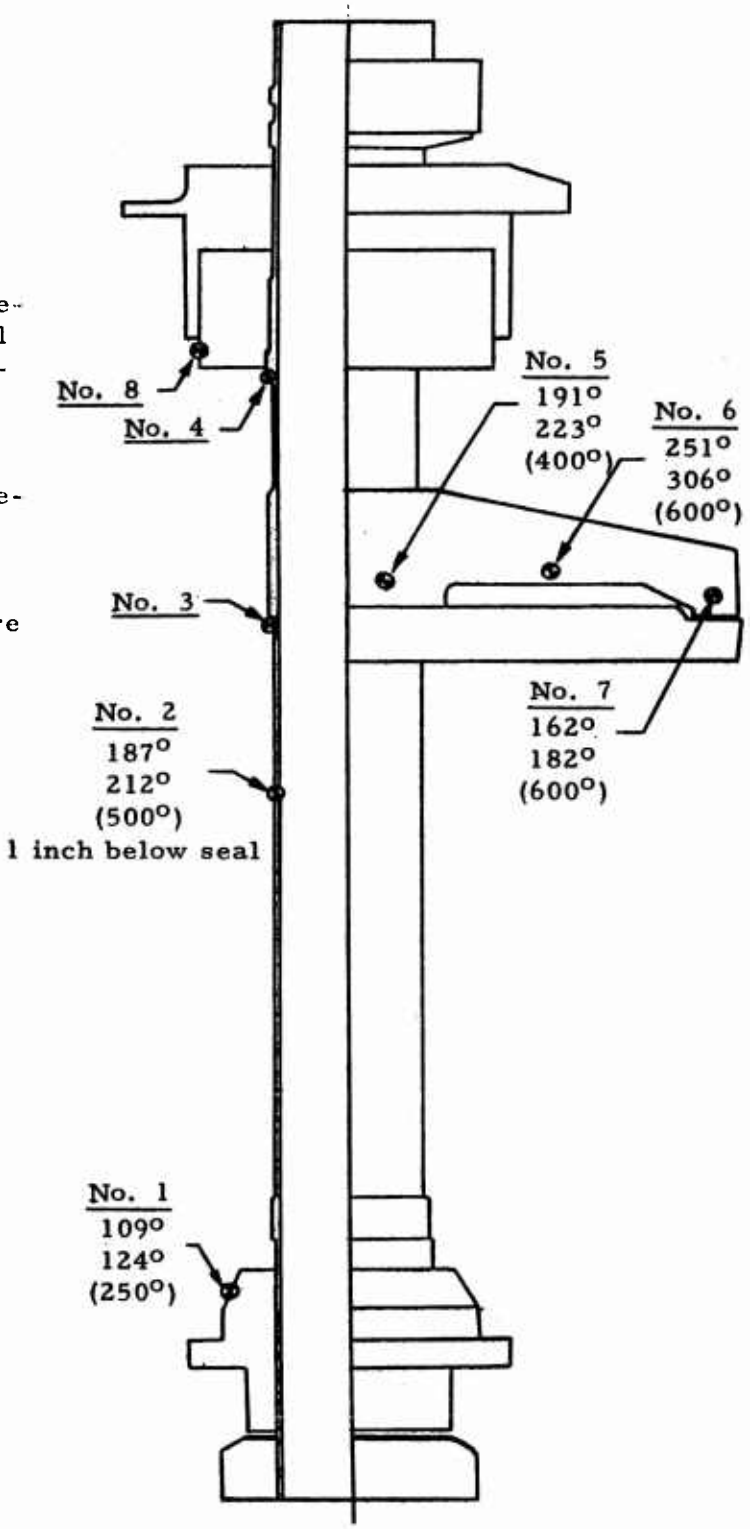

Figure 6.2-2 Distribution of Temperature in the Hub

Location of Thermocouples:

1. **Front spar, center web outside at station 135**
2. **Rear spar, center web outside at station 135**
3. **Rear spar top flange at station 270**
   (This is the highest recorded temperature of a spar at any section.)

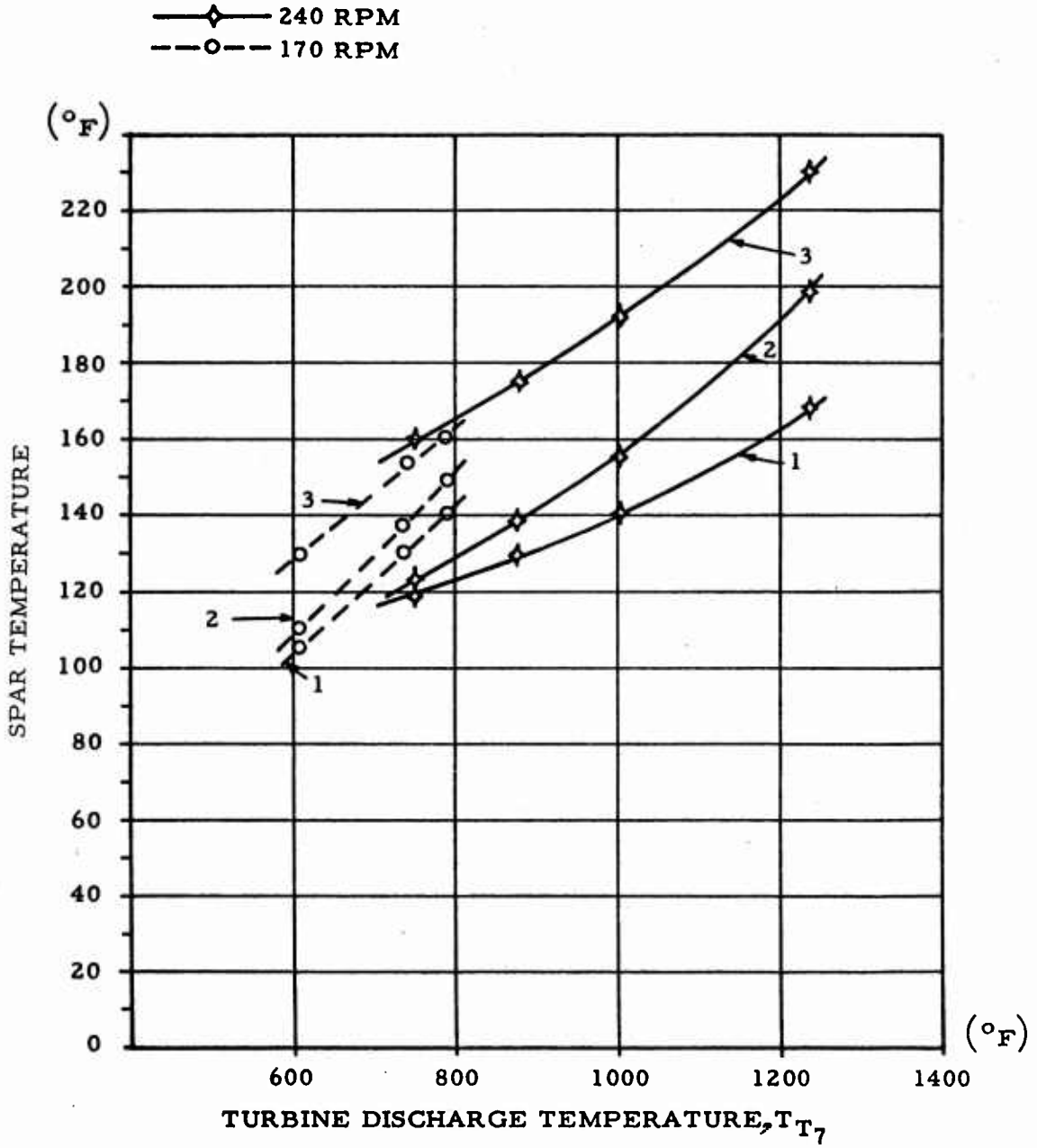

Figure 6.2-3 Temperature of Blade Spars at Various Power Levels

Location of Thermocouples:

1. Duct wall as indicated above at station 95
2. Flexure as indicated above at station 105
3. Hub mast 10 in. below seal

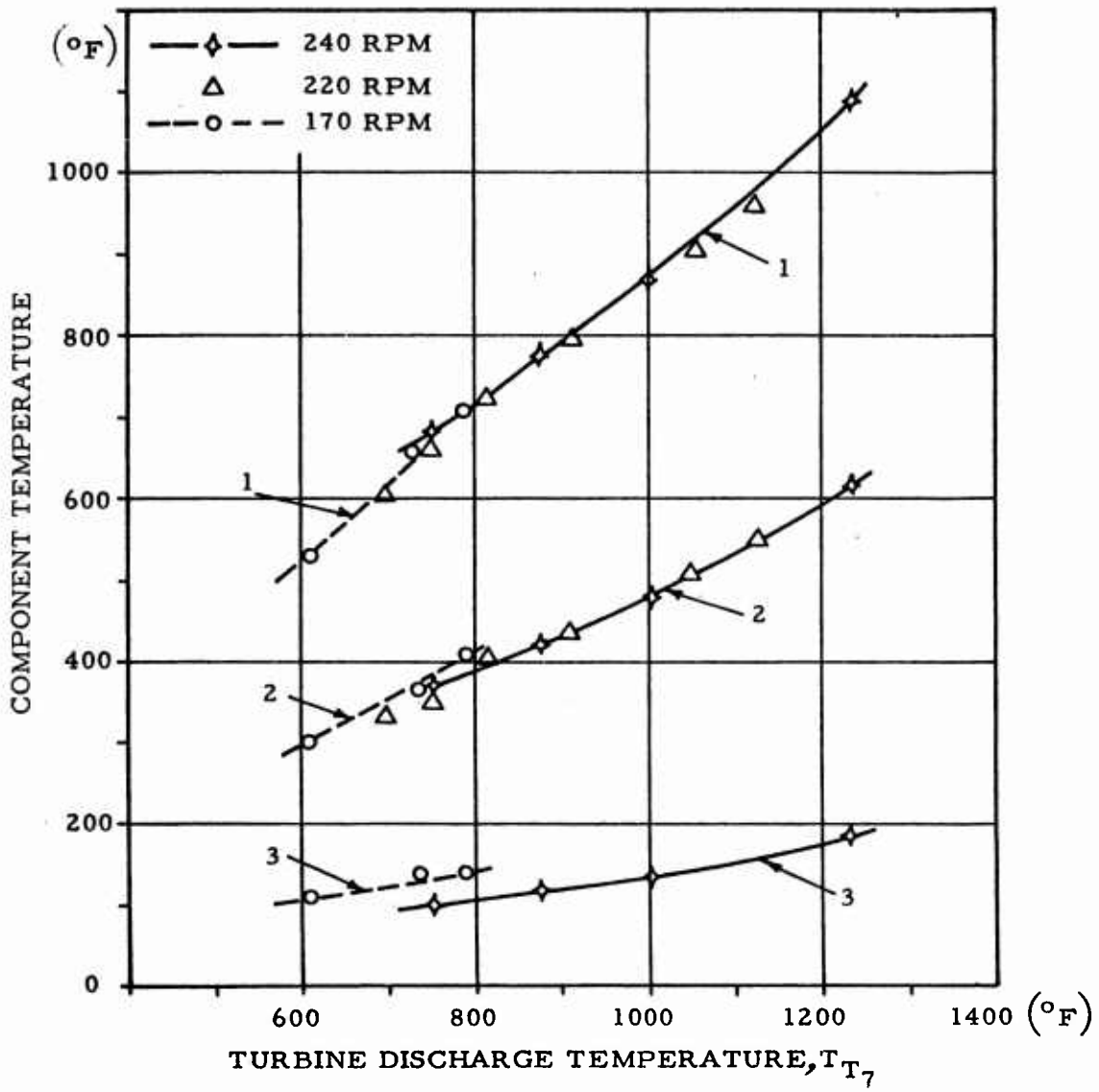

Figure 6.2-4 Temperature of Rotor Components at Various Power Levels

6.3 LEAKAGE SURVEY

The history of rotor system leakage is summarized in Table 6.3-1. It can be seen that the leakage for the various components did not change appreciably from initial installation to final inspection after 60 hours of whirl. The total leakage of less than 0.2% (values are underlined in the table) of total gas flow which did occur is very small and considered completely acceptable. On the other hand, experience gained during the design, fabrication and tests of the current rotor will permit a further substantial reduction of leak paths on future assemblies.

TABLE 6.3-1

LEAKAGE MEASUREMENTS

Assembly Under Test	Hours Whirl Time Before Test	Duct Test Pressure P_1(psig)	Meter Flow Rate Q(cfm)	Corrected Leakage W_w(#/sec)	Leakage (% of Component Flow)	Remarks
Blue Blade	0	23.6	< 1 cfm	0.0039	0.027	
Red Blade	0	23.6	"	0.0039	0.027	
Yellow Blade	0	23.6	"	0.0039	0.027	
Hub Assembly	0	23.6	"	0.0039	0.009	
Blue Blade	18	23.6	0.9	0.0036	0.024	
Red Blade	18	23.6	1.5	0.0059	0.038	
Yellow Blade	18	23.6	2.8	0.0111	0.072	
Rotor System*	18	23.6	17.0	0.0672	0.146	
Rotor System*	18	20	17.0	0.0767	0.168	Reassembled on Tower
Blue Blade	35	23.6	1.5	0.0059	0.039	
Red Blade	35	23.6	2.7	0.0109	0.070	
Yellow Blade	35	23.6	2.7	0.0107	0.070	
Hub Assembly	35	23.6	4.5	0.0178	0.039	
Rotor System*	35	23.6			0.098	Sum of Above
Rotor System*	35	20	17	0.0767	0.168	Reassembled After Teardown
Blue Blade	60	23.6	2.0	0.0079	0.052	
Red Blade	60	23.6	4.0	0.0158	0.103	
Yellow Blade	60	23.6	3.2	0.0131	0.086	
Hub Assembly	60	23.6	13.2	0.0523	0.114	
Rotor System*	60	23.6			0.194	Sum of Above

* Rotor System includes the hub plus the three blades

6.4 PERFORMANCE

6.4.1 Summary

Presented here are the results of performance measurements made during the 60 hour hours of whirl test. It is shown that the two key parameters affecting the conversion of engine gas power to rotor power (duct friction coefficient and nozzle velocity coefficient) are both better than originally estimated. The duct friction coefficient (and hence the pressure loss) for the test rotor is actually less than the value of .004 used for performance estimates. Also, nozzle velocity coefficient, which is a measure of efficiency of the tip nozzle in converting pressure energy to jet velocity is about 2-1/2% better than the value of .955 used for performance estimates.

As an over-all check of the performance of the test rotor and propulsion system, Figure 6.4-1 presents a comparison of measured and predicted rotor thrust. In this figure, the values of thrust are plotted against total pressures at the rotating seal and show good agreement with the analytical estimates. Also, Figure 6.4-1 shows a maximum value of measured thrust of about 22,000 pounds. For the higher pressure ratio which will be available from the T64 gas generators (2.82 atmospheres), the maximum thrust will be about 28,000 pounds.

6.4.2 Temperature and Pressure Losses

Temperature loss in the duct from the turbine exhaust to the hub rotating seal station was 80 to 100°F for the high power runs. This value was fairly constant despite the fact that the insulation blanket around the ducts was sometimes

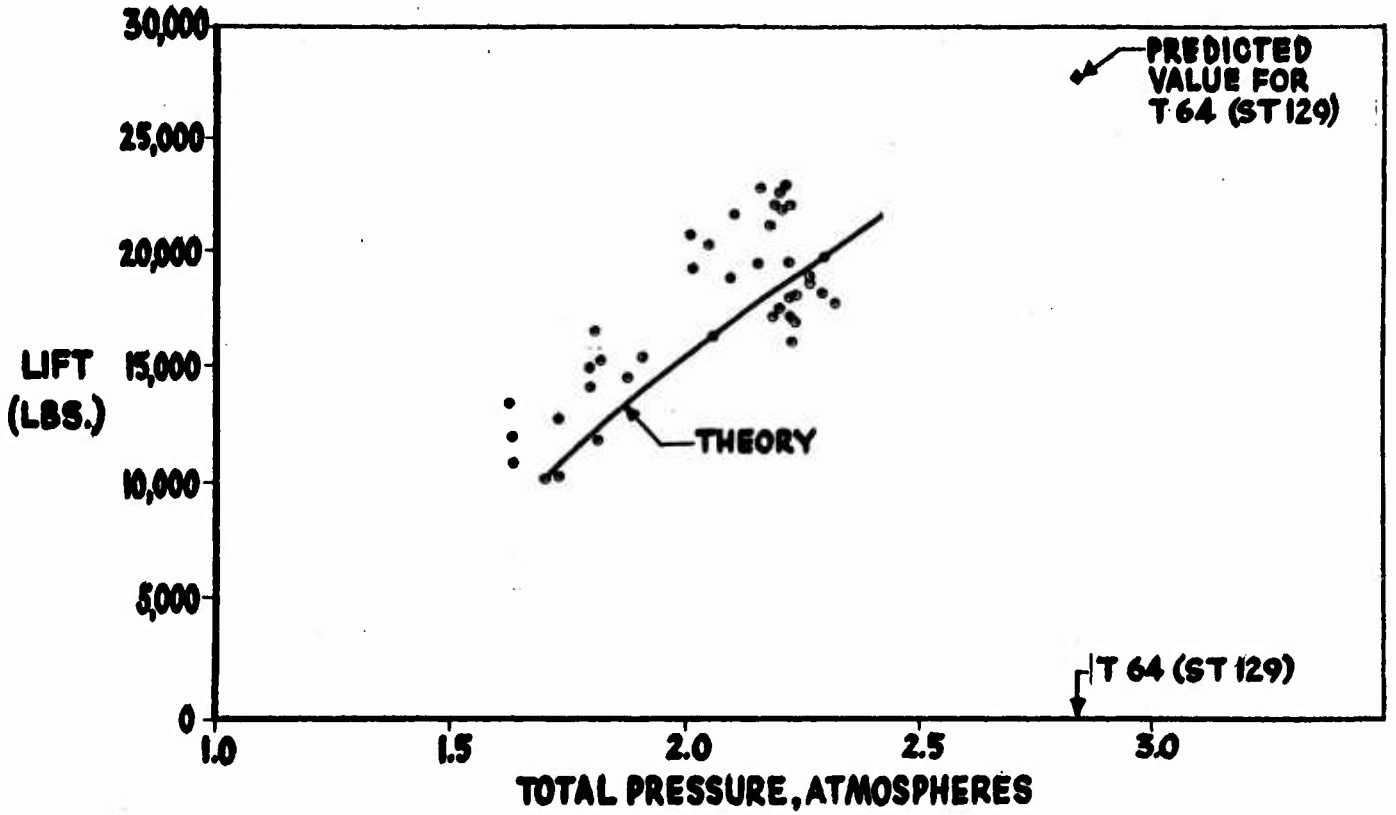

Figure 6.4-1 Hot Cycle Whirl Test Performance

saturated with rain water. Also, for high power runs, the loss in temperature from the hub rotating seal station to the tip nozzles was approximately equal to the temperature rise due to centrifugal compression (35 to 40°F) so that measurements at the flow measuring stations just below the rotating seal indicated quite similar temperatures to those measured at the nozzle inlet stations.

Total pressure loss between the engine and the rotating seal station was from 7.1 to 9.8% of engine discharge pressure. This range of variation of pressure loss was due mostly to changing the butterfly angle in the exhaust dump valve for engine off-line operation as compressor stall is approached. These losses agree well with the predicted values for the whirl test installation.

6.4.3 Tip Nozzle Effective Velocity Coefficient

The effective velocity coefficient, C_{vf}, defined (Report 285-9-7) as the ratio of jet velocity for full expansion to ambient pressure, to jet velocity for full isentropic expansion to ambient pressure (both based on nozzle inlet conditions), was measured to be 0.98 in the choked regime. This is approximately 2.5% better than the 0.955 value used in earlier performance predictions.

6.4.4 Rotor Power

To determine the rotor power through aerothermal analysis, the system is separated into two components (rotating and non-rotating) and the corresponding analyses are programmed for the IBM 7090 in subroutine form. The input and output formats are given in Appendix F, Report 285-16.

6.4.4.1 Non-Rotating Components

The non-rotating components include the J57 gas generator and ducts required to deliver the hot gas to the rotor hub. Details of the calculation are given in Appendix D of Report 285-16.

6.4.4.2 Rotor Power Available

Rotor power available is computed from gas conditions of mass flow, temperature, and pressure existing at the tips of the rotating blades. These conditions differ from those at the rotor hub because of friction and centrifugal force acting on the gas. The gas conditions at the rotor hub are assumed equal to those discharging from the non-rotating duct. (This is described in Section 5.1.5.1 of Report 285-16, while the calculation procedure for computing the changes of gas conditions in going from hub to blade tip is described in Report 285-20.)

Following the procedure of Section 5.1.5.2 of Report 285-16, the gas conditions of mass flow, temperature and pressure at the blade tip are determined. Jet velocity is then computed utilizing the effective velocity coefficient discussed in Section 6.4.3. Finally, rotor power available is computed:

$$RHP = \frac{W_g (V_j - V_T) V_T}{g \times 550}, \text{ where}$$

g = Acceleration due to gravity, 32.2 feet/second/second.

V_j = Jet velocity at blade tip, feet/second

V_T = Blade tip speed, feet/second

W_g = Engine gas flow, pounds/second

6.4.5 Rotor Thrust

The computed thrust of the rotor in hovering is determined from the rotor power available and the rotor geometry using standard NASA methods presented in Reference 2. The approach is to make the power available equal to the power required. The power required equation is then iterated for various values of thrust until the power required is equal to the power available from Section 6.4.4.

The best evidence of the performance of the hot cycle rotor is a direct comparison of measured and computed rotor thrust as a function of engine power. Measured data were reduced according to the procedures discussed in Report 285-16. Figure 6.4-1 shows that measured rotor thrust agrees very well with the computed rotor thrust as a function of rotating seal pressure ratio, up to the maximum value available from the J57 turbojet used during the whirl tests. The calculated curve on Figure 6.4-1 includes an allowance for the power required to centrifically pump the spar cooling air on the test rotor.

The mean value of maximum measured lift was approximately 22,000 pounds, at a seal pressure ratio of 2.2 atmospheres. It should be emphasized that extrapolation of the J57 data (which agrees very well with theory) indicates that at the 2.82 pressure ratio which is available from the advanced (ST 129) model of the T64 gas generator, the rotor will produce over 28,000 pounds of lift.

6.5 ROTOR DYNAMICS AND STABILITY

6.5.1 A free-floating hub configuration was selected for the Hot Cycle Rotor to avoid the need for lead-lag hinges. Figure 6.5-1 presents the predicted blade elastic resonant conditions for the Hot Cycle whirl test rotor. This figure indicates the rotor should be free of resonance within the operating range. No dynamic or flutter problems were evidenced during the entire whirl test program. During the early phases of the program, while building up to higher values of rpm and collective pitch, the cyclic and collective controls were pulsed to establish proximity to resonance of flutter conditions. At no time were such conditions in evidence, substantiating the prediction noted above.

6.5.2 The frequencies given in Figure 6.5-1 were calculated by the Myklestad method (discussed in Appendix of Report 285-14). The values at zero rotor speed were adjusted where necessary to match measured values of non-rotating natural frequencies. The natural frequencies are plotted as Frequency squared versus Rotor Speed squared because in this form the variation of frequency with rotor speed appears as a straight line. Also shown in the figure are the forcing frequencies at integer multiples of rotor speed up through 9 per rev. Intersections of a forcing frequency with a natural frequency is a point of resonance and is indicated by a heavy dot. It can be seen that there are no resonant conditions throughout the normal rotor speed range. The intersection of the 6 per rev forcing frequency with second mode chordwise cantilever frequency is not a point of resonance because on a three bladed rotor a 6 per rev

forcing frequency excites a pin-ended mode only and cannot excite a cantilever mode.

6.5.3 During the measurements of blade non-rotating natural frequencies it was noted that the blade motion damped out very quickly when the excitation was eliminated. Measurements were made of the rate of decay and converted to values of critical damping. Measured damping (first mode flapwise bending) was about 8% of critical. This compares with measurements of about 1% of critical for blades of conventional construction presented in Reference 3. This increase in structural damping is attributed to the slip joint design (refer to Section 5.2 of this report) and should be of significant value in preventing resonance amplification during rotor rev up or, for a compound helicopter configuration, during transition to the unloaded rotor regime.

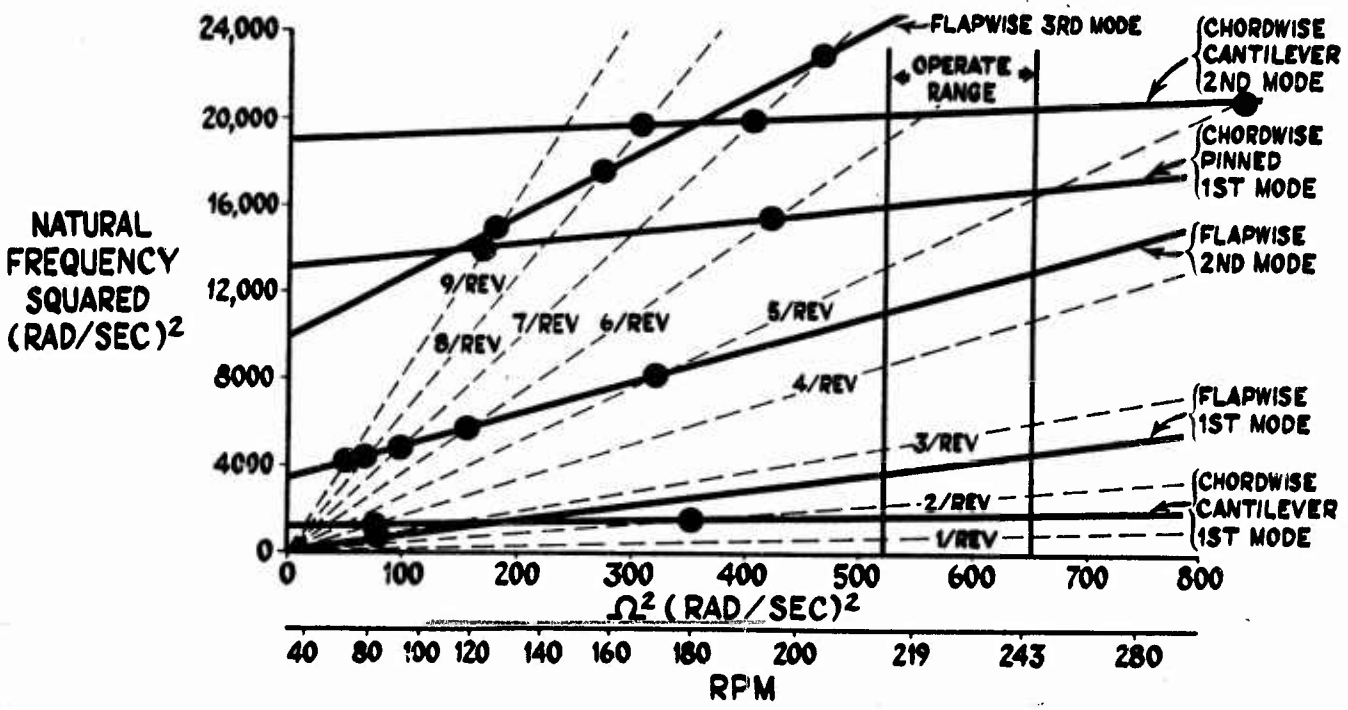

Figure 6.5-1 Predicted Resonances

6.6 ENGINE-ROTOR CONTROL

6.6.1 Study of the engine-rotor control for a hot cycle rotor powered by two General Electric T64 gas generators included a comparison of the techniques currently used for governing free turbine turboshaft engines, both in single and dual installations. All of the free turbine turboshaft engines investigated, including the T64, have droop-stabilized governors to provide essentially constant rotor rpm. Each governor has within it two flyball-type governors, one to measure and control free turbine or rotor speed, and the other to measure and control gas generator speed or engine power. The value of governed rotor speed is selected by the pilot by movement of a lever which changes the reference load on the free turbine speed governor. Engine output power is selected indirectly by the aircraft controls by means of increasing or decreasing the load on the engine (i.e., helicopter rotor collective pitch). The rotor (free turbine) governor controls the gas generator governor to match engine power to load power and thus maintain rotor speed essentially constant. The flyball type governors employed are simple and very reliable, but they permit a small change of rotor rpm with load. This speed change is felt as a reduction of 6-10% in governed rotor rpm as collective pitch is increased from idle to full load. This speed decrease is known as "droop" and is generally removed by resetting the reference rotor speed in proportion to the change of collective pitch to maintain essentially constant rotor rpm. This is effectively shown on Figure 6.6-1.

It was found that the present control system for the YT64 turboshaft engine can successfully govern the hot cycle rotor with no modification in the basic governing circuitry and mechanism. The dynamic behavior of this system for load disturbances, frequency response, behavior after one engine failure, and for power recovery from practice autorotation will be similar to or better than that of other current free turbine turboshaft engine installations.

6.6.2 A design study was also made of the one-engine-out condition to establish requirements for diverter valves and blade duct valves. It was found that one engine operation can be readily obtained. Numerous diverter valve and blade duct valve configurations were studied. Many combinations of these can be used successfully with little or no effect on the dynamic performance of the control system. A detailed discussion of the operation of the over-all system is given in Report 285-19

A brief pre-flight whirl test program utilizing the T64 gas generators is recommended to prove the control concepts.

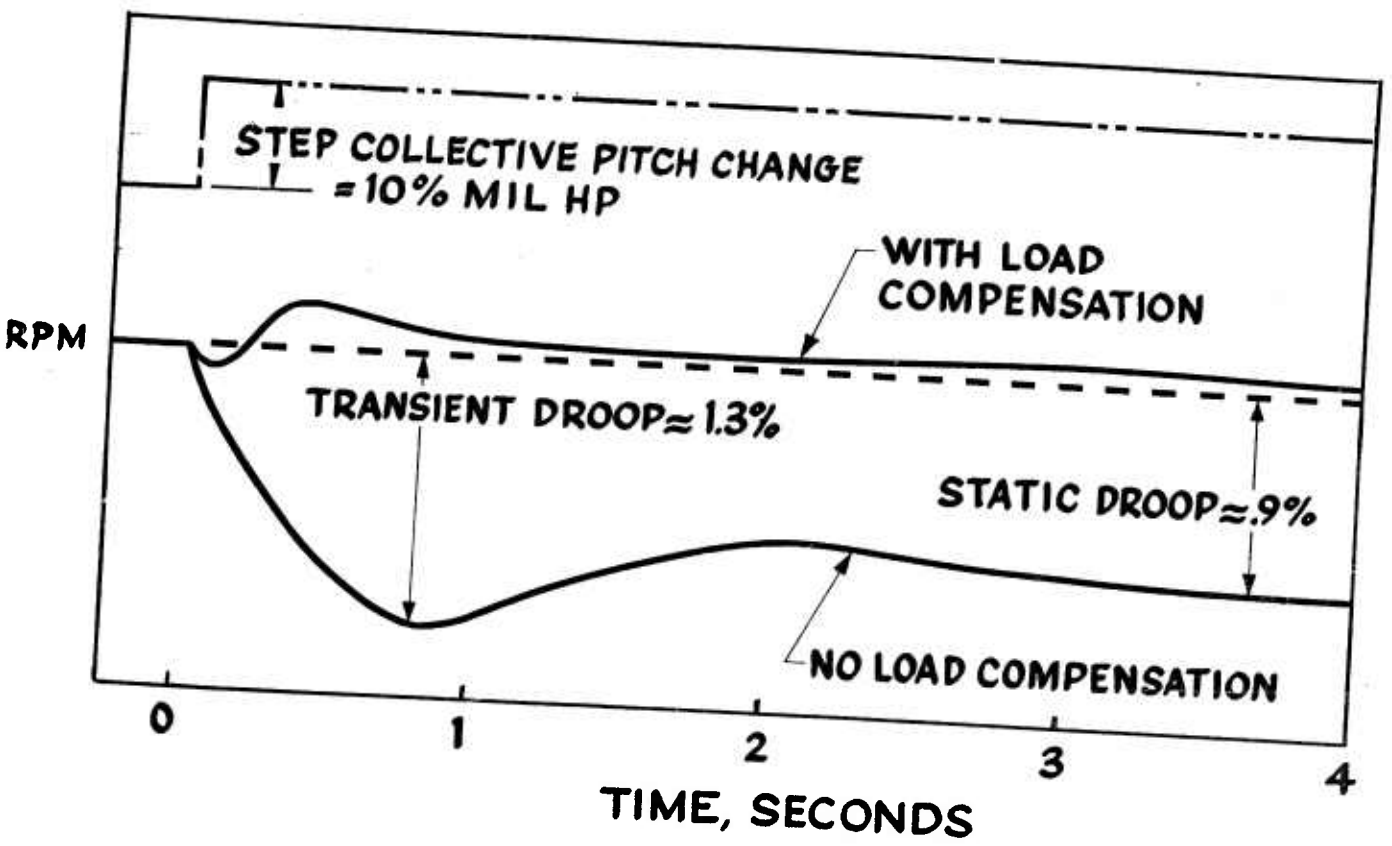

Figure 6.6-1 Rotor RPM Control Utilizing Existing Governors with Droop Compensation

6.7 SOUND LEVEL MEASUREMENT

Due to the fact that only about one third of the J57 exhaust flow was used to power the rotor, and the surplus flow was exhausted directly to the atmosphere, noise associated with this surplus exhaust flow proved bothersome and inconvenient. To lower the sound levels to an acceptable range, sound suppressors were installed at both intake and exhaust ends of the J57 engine. Following this, over-all sound pressure levels were measured close to the test site so that a preliminary study of rotor blade tip exhaust sound levels could be made.

A representative curve is shown on Figure 6.7-1. This is replotted on Figure 6.7-2 in the form of a comparison with other large helicopters and fixed-wing aircraft. The comparison is made for the take-off condition, and presents the over-all sound power level as a function of distance from the aircraft to the observer. It can be seen that the sound level of a hot cycle helicopter is much lower than a typical jet or piston airplane, 22 db lower than (or about 1/2 of 1 percent of) the sound power level of a DC-7. Significantly lower noise than recorded for the H-37A helicopter was also observed during the whirl testing. This measured result was verified by personal observations of individuals who observed the whirl testing and who were also experienced in H-37A operations.

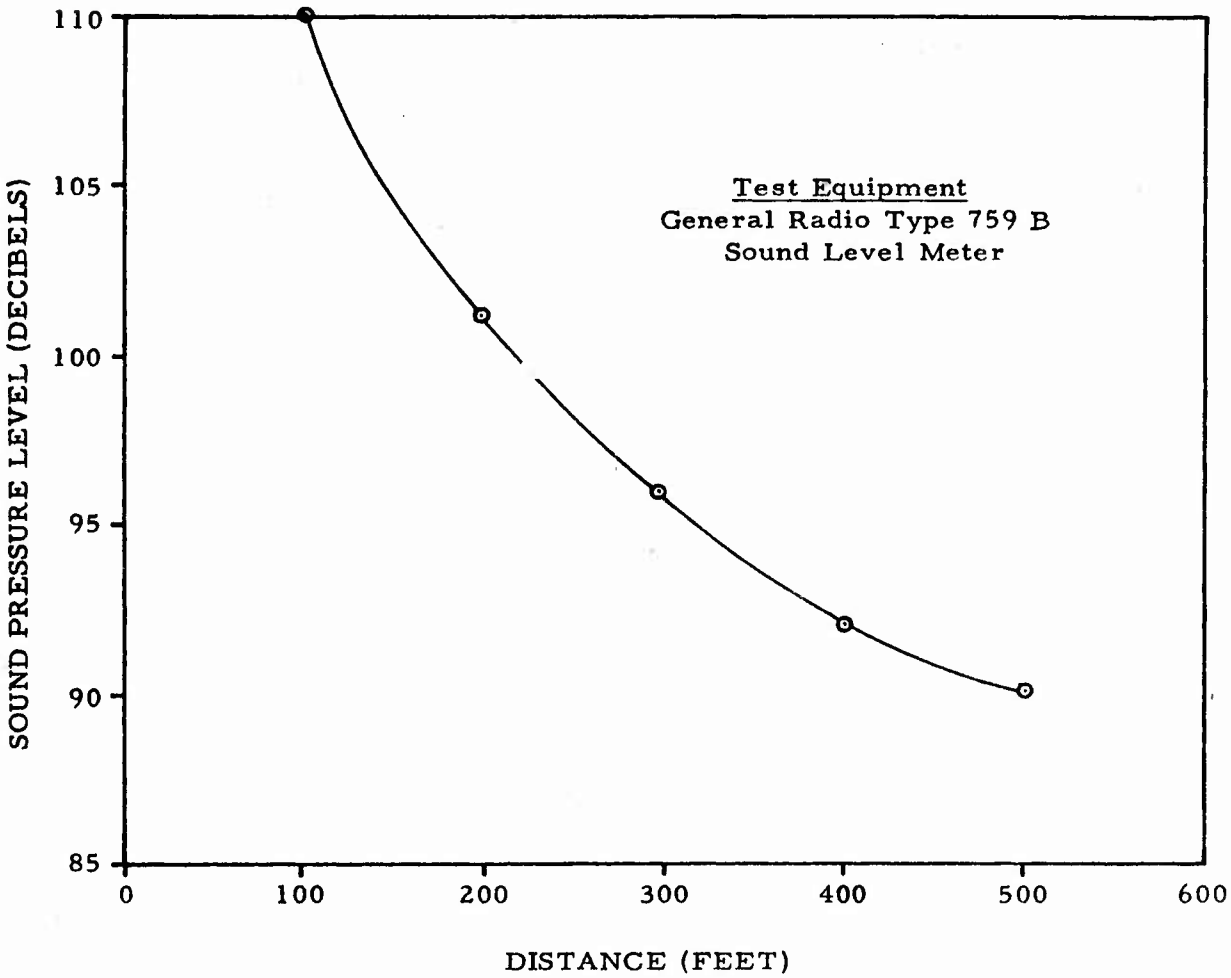

Figure 6.7-1 Sound Pressure Level vs. Distance
(Hot Cycle Rotor plus Suppressed Engine at Full Power)

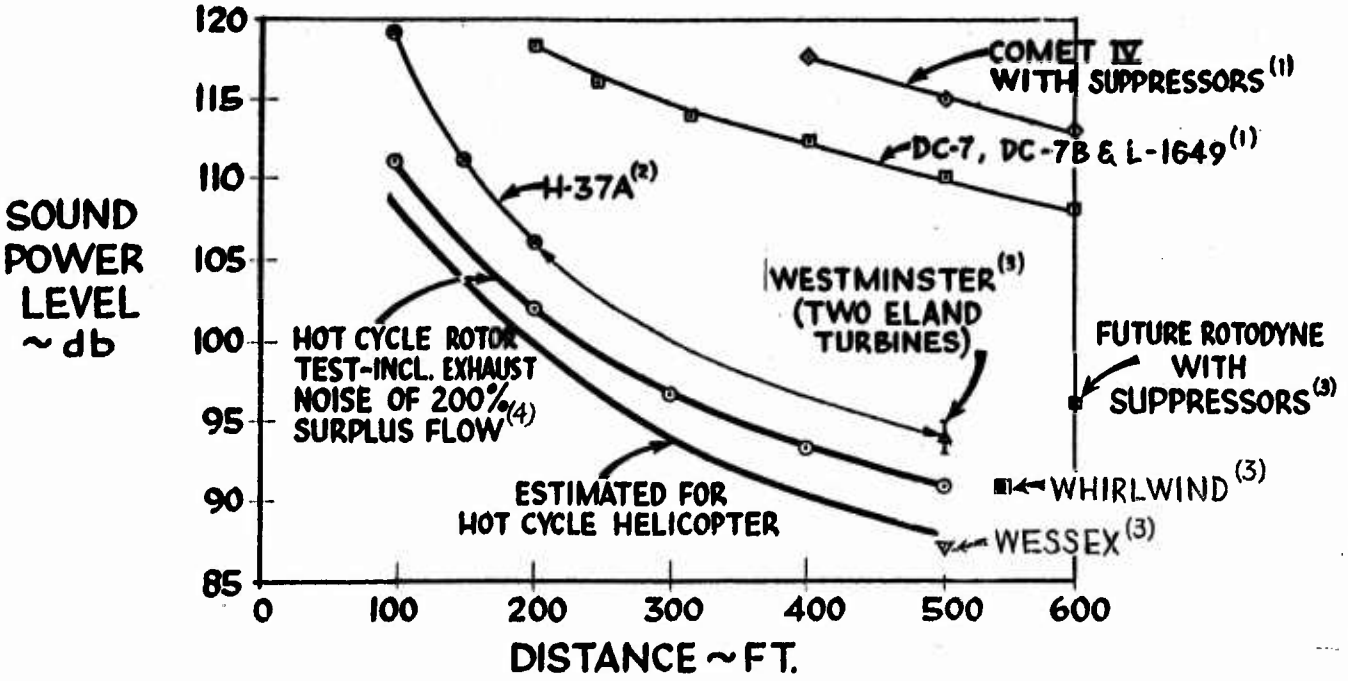

Figure 6.7-2 Noise Comparison for Take-Off Condition

REFERENCES:

1. Studies of the noise characteristics of the Comet IV Jet Airliner and of large propeller driven airliners by Bolt, Beranek and Newman for the Port of New York Authority, October 1958.

2. ARDC H-37A limited stability and control evaluation, AFFTC-TR-60-15.

3. Helicopter noise suppression; H. B. Irving, Journal of the Helicopter Association of Great Britain, Aug. 1959.

Type	Engine(s)	Horsepower
Westminster (S-56)	2 Elands	5000
Whirlwind (S-55)	Gnome	750
Wessex (S-58)	Gazelle	1450

4. Excess flow from J 57 exhausted thru suppressor.

7. REFERENCES

1. Harned, Malcolm; "The Hot Cycle Jet Rotor for Economical VTOL Transport"; Presented at the IAS 30th Annual Meeting New York, New York January 22-24, 1962. IAS Paper No. 62-62.

2. Gessow, A. and Myers G.; "Aerodynamics of the Helicopter"; The Mac-Millan Company, New York, 1952.

3. Gibson, Frederick W.; "Determination of the Structural Damping Coefficients of Six Full-Scale Helicopter Rotor Blades of Different Materials and Methods of Construction"; NASA Technical Note 3862, December 1956.

APPENDICES

INDICES OF ALL REPORTS

UNDER

CONTRACT AF 33(600)-30271

A. Numerical

B. By Contract Item Number

APPENDIX A

INDEX OF

HOT CYCLE PROGRAM REPORTS

IN

NUMERICAL SEQUENCE

Report No.	Title
285-1	Hot Cycle Rotor System, Final Report - Item 2. PART 1 - SUMMARY, 29 February 1956.
285-2	Hot Cycle Rotor System, Final Report - Item 2. PART 2 - STRUCTURAL DESIGN, 29 February 1956.
285-3	Hot Cycle Rotor System, Final Report - Item 2. PART 3 - STRESS ANALYSIS, 29 February 1956.
285-4	Hot Cycle Rotor System, Final Report - Item 2. PART 4 - SYSTEMS STUDY, AERODYNAMICS AND HEAT TRANSFER, 29 February 1956.
285-5	Hot Cycle Rotor System, Final Report - Item 2. PART 5 - WEIGHT AND BALANCE, 29 February 1956.
285-6	Hot Cycle Rotor System, Final Report - Item 1. APPLICATION STUDY, 25 February 1957.
285-7	Hot Cycle Rotor System, Final Report - Item 3. ROTOR SYSTEM PRELIMINARY DESIGN, 30 September 1956.
285-8-1	Anticipated Tests, Component Test Program, Hot Cycle Rotor System, PART I - COMPONENT AND SPECIMEN TESTS NECESSARY TO DEFINE THE STRUCTURE AND CONFIGURATION, 18 December 1956.
285-8-2 (61-14)	Hot Cycle Rotor System, ANTICIPATED TESTS, BLADE FULL SCALE FATIGUE, Specimen Tests Necessary to Define Structure, February 1961.

Report No.	Title
285-8-2S (61-14S)	Hot Cycle Rotor System, ANTICIPATED TESTS, BLADE FULL SCALE FATIGUE, Specimen Tests Necessary to Define Structure, May 1961.(Supplement to 285-8-2)
285-8-3 (61-23)	Hot Cycle Rotor System, ANTICIPATED TESTS, FULL SCALE STATIC AND WHIRL, February 1961.
285-8-3S (61-23S)	Hot Cycle Rotor System, ANTICIPATED TESTS PROPOSED WHIRL TOWER PROGRAM, May 1961. (Supplement to 285-8-3)
285-8-3SR (61-23SR)	Hot Cycle Rotor System, ANTICIPATED TESTS, PROPOSED WHIRL TOWER PROGRAM, November 1961. (Revision of 285-8-3S)
285-9-1	Results of Component Test Program, Hot Cycle Rotor System, TEST NO. 1 - STATIC AND FATIGUE TESTS OF PURE ELECTROFORMED NICKEL, 25 February 1957.
285-9-2	Results of Component Test Program, Hot Cycle Rotor System, TEST NO. 2 - STATIC AND FATIGUE TESTS OF PLAIN AND BRAZED 17-7 PH STAINLESS STEEL SHEET, 4 March 1957.
285-9-3	Results of Component Test Program, Hot Cycle Rotor System, TEST NO. 3 - FATIGUE TESTS OF POKE WELDED 17-7 PH STAINLESS STEEL SHEET, 3 May 1957.
285-9-4	Results of Component Test Program, Hot Cycle Rotor System, TEST NO. 4 - FLOW DISTRIBUTION STUDIES OF THE UPPER STATIC DUCT, 30 August 1957.
285-9-5	Results of Component Test Program, Hot Cycle Rotor System, TEST NO. 5 - BLADE SCREENING FATIGUE TEST, 1 May 1959.
285-9-6	Results of Component Test Program, Hot Cycle Rotor System, TEST NO. 6 - FABROID VS. ARMALON ANTI-FRETTING TEST, 20 May 1959.
285-9-7	Results of Static Test Program, Hot Cycle Rotor System, GAS FLOWS AND TEMPERATURES, February 1962.

Report No.	Title
285-9-8 (62-8)	Hot Cycle Rotor System, Results of Component Test Program, FINAL REPORT, March 1962.
285-10	Hot Cycle Rotor System, Final Report - Item 4, THERMAL ANALYSIS, PART I, June 1960.
285-11 (62-11)	Hot Cycle Rotor System, THERMAL ANALYSIS, PART II, March 1962.
285-12 (62-12)	Hot Cycle Rotor System, DETAIL DESIGN OF ROTOR, March 1962.
285-13 (62-13)	Hot Cycle Rotor System, STRUCTURAL ANALYSIS, March 1962. Vol. I - Structural Analysis Vol. II - Rotor Blade Analysis Vol. III - Hub and Control System Analysis
285-14 (62-14)	Hot Cycle Rotor System, ROTOR DYNAMICS, March 1962.
285-15 (62-15)	Hot Cycle Rotor System, FABRICATION EFFORT, March 1962.
285-16 (62-16)	Hot Cycle Rotor System, WHIRL TESTS, March 1962.
285-17 (62-17)	Hot Cycle Design and Development Program, TECHNICAL SUMMARY REPORT, March 1962.
285-18 (62-18)	Hot Cycle Rotor System, MATERIALS AND PROCESSES, March 1962.
285-19 (62-19)	Hot Cycle Rotor System, ENGINE-ROTOR CONTROL STUDY, March 1962.
285-20 (62-20)	Hot Cycle Rotor System, PERFORMANCE CALCULATION METHOD, March 1962.
285-Pr-1 through -37	PROGRESS REPORTS, January 1956 through April 1962.

APPENDIX B

INDEX

OF

HOT CYCLE PROGRAM REPORTS

BY

CONTRACT ITEM

Item 1b: APPLICATION OF SYSTEM TO HELICOPTERS AND CONVERTIPLANES

285-6 Application Study, 25 February 1957.

Item 2b: DESIGN STUDY OF HOT CYCLE POWERED HELICOPTER

285-1 Part 1 - Summary, 29 February 1956.

285-2 Part 2 - Structural Design, 29 February 1956.

285-3 Part 3 - Stress Analysis, 29 February 1956.

285-4 Part 4- Systems Study, Aerodynamics and Heat Transfer, 29 February, 1956.

285-5 Part 5 - Weight and Balance, 29 February 1956.

Item 3b: PRELIMINARY DESIGN OF ROTOR

285-7 Rotor System Preliminary Design, 30 September 1956.

Item 4e: DETAIL DESIGN OF ROTOR AND EQUIPMENT

285-10 Thermal Analysis, Part I, June 1960.

285-11
(62-11) Thermal Analysis, Part II, March 1962.

285-12
(62-12) Detail Design of Rotor, March 1962.

285-13
(62-13) Structural Analysis, March 1962.
Vol. I: Structural Analysis
Vol. II: Rotor Blade Analysis
Vol. III: Hub and Control System Analysis

285-14
(62-14) Rotor Dynamics, March 1962.

285-20
(62-20) Performance Calculation Method, March 1962.

Item 5n: FABRICATION OF ROTOR AND EQUIPMENT

285-15
(62-15) Fabrication Effort, March 1962.

Item 6b: OUTLINE OF COMPONENT TESTS

285-8-1 Component and Specimen Tests Necessary to Define The Structure and Configuration, 18 December 1956.

285-8-2
(61-14) Anticipated Tests, Blade Full Scale Fatigue, February 1961.

285-8-28
(61-14S) Anticipated Tests, Blade Full Scale Fatigue, May 1961. (Supplement to 285-8-2)

Item 6c: COMPONENT AND NON-ROTATING TESTS

285-9-1 Static and Fatigue Tests of Pure Electroformed Nickel, 25 February 1957.

285-9-2 Static and Fatigue Tests of Plain and Brazed 17-7 PH Stainless Steel Sheet, 4 March 1957.

285-9-3 Fatigue Tests of Poke Welded 17-7 PH Stainless Steel Sheet, 3 May 1957.

285-9-4 Flow Distribution Studies of The Upper Static Duct, 30 August 1957.

285-9-5 Blade Screening Fatigue Test, 1 May 1959.

285-9-6 Fabroid vs. Armalon Anti-Fretting Test, 20 May 1959

285-9-7
(61-79) Gas Flows and Temperatures, February 1962.

285-9-8
(62-8) Results of Component Test Program, Final Report, March 1962.

Item 7b: OUTLINE OF WHIRL TESTS

285-8-3
(61-23) Anticipated Tests, Full Scale Static and Whirl, February 1961.

285-8-3S
(61-23S) Anticipated Tests Proposed Whirl Tower Program, May 1961, (Supplement to 285-8-3).

285-8-3SR
(61-23SR) Anticipated Tests, Proposed Whirl Tower Program, November 1961, (Revision of 285-8-3S).

Item 7c: WHIRL TESTS

285-16
(62-16) Whirl Tests, March 1962.

Item 8: PROGRESS REPORTS

285-Pr-1 dated January 1956

through

285-Pr-37 dated April 1962

Item 9: TECHNICAL SUMMARY OF PROGRAM

285-17
(62-17) Technical Summary Report, March 1962.

Item 10: MATERIALS AND PROCESSES

285-18
(62-18) Materials and Processes, March 1962.

Item 12: STUDY OF ENGINE AND ROTOR CONTROL INTERACTION

285-19
(62-19) Engine-Rotor Control Study, March 1962.

UNCLASSIFIED